ON THE FUKAYA CATEGORY OF GRASSMANNIANS

By

MARCO CASTRONOVO

A dissertation submitted to the

School of Graduate Studies

Rutgers, The State University of New Jersey

In partial fulfillment of the requirements

For the degree of

Doctor of Philosophy

Graduate Program in Mathematics

Written under the direction of

Christopher Thomas Woodward

And approved by

____

____

____

____

New Brunswick, New Jersey

May, 2021

ABSTRACT OF THE DISSERTATION

On the Fukaya category of Grassmannians

by MARCO CASTRONOVO

Dissertation Director:

Christopher Thomas Woodward

The Grassmannian of k-dimensional planes in a complex n-dimensional vector space has a natural symplectic structure, that one can use to construct a deformation of its cohomology ring. We begin the study of its Fukaya category, which is a refinement of the category of modules over this ring. When n is a prime number, we prove that a fiber of an integrable system introduced by Guillemin-Sternberg split-generates the Fukaya category. If n is not prime this generally fails, and we construct examples of Lagrangian tori that support nonzero objects in the missing part of the Fukaya category. The tori are parametrized by seeds of a cluster algebra in the sense of Fomin-Zelevinsky, and have associated Laurent polynomials with positive integer coefficients. We program a random walk that computes these Laurent polynomials explicitly, and observe that they encode the open genus zero Gromov-Witten invariants of the tori in some cases. We put forth a conjecture on the general meaning of the Laurent polynomials, which can be considered as a Symplectic Field Theory interpretation of the notion of scattering diagram proposed by Gross-Hacking-Keel-Kontsevich.

DEDICATION

To New Jersey Transit

ACKNOWLEDGMENTS

This thesis would not have been possible without Chris Woodward, whom I wish to thank for taking up the burden of my doctoral education. Besides the many meetings, emails and the support from his grants, Chris shared his sense of what are the most interesting questions in Symplectic Topology today. Instead of imposing some grand research plan that I could barely understand (a popular trend that crushes many students in the field), he suggested examples that I could play with, whose features raised many puzzling questions. This gave me the opportunity to develop independence and confidence, hopefully laying the ground for depth and sophistication in the future.

The city of New York, where I lived in the past five years, also had a strong impact. Although it is possble to explore mathematics in some degree of isolation, the city's music, food, parks, art, events, etc. gave an extra kick to my intellectual life. When mathematics didn't work, the city reminded me that I'm just a human on planet Earth. When it did work, the city simply ignored me and carried on with its usual humming.

Most of the writing I have done in these years has been carried out at the Columbia University Mathematics Department. While there, I have had the chance to attend many inspiring seminars. Mohammed Abouzaid often sat in the last row, and I learned a great deal from his questions and comments. Off the books, Mohammed always found some space for me in his schedule, and his feedback ruled out many of my attempts to pursue goals too vague or too false.

The Rutgers University Mathematics Department provided excellent conditions for my growth: funding, library access, teaching training. I wish to thank Lev Borisov and Anders Buch in particular, who provided useful inputs on some topics related to this thesis. Something quite unique that I had the chance to experience while at Rutgers is the Geometry, Physics and Symmetry seminar, an attempt to bring mathematicians and physicists together. I look forward to having more of these interactions in the future.

I think this is also the right place to thank some people who believed, before anybody else, that I could complete this PhD. Peter Teichner gave me the chance to spend one year at the Max Planck Institute for Mathematics in Bonn, then helped me to come to

the United States. Dylan Thurston at Indiana University Bloomington first taught me a lot about Heegaard Floer Theory, then helped me to come to New York.

There are many more mathematicians who, for one reason or another, I got to know better and made me feel part of a beautiful community. In alphabetical order: Antonio Alfieri, Akram Alishahi, Catherine Cannizzo, Soham Chanda, Luis Diogo, Andrew Hanlon, Jeff Hicks, Ailsa Keating, Lea Kenigsberg, Artem Kotelskiy, Oleg Lazarev, Yanki Lekili, Francesco Lin, Joseph Palmer, Semon Rezchikov, Douglas Schultz, Kyler Siegel, Jack Smith, Yuhan Sun, Dmitry Tonkonog, Umut Varolgunes, Sara Venkatesh, Xindi Zhang. I thank you all.

Chapter 3 has appeared in different form as arXiv preprint 1808.02955, and was then published on Advances in Mathematics, Volume 372, 107287 (October 2020). Chapter 4 has appeared in different form as arXiv preprint 1910.10888, and has been submitted for publication. Chapter 5 is written in the programming language Python, and uses some libraries from the open-source software SageMath, downloadable from

`https://www.sagemath.org/` .

Tests have been performed with SageMath 8.6; compatibility with other versions is not guaranteed. The code has been released under the open-source license GNU GPLv3, and is available on GitLab at

`https://gitlab.com/castronovo/clusterexplorer` .

Appendix A and B summarize, for the reader's convenience, results obtained by others, and we claim no originality for material contained there.

Contents

Chapter 1

INTRODUCTION

In this chapter, we introduce the main questions around which this thesis revolves, and explain how they fit more broadly in the context of Symplectic Topology, Floer Theory, and Mirror Symmetry. We then describe what was known about these questions when this thesis began, and summarize the results obtained in the years 2017-2019. Finally, we describe some future directions whose exploration started in 2020.

1.1. Why are symplectic computations hard?

The promise of Topology is to build a bridge between continuous and discrete phenomena. Since the early days of Betti, Riemann, Poincaré, etc. the following strategy has been the blueprint for the construction of topological invariants of an object X:

1. define what it means to deform X ;
2. construct a discrete deformation invariant ;
3. develop techniques to compute the invariant .

The reader can think of homotopy equivalence and cohomology theories as an instance of this paradigm, with exact or spectral sequences being the main computational tool. The specific interest of topological (as opposed to general) invariants is that deformations of X are typically hard to classify, whereas discrete invariants are much simpler to handle. One typically judges the strength of the invariant not by how faithfully it encodes the deformation class of X, but rather by that relative to its computability.

Beginning with Lefschetz, Hodge, Hirzebruch, etc. a particular focus has been on computing topological invariants of objects X defined by algebraic (or analytic) equations. Say X is a smooth projective variety over $\mathbb{C}$; singularities are welcome in topology, and étale techniques are available in positive characteristic, but simpler things first. Surprisingly, the invariants of X tend to acquire extra properties and structure in this case. Most relevant for us is the insight of Witten [83], who observed that the cohomology ring has a refinement where the cup product $\Delta_a \Delta_b$ of two classes in a basis $\Delta_\bullet$ with Poincaré dual $\Delta^\bullet$ is replaced by

$$\Delta_a \star \Delta_b = \sum_c \frac{\partial^3 \Phi}{\partial t_a \partial t_b \partial t_c} \Delta^c \quad ,$$

which involves derivatives of a generating function

$$\Phi = \sum_{n \in \mathbb{N}} \frac{1}{n!} \sum_{i_1, \ldots, i_n} \left(\sum_\beta \langle \Delta_{i_1} \cdots \Delta_{i_n} \rangle_\beta q^\beta \right) t_{i_1} \cdots t_{i_n} \quad .$$

The quantities $\langle \Delta_{i_1} \cdots \Delta_{i_n} \rangle_\beta \in \mathbb{Q}$ are known today as closed genus zero Gromov-Witten numbers, and the resulting ring as (big) quantum cohomology $\mathrm{QH}(X)$. Roughly, these are counts of rational curves (or holomorphic spheres) with homology class $\beta \in H_2(X)$, passing through n points on cycles dual to $\Delta_{i_1}, \ldots, \Delta_{i_n}$. Gromov [34] had previously realized that they do not actually depend on the complex structure of X, but only on the deformation class of a compatible symplectic structure, and thus are invariants in the sense of Symplectic Topology.

From the enumerative point of view, where Φ is the central object of study, quantum cohomology is a rather odd invariant that does not fit squarely in the framework of homological algebra: what complex is it the cohomology of? This perhaps explains why, throughout the years, the main computational techniques came from Algebraic Geometry and heuristics in String Theory; see the monograph by Cox-Katz [19].

The topological point of view allows to resolve this difficulty, the main input being an infinite-dimensional version of Morse theory for the loop space $\mathcal{L}X$ known as Hamiltonian Floer theory; see Salamon [72] for a survey and Piunikhin-Salamon-Schwarz [65] for the relation to quantum cohomology. The remarkable technical difficulties involved in establishing Hamiltonian Floer theory in full generality have constrained the development of the subject to foundational matters until recently; see Pardon [64] for the most recent construction of the relevant virtual fundamental classes. However, at the time of writing Varolgunes [82] moved the first steps towards establishing purely topological computational methods, such as a Mayer-Vietoris property and functoriality.

Summarizing, with the benefit of the hindsight the sophisticated invariants of Symplectic Topology can be constructed by means of Floer theory, and there is a good chance that they will be computable by homological techniques. However, much of the intuition along the way came from the case where X is algebraic (or analytic) and computations from Algebraic Geometry or heuristics from String Theory.

1.2. From closed to open strings

Informally speaking, Hamiltonian Floer theory replaces gradient flow lines between critical points of a Morse function H with cylinders connecting periodic orbits of an associated vector field X_H. The cylinders satisfy an analogue of the Cauchy-Riemann equations from complex analysis, and one can think of them as the trace of a closed string moving inside the target symplectic manifold X.

If $L \subset X$ is a Lagrangian submanifold, there is version of this picture where closed strings are replaced by open strings: Lagrangian Floer theory. Instead of cylinders, one looks at strips whose boundary lines lie on L and a transverse perturbation $\phi^1_H(L)$, where ϕ^1_H is the flow of X_H at time one. Recall that L is half-dimensional, so that the set $L \cap \phi^1_H(L)$ consists of finitely many points, and the ends of a strip are asymptotic to a pair of such points; see the survey by Auroux [7] and Appendix A for more details.

Formal analogy with Hamiltonian Floer theory suggests that Lagrangian Floer theory should lead to a deformation of the cohomology ring of L. Although this is true in some cases, the story is in general more complicated. Recall that all enumerative theories rely on having compact moduli spaces. The appropriate compactification for the moduli space of strips is known: it includes the expected configurations with sphere bubbles as well as new disk bubbles. Lagrangian Floer theory leads to a natural guess for a complex $CF(L)$ deforming the singular cochain complex, but disk bubbling prevents the new differential from squaring to zero. In fact, $CF(L)$ has a much richer structure of curved A_∞-algebra, and L can be thought of as an object of an A_∞-category called Fukaya category $\mathcal{F}(X)$; see the monograph by Fukaya-Oh-Ohta-Ono [28].

In this thesis, we work with a simplified version of the Fukaya category, where both X and the Lagrangian $L \subset X$ satisfy a condition called monotonicity; see Appendix B for more details. Monotonicity of X is a geometric assumption, that can be achieved whenever X is Fano. Instead, monotonicity of L is a technical restriction that suffices for our purposes but should be lifted in future work; compare Charest-Woodward [13] for a possible approach. Moreover, we will be focused on the case in which L is a torus. Following a proposal of Strominger-Yau-Zaslow [80], it is widely believed that Lagrangian tori should determine much of the information contained in the Fukaya category $\mathcal{F}(X)$; see Abouzaid [2] for a result in this direction when X is fibered by Lagrangian tori bounding no holomorphic disks.

Recall that the cohomology ring of an N-dimensional torus L can be described as the exterior algebra of $H^1(L)$. One can deform this to a different Clifford algebra, by replacing the trivial quadratic form with one encoding symplectic information. As in the closed-string case, consider the generating function

$$W_L = \sum_\beta c_\beta(L) x^{\partial\beta} \quad ,$$

where $c_\beta(L) \in \mathbb{Q}$ roughly counts holomorphic disks with homology class $\beta \in H_2(X, L)$ and boundary homology class $\partial\beta \in H_1(L)$; under our assumptions the numbers $c_\beta(L)$ are nonzero integers for finitely many β. After choosing a basis $\gamma_\bullet \in H_1(L)$, one can think of the formal variables $x_\bullet$ as holonomies of a rank one local system ξ on L, so that its holonomy around $\partial\beta$ corresponds in the sum above to the weight

$$x^{\partial\beta} = x_1^{k_1} \cdots x_N^{k_N} \quad , \quad \partial\beta = k_1\gamma_1 + \ldots + k_N\gamma_N \quad .$$

Since local systems are classified by their holonomy, the moduli space of such ξ is a complex torus $\mathrm{Hom}(H_1(L), \mathbb{C}^\times) = (\mathbb{C}^\times)^N$, and W_L is a regular function on this torus. If ξ is a critical point of W_L, then its Hessian at ξ defines a quadratic form on $H^1(L;\mathbb{C})$ encoding enumerative information about the Lagrangian embedding $L \subset X$.

Lagrangian Floer theory twisted by the local system ξ gives now a honest complex $CF(L_\xi)$, and its cohomology $HF(L_\xi)$ is the Clifford algebra just described. For any $\lambda \in \mathbb{C}$, one then constructs a Fukaya category $\mathcal{F}_\lambda(X)$ containing objects L_ξ such that $W_L(\xi) = \lambda$. This is a categorification of a subring $\mathrm{QH}_\lambda(X) \subset \mathrm{QH}(X)$ of quantum cohomology; see Sanda [73] and Appendix B. The formal sum

$$\mathcal{F}(X) = \bigoplus_{\lambda} \mathcal{F}_{\lambda}(X)$$

is referred to as the spectral decomposition of the Fukaya category.

1.3. Main questions and state of the art

There are very few topological techniques to compute open-string invariants. Once again, the first insights are coming from Algebraic Geometry and String Theory. We assume from now on that X is a smooth complex projective variety of Fano type, and that D is a fixed effective anti-canonical divisor.

As described in Auroux [6], there should be a construction of a complex variety $X^\vee$, referred to as a Landau-Ginzburg model, with a regular function $W \in \mathcal{O}(X^\vee)$ called potential. Roughly speaking, $X^\vee$ should arise as moduli space of Lagrangian tori $L \subset X \backslash D$ equipped with rank one local systems ξ. The potential W should describe, in suitable complex torus charts $T_L \subset X^\vee$, the obstruction to the Floer differential squaring to zero in $CF(L)$; in other words $W_{|T_L} = W_L$ holds. This description is expected to have a purely topological translation when X is a general compact symplectic manifold, with D replaced by a symplectic divisor in the sense of McLean-Therani-Zinger [57], and $X^\vee$ by a rigid analytic space over the Novikov field. Recent work of Yuan [84] constructs candidates Landau-Ginzburg model and potential when $X \backslash D$ is generically fibered by Lagrangian tori bounding no holomorphic disks with negative Maslov index.

Following Kontsevich [49], once a candidate Landau-Ginzburg model $(X^\vee, W)$ for (X, D) is known one says that Homological Mirror Symmetry holds if

$$\mathbf{D}\mathcal{F}_{\lambda}(X) \simeq \mathbf{D}\mathcal{S}(W^{-1}(\lambda)) \quad \forall \lambda \in \mathbb{C} \quad .$$

This is the statement that two triangulated categories are equivalent: one is the derived category of $\mathcal{F}_{\lambda}(X)$; the other is the derived category of singularities of the fiber $W^{-1}(\lambda)$ introduced by Orlov [62], which measures to what extent coherent sheaves fail to have finite resolutions by locally free sheaves. See Appendix B for more details on these categories.

Dyckerhoff [23] showed that, whenever W has critical locus of dimension zero, the category of singularities is generated by skyscraper sheaves at the critical points. On the symplectic side no such general statement is known, but it is natural to ask the following.

Question 1.3.1. *(General) Think of a smooth complex projective Fano variety X as a compact manifold with symplectic structure ω such that $[\omega] = c_1(X)$. Is $\mathcal{F}(X)$ generated by objects supported on Lagrangian tori? If yes, how to construct a set of generators in practice?*

For $X = \mathbb{P}^N$ and D union of coordinate hyperplanes, Cho [14] showed that a fiber of the moment map supports $N+1$ nonzero objects that generate all the summands of $\mathbf{D}\mathcal{F}(X)$, corresponding to the critical points of the potential $W \in \mathcal{O}(X^\vee)$ with $X^\vee = (\mathbb{C}^*)^N$ and

$$W = x_1 + \ldots + x_N + x_1^{-1} \cdots x_N^{-1} \quad .$$

This was later generalized to arbitrary smooth projective Fano toric varieties $X(\Sigma)$ by Fukaya-Oh-Ohta-Ono [29], with $D = D_\Sigma$ torus invariant anti-canonical divisor, Landau-Ginzburg model $X^\vee = (\mathbb{C}^*)^N$ and potential W determined by the primitive lattice vectors generating the rays of Σ.

The goal of this thesis is to investigate the question of generation by Lagrangian tori when X is not toric, focusing on complex Grassmannians $X = \mathrm{Gr}_k(n)$ of k-planes in $\mathbb{C}^n$. We believe that this is the next easiest case after toric for the following reasons.

1. Based on ideas from representation theory, Rietsch [69] constructed candidate Landau-Ginzburg models $(X^\vee, W)$ for general homogeneous varieties $X = G/P$, and showed that the coordinate ring of the critical locus of W matches the quantum cohomology ring $\mathrm{QH}(G/P)$. This is an indication that Homological Mirror Symmetry, which is a categorification of this statement, could hold and serve as a guide in the calculation of $\mathcal{F}(G/P)$.

2. The Landau-Ginzburg model $X^\vee$ is an open projected Richardson variety in the sense of Knutson-Lam-Speyer [48]. These are smooth affine varieties, and Leclerc [51] showed that their coordinate rings admit a cluster structure in many cases. The notion of cluster algebra was introduced by Fomin-Zelevinsky [26], and roughly says that $X^\vee$ has an atlas of complex torus charts related by special birational

transition functions. It is natural to speculate that these charts are mirror to Lagrangian tori $L \subset G/P$, and that W locally agrees with their disk potential W_L. Since W and the cluster charts can be computed in practice, this gives precise predictions on the open Gromov-Witten numbers of Lagrangian tori in G/P by restricting W to the cluster charts.

3. Starting from type A, the variety $X = G/P = SL_n/P$ parametrizes partial flags in $\mathbb{C}^n$. If P is the subgroup of matrices with a $k \times k$ block then $X = \mathrm{Gr}_k(n)$, and much of what discussed so far can be recasted in elementary terms using the classical Plücker coordinates; see Marsh-Rietsch [53] for the description of the Landau-Ginzburg model, and Scott [74] for its cluster structure. We point out that in this case the Landau-Ginzburg model is also known as open positroid stratum, and its properties have been the focus of several works in representation theory, combinatorics and topology [52, 66, 47, 76].

Therefore we are lead to the following, more specific.

Question 1.3.2. *(Specific) Is $\mathcal{F}(\mathrm{Gr}_k(n))$ generated by objects supported on Lagrangian tori? If yes, how to construct a set of generators in practice?*

As of November 2017 (the beginning of this thesis) no one had investigated the question beyond the toric cases $\mathrm{Gr}_1(n) = \mathbb{P}^{n-1}$. The Grassmannian $\mathrm{Gr}_2(4)$ can be presented as a quadric hypersurface in $\mathbb{P}^5$, and the work of Sheridan [77] on the Fukaya category of Fano hypersurfaces applies, but it focuses on Lagrangian spheres as opposed to tori. The results that back then were closest to the spirit of the question are listed below in chronological order.

1. Guillemin-Sternberg [40] constructed an integrable system on $\mathrm{Gr}_k(n)$ and more general partial flag manifolds, called Gelfand-Zetlin system, by thinking of the Grassmannian as coadjoint orbit of $U(n)$; their construction is recalled in Section 3.2. In particular, the generic fiber of this integrable system is a Lagrangian torus, and the the image of its Hamiltonians is a lattice polytope $\Delta_{GZ} \subset \mathbb{R}^{k(n-k)}$.

2. Nishinou-Nohara-Ueda [58] observed that the polytope Δ_{GZ} is the moment polytope of a (typically) singular toric variety, and that the Lagrangian torus fibers of the Gelfand-Zetlin system are deformations of toric moment fibers in a suitable

sense; they used this to establish a bijection between rigid holomorphic disks on Gelfand-Zetlin fibers and codimension one faces of the polytope Δ_{GZ}.

3. Nohara-Ueda [59, 60] used symplectic reduction techniques to construct a Catalan number C_{n-2} of integrable systems on $\mathrm{Gr}_2(n)$, each labeled by a triangulation Γ of the n-gon; the generic fibers of these systems are Lagrangian tori $L_\Gamma \subset \mathrm{Gr}_2(n)$, and the images of their Hamiltonians are lattice polytopes Δ_Γ (one of them matches Δ_{GZ} for each n). Explicit formulas for the disk potentials W_{L_Γ} were given as sums over edges of the triangulation Γ, and disk potentials of tori whose triangulations are related by a flip were shown to be related by a cluster mutation in the sense of Fomin-Zelevinsky [26].

4. Rietsch-Willams [70] investigated a special collection of cluster charts $T_G \subset X^\vee$ in the Landau-Ginzburg model for $X = \mathrm{Gr}_k(n)$ proposed by Marsh-Rietsch [53], parametrized by combinatorial objects G known as plabic graphs. They gave combinatorial formulas for the restriction of the potential $W_{|T_G}$ to each chart in terms of matchings on the graph G, and observed that a procedure called positive tropicalization produces, when applied to $W_{|T_G}$, a rational polytope $\Delta_G(D_{FZ})$ which is an Okounkov body for a natural anti-canonical divisor $D_{FZ} \subset \mathrm{Gr}_k(n)$. For each k and n there is a special Okounkov body $\Delta_G(D_{FZ})$ the matches the Gelfand-Zetlin polytope Δ_{GZ}.

1.4. Results

The first step in the computation of the Fukaya category of Grassmannians is the description of its spectral decomposition. It is known (Theorem B.3.2) that the summand $\mathcal{F}_\lambda(\mathrm{Gr}_k(n))$ can be nonzero only if λ is an eigenvalue of the operator $c_1\star$ acting on $\mathrm{QH}(\mathrm{Gr}_k(n))$. We describe this spectrum below; see Figure 1.1 for some examples.

Proposition 1.4.1. *(3.1.4) The eigenvalues of $c_1\star$ acting on $\mathrm{QH}(\mathrm{Gr}_k(n))$ (evaluated at $q = 1$) are given by $n(\zeta_1 + \ldots + \zeta_k)$, with $\{\zeta_1, \ldots \zeta_k\}$ varying among the size k sets of roots of $x^n = (-1)^{k+1}$.*

In principle, one could use known combinatorial formulas for the quantum product of Schubert classes in $\mathrm{QH}(\mathrm{Gr}_k(n))$ to compute this spectrum in specific cases. Instead, we deduce the result in a uniform way for all Grassmannians, relying on the existence of a basis of quantum cohomology that simultaneously diagonalizes all operators of multiplication by a Schubert class; see Section 3.1 for more details. The existence of such basis seems to have been observed by physicists in the early days of quantum cohomology; we learned of it from a paper of Rietsch [67]. The cited paper does not spell out a proof of its remarkable property; we derive it in Lemma 3.1.3.

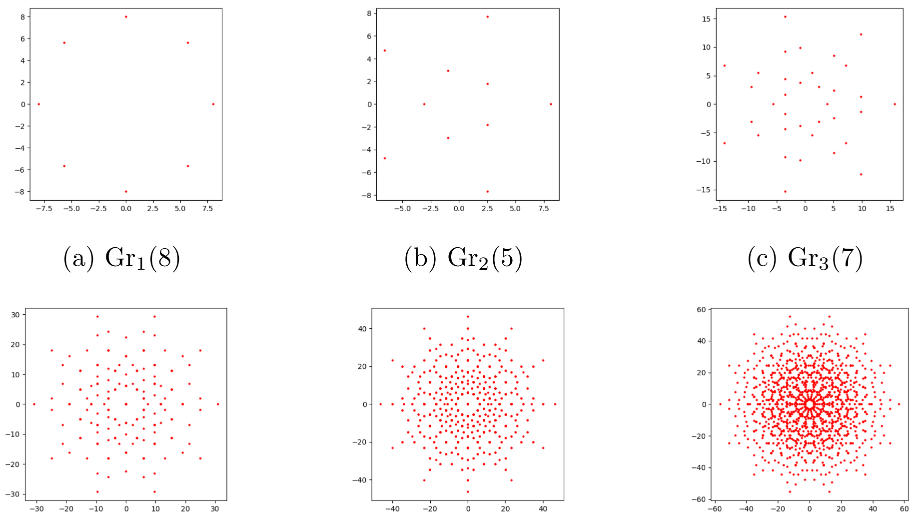

(a) $\mathrm{Gr}_1(8)$ (b) $\mathrm{Gr}_2(5)$ (c) $\mathrm{Gr}_3(7)$

(d) $\mathrm{Gr}_4(10)$ (e) $\mathrm{Gr}_6(12)$ (f) $\mathrm{Gr}_5(14)$

Figure 1.1: Eigenvalues of $c_1\star$ acting on $\mathrm{QH}(\mathrm{Gr}_k(n))$.

In Section 3.2 we focus on the monotone Lagrangian torus fiber of the Gelfand-Zetlin integrable system $L_{GZ} \subset \mathrm{Gr}_k(n)$ introduced by Guillemin-Sternberg [40]. From the work of Nishinou-Nohara-Ueda [58], it is known that its disk potential $W_{L_{GZ}}$ has one monomial for each codimension one face of Δ_{GZ}. We work out a more explicit formula.

Proposition 1.4.2. *(3.2.6) If $L_{GZ} \subset \mathrm{Gr}_k(n)$ is the Gelfand-Zetlin torus, its disk potential is*

$$W_{L_{GZ}} = \sum_{i=1}^{k-1}\sum_{j=1}^{n-k} \frac{x_{i,j}}{x_{i+1,j}} + \sum_{i=1}^{k}\sum_{j=1}^{n-k-1} \frac{x_{i,j+1}}{x_{i,j}} + \frac{1}{x_{1,n-k}} + x_{k,1} \quad .$$

The proof of this formula relies on a description of the face poset of Δ_{GZ} found by An-Cho-Kim [5] in terms of certain planar diagrams. Thinking of $\mathrm{Gr}_k(n)$ as a $U(n)$ coadjoint orbit in the space of $n \times n$ Hermitian matrices H, the Hamiltonians of the Gelfand-Zetlin system are eigenvalues of H and its minors, and their image is a convex polytope Δ_{GZ} cut out by interlacing inequalities among the eigenvalues of nested minors. The planar diagrams mentioned above roughly encode which of these inequalities are equalities in each face of the polytope.

The main goal of Chapter 3 is to investigate what nonzero objects of the Fukaya category are supported on the Lagrangian torus L_{GZ}. Recall that objects are of the form $(L_{GZ})_\xi$ for some rank one local system ξ on the torus. It is known that $HF((L_{GZ})_\xi) \neq 0$ if and only if the holonomies of ξ around a fixed basis of $H_1(L)$ give a critical point of the disk potential $W_{L_{GZ}}$ (Theorem B.3.3). Nishinou-Nohara-Ueda [58] proved that $W_{L_{GZ}}$ must have some critical point, but this is not sufficient to describe all critical points and study their critical values, which determine in which summand of the Fukaya category the object $(L_{GZ})_\xi$ lives. This is the first place where we take advantage of the Landau-Ginzburg model described by Marsh-Rietsch [53]; see Section 2.3.3 for the definition. The key observation is that, up to an automorphism of a complex torus, one has

$$W_{L_{GZ}} = W_{|T_{\mathcal{C}^R}} \quad ,$$

for a specific chart $T_{\mathcal{C}^R} \subset \mathcal{U}_{k,n}$ in the cluster structure of $\mathcal{U}_{k,n}$.

There are two obstacles to overcome to prove this equality. First, it is crucial to guess what the correct complex torus chart $T_{L_{GZ}} \subset \mathcal{U}_{k,n}$ corresponding to $L_{GZ} \subset \mathrm{Gr}_k(n)$ is, and the answer is the so called rectangular chart $T_{L_{GZ}} = T_{\mathcal{C}^R}$, which corresponds to the initial seed of the cluster structure of $\mathcal{U}_{k,n}$; see Section 3.3. In general there are many charts, and choosing a different one can lead to obstructions to the equality above; we return to this point in Chapter 4 of the thesis. The second obstacle is that the equality is not true on the nose, but only after an automorphisms of the complex torus chart; we work out this change of coordinates in Section 3.4. This step relies on the previous explicit formula for $W_{L_{GZ}}$ and the fact that $W_{|T_{\mathcal{C}^R}}$ has been computed by Marsh-Rietsch [53]. The unpleasant change of coordinates suggests that the Gelfand-Zetlin system, which is responsible for the choice of basis of $H_1(L_{GZ})$ used to write down $W_{L_{GZ}}$, is perhaps a bad choice from the point of view of mirror symmetry. In Chapter 4 of the thesis, the newly constructed Lagrangian tori will have instead canonical bases of cycles coming from the data of a toric degeneration of $\mathrm{Gr}_k(n)$, thus giving a geometric solution to the problem of fixing coordinates.

Once the equality $W_{L_{GZ}} = W_{|T_{\mathcal{C}^R}}$ is established, asking what nonzero objects of the

Fukaya category are supported on L_{GZ} becomes equivalent to understanding which of the critical points of the global potential $W \in \mathcal{O}(\mathcal{U}_{k,n})$ fall in the rectangular cluster chart $T_{\mathcal{C}^R} \subset \mathcal{U}_{k,n}$. The critical points of W are well understood, see e.g. Karp [42], and the condition of being contained in $T_{\mathcal{C}^R}$ can be rephrased in terms of vanishing of certain Schur polynomials at the roots of unity. This leads to the following theorems; compare Figure 1.2.

Theorem 1.4.3. *(3.4.4) The Gelfand-Zetlin torus L_{GZ} supports n objects that split-generate the summands $\mathcal{F}_\lambda(\mathrm{Gr}_k(n))$ with maximum $|\lambda|$.*

Theorem 1.4.4. *(3.4.6) The dihedral group D_n acts on the set of nonzero objects $(L_{GZ})_\xi$ supported on the Gelfand-Zetlin torus and*

$$(L_{GZ})_\xi \quad \text{in} \quad \mathcal{F}_\lambda(\mathrm{Gr}_k(n)) \implies g \cdot (L_{GZ})_\xi \quad \text{in} \quad \mathcal{F}_{g\cdot\lambda}(\mathrm{Gr}_k(n)) \quad \text{for all} \quad g \in D_n \quad ,$$

where the standard generators of D_n act on $\mathbb{C}$ via $r \cdot \lambda = e^{2\pi i/n}\lambda$ and $s \cdot \lambda = \overline{\lambda}$.

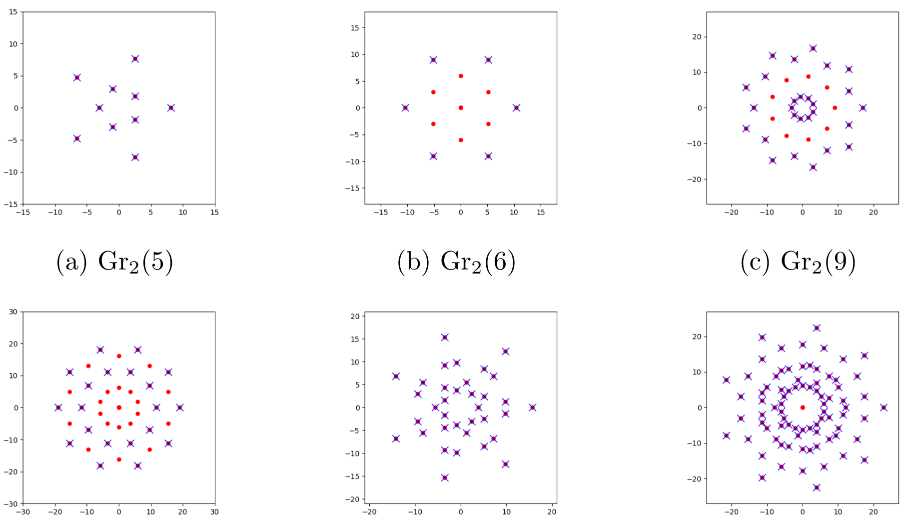

(a) $\mathrm{Gr}_2(5)$ (b) $\mathrm{Gr}_2(6)$ (c) $\mathrm{Gr}_2(9)$

(d) $\mathrm{Gr}_2(10)$ (e) $\mathrm{Gr}_3(7)$ (f) $\mathrm{Gr}_3(9)$

Figure 1.2: Summands of $\mathcal{F}(\mathrm{Gr}_k(n))$ containing objects supported on L_{GZ}.

While writing up these results, we realized that for $n = p$ prime the objects supported on L_{GZ} seemed to always cover all the summands in the spectral decomposition of the Fukaya category, or equivalently that all the critical points of W seemed to be contained in the chart $T_{\mathcal{C}^R} \subset \mathcal{U}_{k,n}$ in this case. Translating this observation into a statement about Schur polynomials at the roots of unity, it is indeed possible to prove it using Stanley's hook-content formula (Theorem 2.1.9).

Theorem 1.4.5. *(3.4.7) When $n = p$ is prime, the Fukaya category of $\mathrm{Gr}_k(p)$ is split-generated by objects supported on L_{GZ}, and for every $\lambda \in \mathbb{C}$ there is an equivalence of triangulated categories*

$$\mathbf{D}\mathcal{F}_\lambda(\mathrm{Gr}_k(p)) \simeq \mathbf{D}\mathcal{S}(W^{-1}(\lambda)) \quad .$$

The equivalence of triangulated categories above is the first instance in which Homological Mirror Symmetry is verified for an infinite class of Grassmannians (beyond projective spaces). Together with the observation, described above, that objects supported on L_{GZ} cover all summands of the spectral decomposition, the proof relies on a version of Abouzaid's generation criterion [1] established by Sheridan [77] for the monotone Fukaya category (Theorems B.3.4, B.3.5). The application of the criterion is particularly simple in this case, thanks to a lucky coincidence: when $n = p$ prime all the eigenvalues of $c_1\star$ acting on $\mathrm{QH}(\mathrm{Gr}_k(p))$ have multiplicity one; this is proved in Proposition 3.1.4.

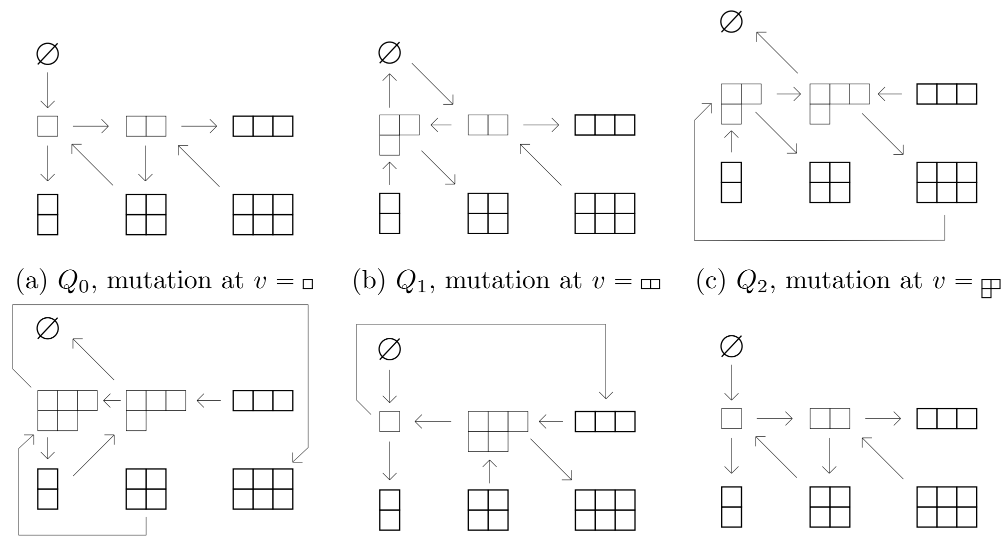

(a) Q_0, mutation at $v = \square$ (b) Q_1, mutation at $v = \square\square$ (c) Q_2, mutation at $v =$ (d) Q_3, mutation at $v =$ (e) Q_4, mutation at $v =$ (f) $Q_5 = Q_0$

Figure 1.3: A Plücker sequence of type $(2, 5)$ and length five. The labeling variables x_d on the nodes are replaced by d for notational convenience.

Starting from Chapter 4, we begin to take the cluster structure of the Landau-Ginzburg model $\mathcal{U}_{k,n}$ seriously, and consider its implications for the Fukaya category of $\mathrm{Gr}_k(n)$. The rectangular chart $T_{\mathcal{C}^R}$ is the first step of an iterative mutation procedure, that produces many other charts $T_{\mathfrak{s}}$ by quiver mutation in the sense of representation theory. At each step of a sequence $\mathfrak{s}$ of mutations, the initial Laurent polynomial $W_{\mathfrak{s}_0} = W_{|T_{\mathcal{C}^R}}$ evolves to become a new rational function $W_{\mathfrak{s}}$, obtained by composing $W_{\mathfrak{s}_0}$ with a sequence of birational maps of complex tori determined by the quivers; this procedure is described in detail in Section 4.1 and is best explained here by an example.

Example 1.4.6. Let $k = 2$ and $n = 5$. Figure 1.3 represents a sequence of mutations

$$\mathfrak{s} : (Q_0, W_0) \to (Q_1, W_1) \to (Q_2, W_2) \to (Q_3, W_3) \to (Q_4, W_4) \to (Q_5, W_5)$$

of length five, where the final step and the initial one coincide. At each step (Q_i, W_i), the graph Q_i is a quiver whose nodes are labeled by Plücker coordinates x_d for some collection of Young diagrams $d \subseteq 2 \times 3$, and W_i is a Laurent polynomial of the variables x_d. A mutation $(Q_i, W_i) \to (Q_{i+1}, W_{i+1})$ in the sequence consists in performing a quiver mutation at a mutable node v of Q_i as described in Section 4.1. This procedure changes the label $l(v)$ of the node v in Q_i to a new label $l'(v)$ of the same node in Q_{i+1}. The two labels are related by the following exchange relation: $l(v)l(v')$ is a sum of two terms, obtained by taking the product of labels $l(w)$ from incoming/outgoing nodes w adjacent to v respectively. The rational function W_{i+1} is obtained from W_i by using the previous relation to replace the label $l(v)$ with $l(v')$, and becomes Laurent modulo Plücker relations, i.e. when interpreted as element of the function field $\mathrm{Frac}(\mathcal{A}_{2,5}) = \mathbb{C}(\mathcal{U}_{2,5})$. The Laurent polynomials are:

$$W_0 = x_{\ydiagram{1}} + \frac{x_{\ydiagram{1,1}}}{x_{\ydiagram{1}}} + \frac{x_{\ydiagram{2,2}}x_{\varnothing}}{x_{\ydiagram{1}}x_{\ydiagram{2}}} + \frac{x_{\ydiagram{3,3}}x_{\varnothing}}{x_{\ydiagram{2}}x_{\ydiagram{3}}} + \frac{x_{\ydiagram{2}}}{x_{\ydiagram{3,3}}} + \frac{x_{\ydiagram{2}}}{x_{\ydiagram{1}}} + \frac{x_{\ydiagram{3}}}{x_{\ydiagram{2}}} + \frac{x_{\ydiagram{2,2}}x_{\varnothing}}{x_{\ydiagram{1}}x_{\ydiagram{1,1}}} + \frac{x_{\ydiagram{3,3}}x_{\ydiagram{1}}}{x_{\ydiagram{2}}x_{\ydiagram{2,2}}} \quad ;$$

$$W_1 = \frac{x_{\varnothing}x_{\ydiagram{2,2}}}{x_{\ydiagram{2,1}}} + \frac{x_{\ydiagram{2}}x_{\ydiagram{1,1}}}{x_{\ydiagram{2,1}}} + \frac{x_{\ydiagram{3,3}}x_{\varnothing}}{x_{\ydiagram{2}}x_{\ydiagram{2,1}}} + \frac{x_{\ydiagram{3,3}}x_{\ydiagram{1,1}}}{x_{\ydiagram{2,2}}x_{\ydiagram{2,1}}} + \frac{x_{\ydiagram{2,1}}}{x_{\ydiagram{2}}} + \frac{x_{\ydiagram{2,1}}}{x_{\ydiagram{1,1}}} + \frac{x_{\ydiagram{3,3}}x_{\varnothing}}{x_{\ydiagram{2}}x_{\ydiagram{3}}} + \frac{x_{\ydiagram{2}}}{x_{\ydiagram{3,3}}} + \frac{x_{\ydiagram{3}}}{x_{\ydiagram{2}}} \quad ;$$

$$W_2 = \frac{x_{\varnothing}x_{\ydiagram{3,3}}x_{\ydiagram{1,1}}}{x_{\ydiagram{3,1}}x_{\ydiagram{2,1}}} + \frac{x_{\varnothing}}{x_{\ydiagram{3,1}}} + \frac{x_{\ydiagram{3}}x_{\ydiagram{1,1}}}{x_{\ydiagram{3,1}}} + \frac{x_{\ydiagram{2,1}}x_{\ydiagram{3}}}{x_{\ydiagram{3,1}}x_{\ydiagram{3,3}}} + \frac{x_{\ydiagram{3,1}}}{x_{\ydiagram{2,1}}} + \frac{x_{\ydiagram{3,1}}}{x_{\ydiagram{3}}} + \frac{x_{\varnothing}x_{\ydiagram{2,2}}}{x_{\ydiagram{2,1}}} + \frac{x_{\ydiagram{3,3}}x_{\ydiagram{1,1}}}{x_{\ydiagram{2,2}}x_{\ydiagram{2,1}}} + \frac{x_{\ydiagram{2,1}}}{x_{\ydiagram{1,1}}} \quad ;$$

$$W_3 = \frac{x_{\varnothing}}{x_{\ydiagram{3,1}}} + \frac{x_{\ydiagram{3}}x_{\ydiagram{1,1}}}{x_{\ydiagram{3,1}}} + \frac{x_{\ydiagram{3,1}}}{x_{\ydiagram{3}}} + \frac{x_{\ydiagram{3,2}}x_{\varnothing}}{x_{\ydiagram{3,1}}} + \frac{x_{\ydiagram{3,2}}}{x_{\ydiagram{2,2}}} + \frac{x_{\ydiagram{1,1}}x_{\ydiagram{3}}}{x_{\ydiagram{3,2}}x_{\ydiagram{3,1}}} + \frac{x_{\ydiagram{3,3}}}{x_{\ydiagram{3,2}}} + \frac{x_{\ydiagram{2,2}}x_{\ydiagram{3}}}{x_{\ydiagram{3,2}}x_{\ydiagram{3,3}}} + \frac{x_{\ydiagram{3,1}}x_{\ydiagram{2,2}}}{x_{\ydiagram{3,2}}x_{\ydiagram{1,1}}} \quad ;$$

$$W_4 = \frac{x_{\ydiagram{3,2}}}{x_{\ydiagram{2,2}}} + \frac{x_{\ydiagram{3,3}}}{x_{\ydiagram{3,2}}} + \frac{x_{\ydiagram{2,2}}x_{\ydiagram{3}}}{x_{\ydiagram{3,2}}x_{\ydiagram{3,3}}} + \frac{x_{\ydiagram{1}}}{x_{\ydiagram{3,2}}} + x_{\ydiagram{1}} + \frac{x_{\varnothing}x_{\ydiagram{3,2}}}{x_{\ydiagram{1}}x_{\ydiagram{3}}} + \frac{x_{\varnothing}x_{\ydiagram{2,2}}}{x_{\ydiagram{1}}x_{\ydiagram{1,1}}} + \frac{x_{\ydiagram{1,1}}}{x_{\ydiagram{1}}} + \frac{x_{\ydiagram{3}}x_{\ydiagram{2,2}}}{x_{\ydiagram{1}}x_{\ydiagram{3,2}}} \quad .$$

By computing a few instances of $W_{\mathfrak{s}}$ in more examples, one quickly notices the following two general phenomena, which are not a direct consequence of the construction:

1. modulo Plücker relations, each $W_{\mathfrak{s}}$ is a Laurent polynomial ;

2. the coefficients of each Laurent polynomial $W_{\mathfrak{s}}$ are natural numbers .

Property (1) is related to the Laurent phenomenon of cluster algebras in the sense of Fomin-Zelevinsky [26]. Think each x_d as a Plücker coordinate on the dual Grassmannian $\mathrm{Gr}_k^{\vee}(n) = \mathrm{Gr}_{n-k}(n) \subset \mathbb{P}^{\binom{n}{k}-1}$ in its Plücker embedding; the definition of Plücker coordinate is recalled in Definition 2.2.1. Each Plücker sequence $\mathfrak{s}$ singles out an open algebraic torus chart $T_{\mathfrak{s}} \subset \mathcal{U}_{k,n}$, and the global regular functions $\mathcal{A}_{k,n} = \mathcal{O}(\mathcal{U}_{k,n})$ form a cluster algebra; see Scott [74]. In fact, Marsh-Rietsch [53] prove that each $W_{\mathfrak{s}}$ is the restriction $W_{\mathfrak{s}} = W_{|T_{\mathfrak{s}}}$ of the Landau-Ginzburg potential $W \in \mathcal{A}_{k,n}$ to the corresponding cluster chart $T_{\mathfrak{s}}$, and in particular it is a regular function on that chart. Property (2) is related to positivity of cluster algebras, which has been proved by Gross-Hacking-Keel-Kontsevich [35]. Their proof consists in interpreting the coefficients as generating functions of tropical curves called broken lines. Broken lines are expected to correspond to the holomorphic disks of Symplectic Topology. The key observation for us is that, for certain sequences $\mathfrak{s}$, each step of this process produces a Lagrangian torus $L_{\mathfrak{s}} \subset \mathrm{Gr}_k(n)$ with a basis of cycles $\gamma_d \in H_1(L_{\mathfrak{s}})$ labeled by a collection of Young diagrams d in the $k \times (n-k)$ grid.

This is how the construction goes. It is known from the work of Rietsch-Williams [70] that each step of $\mathfrak{s}$ produces a degeneration $\mathrm{Gr}_k(n) \rightsquigarrow X(\Sigma_{\mathfrak{s}})$ of the Grassmannian to a toric variety with polyhedral fan $\Sigma_{\mathfrak{s}}$. The limit toric variety is typically singular, and the fan $\Sigma_{\mathfrak{s}}$ is made up of cones over the faces of the Newton polytope $\mathrm{Newt}(W_{\mathfrak{s}})$ of the Laurent polynomial $W_{\mathfrak{s}}$; see Definition 4.2.1 for the precise meaning of the word degeneration. From this degeneration data one gets an open set $U_{\mathfrak{s}} \subset \mathrm{Gr}_k(n)$ (in the analytic topology) carrying a regular Lagrangian torus fibration, obtained by deforming the one given by the moment map on the maximal torus orbit of $X(\Sigma_{\mathfrak{s}})$. The Lagrangian torus $L_{\mathfrak{s}} \subset U_{\mathfrak{s}} \subset \mathrm{Gr}_k(n)$ is a particular torus in this fibration. This construction and the extension of this fibration to a completely integrable system away from $U_{\mathfrak{s}}$ has been investigated in great generality by Harada-Kaveh [41], and essentially is available whenever the degeneration comes from the Okounkov body of an ample divisor on a projective variety; see Section 1.5 for more on this.

A result of Nishinou-Nohara-Ueda [58] gives a general sufficient condition for the the Laurent polynomials $W_{\mathfrak{s}}$ to be the disk potentials of the corresponding Lagrangian tori $L_{\mathfrak{s}} \subset \mathrm{Gr}_k(n)$, which also implies monotonicity of $L_{\mathfrak{s}}$. The condition involves the existence of a small toric resolution for the singular toric variety $X(\Sigma_{\mathfrak{s}})$; see Definition 4.2.9. Due to the combinatorial nature of toric varieties, for any given sequence $\mathfrak{s}$ one can check this condition in finitely many steps. In Section 4.3 we use this to describe a sample application in the smallest example not accessible by previous techniques.

Theorem 1.4.7. *(see Theorem 4.3.15) The Grassmannian* $\mathrm{Gr}_3(6)$ *contains* 6 *monotone Lagrangian tori that are not displaceable nor equivalent under Hamiltonian isotopy.*

We call these tori exotic, because only one monotone torus was previously known: the Gelfand-Zetlin torus. The new examples are of the form $L_{\mathfrak{s}}$ for some sequence of mutations $\mathfrak{s}$, and are distinguished by a combination of two invariants: the number of critical points of their disk potential $W_{L_{\mathfrak{s}}}$ and the f-vector of its Newton polytope. This strategy applies without modification to arbitrary Grassmannians, as long as one can check that $X(\Sigma_{\mathfrak{s}})$ has a small resolution. Even when this is not true (we could not find examples), the positivity of the coefficients of $W_{\mathfrak{s}}$ suggests an enumerative interpretation in terms of counts of holomorphic disks with boundary on $L_{\mathfrak{s}}$; see Section 1.5 for a possible interpretation of the symplectic meaning of these Laurent polynomials.

For $k = 1$ one has projective spaces $\mathrm{Gr}_1(n) = \mathbb{P}^{n-1}$, and there is only one Plücker sequence $\mathfrak{s}$ of lenght 0; in this case $W_{\mathfrak{s}}$ is the disk potential of the moment map fiber known to generate the Fukaya category. For $k = 2$ the construction recovers a different one studied by Nohara-Ueda [60] mentioned in Section 1.3 and corresponding to triangulations of the n-gon; the relation is explained in Lemma 4.3.3, which also implies that all toric degenerations have small resolutions when $k = 2$ and the tori $L_{\mathfrak{s}} \subset \mathrm{Gr}_2(n)$ are all monotone. Definition 4.2.5 introduces some natural local systems supported on the Lagrangian tori $L_{\mathfrak{s}} \subset \mathrm{Gr}_k(n)$, that are controlled by the values of k-variables Schur polynomials at certain roots of unity. When $k = 2$, we show that the corresponding objects generate the Fukaya category $\mathcal{F}(\mathrm{Gr}_2(n))$ in examples where objects supported on the Gelfand-Zetlin torus alone fail to do so.

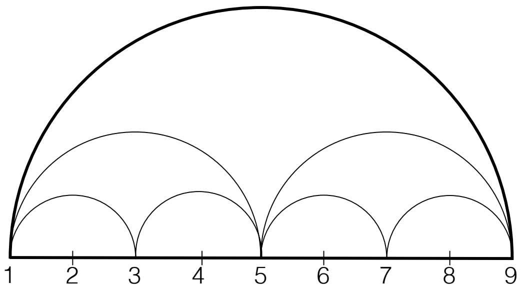

Figure 1.4: The dyadic triangulation of an 9-gon.

Theorem 1.4.8. *(4.3.7) If $n = 2^t + 1$ for some $t \in \mathbb{N}^+$, the derived Fukaya category $\mathbf{D}\mathcal{F}(\mathrm{Gr}(2, 2^t + 1))$ is split-generated by objects supported on a single Plücker torus.*

The Lagrangian torus in the statement is associated to a special triangulation of the n-gon, that we call dyadic; see Figure 1.4 for an example. In fact, Section 4.3 contains a criterion to prove generation of $\mathcal{F}(\mathrm{Gr}_2(n))$ by objects supported on any number of tori $L_{\mathfrak{s}} \subset \mathrm{Gr}_2(n)$, whenever n is odd. The criterion is based on a construction of triangulations of the n-gon whose sides lengths avoid the prime numbers appearing in the factorization of n; see Figure 1.5 for an example.

Theorem 1.4.9. *(4.3.10) Let $n > 2$ be odd, and consider its prime factorization $n = p_1^{e_1} \cdots p_l^{e_l}$. If for all $1 \leqslant i \leqslant l$ there exists a triangulation Γ_i of $[n]$ that is p_i-avoiding, then $\mathbf{D}\mathcal{F}(\mathrm{Gr}(2, n))$ is split generated by objects supported on l Plücker tori.*

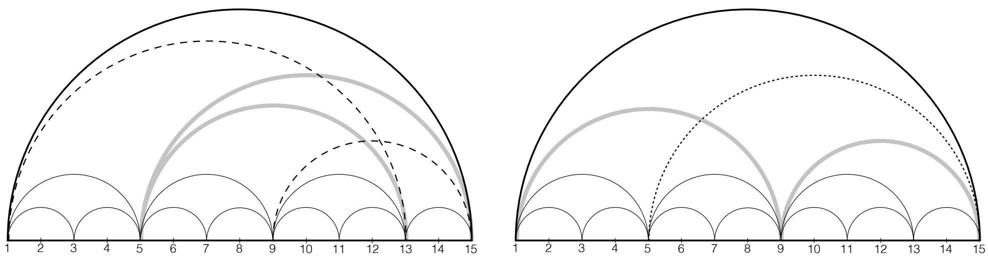

(a) 3-avoiding triangulation (b) 5-avoiding triangulation

Figure 1.5: Two triangulations of a 15-gon.

These results seem to suggest that objects supported on the tori $L_{\mathfrak{s}}$ could generate $\mathcal{F}(\mathrm{Gr}_k(n))$ in general, although generation over $\mathbb{C}$ has a subtle relation with the location of the critical points of $W \in \mathcal{A}_{k,n}$ relative to the torus charts $T_{\mathfrak{s}} \subset \mathcal{U}_{k,n}$. For example, split-generation over $\mathbb{C}$ fails for $\mathrm{Gr}_2(4)$, where W has two critical points in a complex codimension 2 locus of $\mathcal{U}_{k,n}$ which is not covered by cluster charts. We plan to investigate in a separate work how the situation changes when working over the Novikov field $\Lambda_{\mathbb{C}}$ instead and considering bulk-deformations of the Fukaya category in the sense of Fukaya-Oh-Ohta-Ono [28], which categorifies big as opposed to small quantum cohomology.

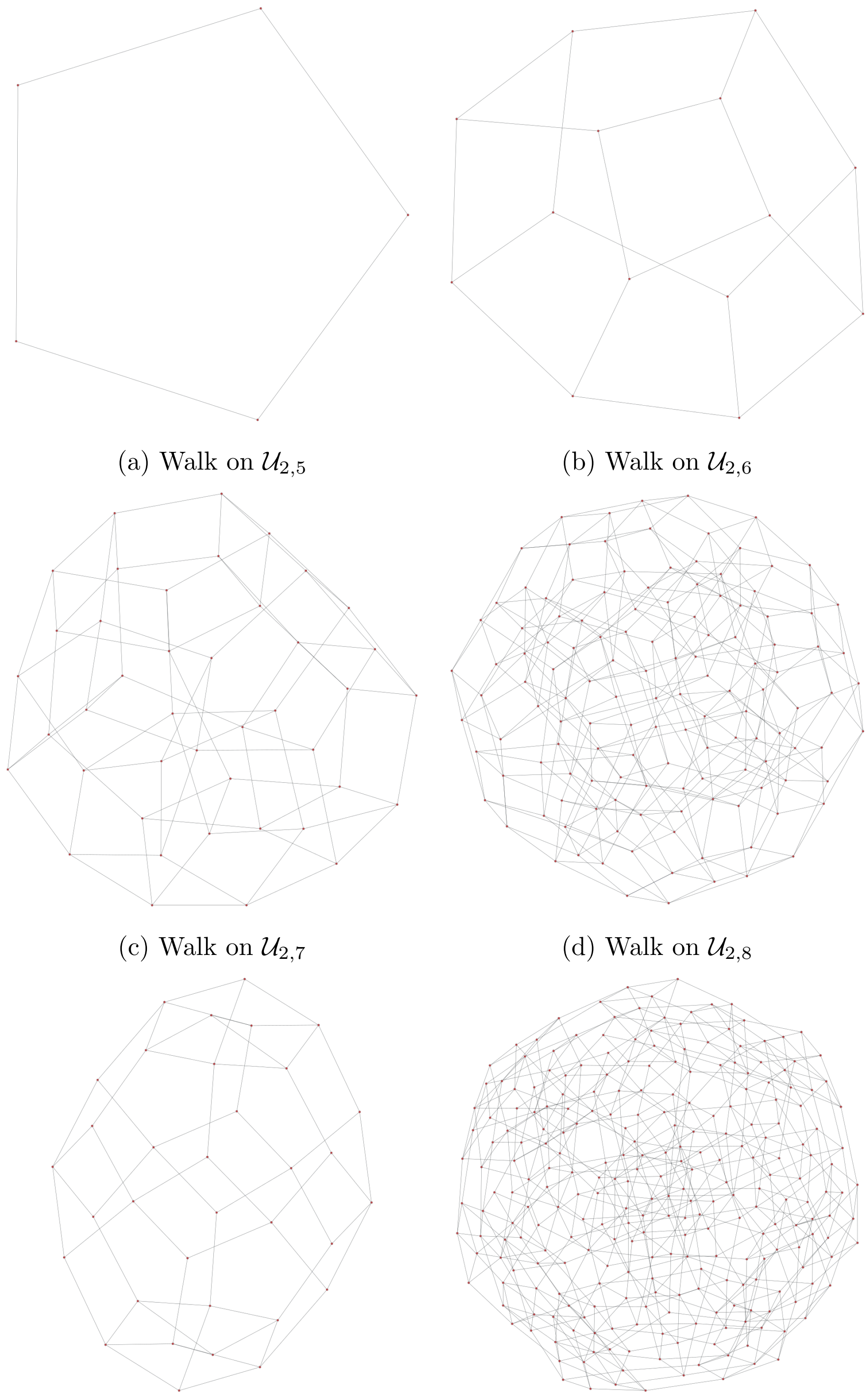

(a) Walk on $\mathcal{U}_{2,5}$ (b) Walk on $\mathcal{U}_{2,6}$

(c) Walk on $\mathcal{U}_{2,7}$ (d) Walk on $\mathcal{U}_{2,8}$

(e) Walk on $\mathcal{U}_{3,6}$ (f) Walk on $\mathcal{U}_{3,7}$

Figure 1.6: Random walk on the cluster graph

The iterative description of the Laurent polynomials $W_\mathfrak{s}$ makes them particularly suitable for computations. Starting from the disk potential of the Gelfand-Zetlin torus, at each step of the mutation process one has finitely many ways to choose how to proceed, encoded by the choice of mutable node of the quiver $Q_\mathfrak{s}$. One can perform this choice uniformly at random at each step, thus obtaining a random walk on the cluster graph, whose nodes are the complex torus charts $T_\mathfrak{s} \subset \mathcal{U}_{k,n}$ and whose edges are mutations. Figure 1.6 represent (typically partial) explorations of the cluster graph for small Grassmannians.

In Chapter 5, we implement this random walk in the programming language Python. The code also relies on some modules from the open-source project SageMath. At each step of the random walk, the algorithm allows to perform the following tasks:

- compute the Laurent polynomial $W_\mathfrak{s} = W_{|T_\mathfrak{s}}$;
- compute the Newton polytope $\mathrm{Newt}(W_\mathfrak{s})$ and its f-vector, its Ehrhart polynomial, whether it is reflexive or not ;
- compute the fan of the toric variety $X(\Sigma_\mathfrak{s})$ obtained as limit of the degeneration $\mathrm{Gr}_k(n) \rightsquigarrow X(\Sigma_\mathfrak{s})$;
- count the critical points of W contained in the cluster chart $T_\mathfrak{s}$, and compute their critical values .

1.5. Future directions

This thesis ends with a puzzling question. The construction of the Lagrangian tori $L_\mathfrak{s} \subset \mathrm{Gr}_k(n)$ works with no assumptions, and one can easily attach to them Laurent polynomials $W_\mathfrak{s}$ with remarkably positive integer coefficients, explicitly computable using the random walk of Chapter 5. Recall that the Laurent polynomial $W_\mathfrak{s}$ computes the Gromov-Witten disk potential $W_{L_\mathfrak{s}}$ of $L_\mathfrak{s} \subset \mathrm{Gr}_k(n)$ whenever $X(\Sigma_\mathfrak{s})$ has a small toric resolution. This naturally rises the following.

Question 1.5.1. *If $X(\Sigma_\mathfrak{s})$ does not have a small toric resolution, does $W_\mathfrak{s}$ encode any symplectic information about the Lagrangian embedding $L_\mathfrak{s} \subset \mathrm{Gr}_k(n)$?*

One tempting guess is that $W_\mathfrak{s}$ encodes counts of holomorphic disks in the singular variety $X(\Sigma_\mathfrak{s})$. For example, Cho-Poddar [18] developed a notion of holomorphic disk in a toric orbifold. However, typically $\Sigma_{\mathfrak{s}}$ is not simplicial, so that $X(\Sigma_{\mathfrak{s}})$ is not an orbifold in a canonical way. Moreover, even for simplicial $\Sigma_{\mathfrak{s}}$ it is not clear how orbifold disks on a moment fiber of $X(\Sigma_{\mathfrak{s}})$ are supposed to relate to holomorphic disks in X with boundary on $L_{\mathfrak{s}}$.

We propose a different point of view. The toric divisor endows any toric variety $X(\Sigma_{\mathfrak{s}})$ with a natural logarithmic structure in the sense of Kato [43, 44], which makes it log-smooth. This weaker smoothness condition is known to be the right generality in which closed Gromov-Witten invariants can be defined by algebraic means; for the foundations of logarithmic Gromov-Witten theory see Gross-Siebert [39] and Abramovich-Chen [15, 3]. Logarithmic structures are a key ingredient in the Gross-Siebert program [36, 37, 38]. There should be a notion of logarithmic disk with boundary on a Lagrangian moment fiber of a Fano projective toric variety $X(\Sigma_{\mathfrak{s}})$ with arbitrary singularities.

The Fano condition should allow to write down a natural Liouville domain $W(\Sigma_{\mathfrak{s}}) \subset X(\Sigma_{\mathfrak{s}})$ which is disjoint from the toric divisor, and in which the moment fiber of interest becomes exact. Crucially, the dynamics of the Reeb vector field on the contact boundary $\partial W(\Sigma_{\mathfrak{s}})$ reflects the combinatorial data of $\Sigma_{\mathfrak{s}}$, or equivalently the intersection data of the components of the toric divisor at infinity in $X(\Sigma_{\mathfrak{s}})$. Lattice points in the cones of $\Sigma_{\mathfrak{s}}$ should parametrize pseudo Morse-Bott families or Reeb orbits in $\partial W(\Sigma_{\mathfrak{s}})$ in the sense of McLean [56] whose dimension depends on the dimension of the cone and whose Conley-Zehnder index depends on the point. In this setting, a natural notion of logarithmic disk is that of holomorphic half-cylinder with boundary on the Lagrangian torus and asymptotic to a Reeb orbit in one of these families. One technical difficulty is that the toric divisor is not normal crossing for arbitrary $\Sigma_{\mathfrak{s}}$, so one has to adapt the techniques available in the literature to this case, which is both more general due to the singularities and less general due to the torus symmetry.

Using the data of the degeneration $\mathrm{Gr}_k(n) \rightsquigarrow X(\Sigma_{\mathfrak{s}})$, one can think $W(\Sigma_{\mathfrak{s}}) \subset U_{\mathfrak{s}} \subset \mathrm{Gr}_k(n)$ as a Liouville subdomain of the original manifold, and $L_{\mathfrak{s}} \subset W(\Sigma) \subset \mathrm{Gr}_k(n)$ as a Lagrangian torus that becomes exact in this Liouville domain, so that every holomorphic disk in $\mathrm{Gr}_k(n)$ with boundary on $L_{\mathfrak{s}}$ must cross the contact hypersurface $\partial W(\Sigma_{\mathfrak{s}}) \subset \mathrm{Gr}_k(n)$. After applying neck-stretching in the sense of Symplectic Field Theory, any rigid holomorphic disk in the ambient will have a trace in the Liouville domain which is a rigid logarithmic disk.

Conjecture 1.5.2. *The Laurent polynomial $W_{\mathfrak{s}}$ is the generating function of rigid logarithmic disks in $W(\Sigma_{\mathfrak{s}})$ with boundary on $L_{\mathfrak{s}}$, obtained by neck-stretching of ambient rigid holomorphic disks along the contact hypersurface $\partial W(\Sigma_{\mathfrak{s}})$. The data of the fan $\Sigma_{\mathfrak{s}}$ determines a symplectic cohomology class $\mathcal{BS}_{\mathfrak{s}} \in \mathrm{SH}(W(\Sigma_{\mathfrak{s}}))$ such that*

$$W_{\mathfrak{s}} = \mathrm{CO}_{L_{\mathfrak{s}}}(\mathcal{BS}_{\mathfrak{s}}) \quad .$$

In the conjecture above, the map $\mathrm{CO}_{L_{\mathfrak{s}}} : \mathrm{SH}(W(\Sigma_{\mathfrak{s}})) \to \mathrm{HF}_{W(\Sigma_{\mathfrak{s}})}(L_{\mathfrak{s}})$ is the closed-open map from symplectic cohomology of the Liouville domain $W(\Sigma_{\mathfrak{s}})$ to Lagrangian Floer cohomology of the exact Lagrangian torus $L_{\mathfrak{s}} \subset W(\Sigma_{\mathfrak{s}})$ (compare Tonkonog [81]).

There should also be an open-string analogue of the result of Abramovich-Wise [4], who showed that closed logarithmic Gromov-Witten invariants do not change under logarithmic modifications, a class of birational transformations of the target that includes mutations coming from cluster algebras. In our setting, we expect that if $\mathrm{Gr}_k(n) \rightsquigarrow X(\Sigma_{\mathfrak{s}}), X(\Sigma_{\mathfrak{s}'})$ are two toric degenerations associated to cluster charts $T_{\mathfrak{s}}, T_{\mathfrak{s}'} \subset \mathcal{U}_{k,n}$ related by a single mutation $\phi_{\mathfrak{s},\mathfrak{s}'} : T_{\mathfrak{s}} \dashrightarrow T_{\mathfrak{s}'}$ then the birational relation

$$W_{\mathfrak{s}} = \phi^*_{\mathfrak{s},\mathfrak{s}'} W_{\mathfrak{s}'}$$

should be the special case of a more general phenomenon. Thinking $W(\Sigma_{\mathfrak{s}})$ as a Lagrangian torus fibration over a smoothing of the Okounkov body $\Delta_{\mathfrak{s}}(D_{FZ})$, the birational map $\phi_{\mathfrak{s},\mathfrak{s}'}$ is known to induce a piece-wise linear homeomorphism $\mathrm{Trop}(\phi_{\mathfrak{s},\mathfrak{s}'}) : \Delta_{\mathfrak{s}}(D_{FZ}) \to \Delta_{\mathfrak{s}'}(D_{FZ})$ by tropicalization. We expect this to induce a map between $\mathrm{SH}(W(\Sigma_{\mathfrak{s}}))$ and $\mathrm{SH}(W(\Sigma_{\mathfrak{s}'}))$ which intertwines the classes $\mathcal{BS}_{\mathfrak{s}}$ and $\mathcal{BS}_{\mathfrak{s}'}$. This map should be highly structured: perhaps already defined at the chain level, and a map of L_∞-algebras.

In our view, this approach has the potential not only to clarify the meaning of the Laurent polynomials $W_{\mathfrak{s}}$, but also suggest a path to develop a purely symplectic framework for wall-crossing formulas of disk potentials of Lagrangian tori in Fano manifolds. As explained by Kaveh-Manon [46], if D is an anti-canonical divisor in a Fano manifold X, one has a natural class of Okounkov bodies $\Delta_c(D)$ parametrized by certain cones c in the tropicalization $\mathrm{Trop}(X)$ of X; see for example Kaveh-Khovanskii [45] for the general theory of Okounkov bodies. Two cones $c, c' \subset \mathrm{Trop}(X)$ are adjacent if they share a codimension one wall. The piece-wise linear map tropicalizing cluster mutations in the discussion above has an analogue in this generality, i.e. a piece-wise linear homeomorphism mapping the Okounkov body $\Delta_c(D)$ to $\Delta_{c'}(D)$; see Escobar-Harada [25]. It is known that each Okounkov body $\Delta_c(D)$ produces a toric degeneration $X \rightsquigarrow X(\Sigma^n \Delta_c(D))$ to the toric variety whose fan is the normal fan of $\Delta_c(D)$ (see [46] and references therein). From the work of Harada-Kaveh [41], one then gets Lagrangian tori $L_{\mathfrak{s}} \subset X$ corresponding to each Okounkov body, and one can draw inspiration from Conjecture 1.5.2 to prove that $\Sigma_{\mathfrak{s}}$ determines a symplectic cohomology class $\mathcal{BS}_{\mathfrak{s}} \in \mathrm{SH}(W(\Sigma_{\mathfrak{s}}))$ and this time use the equation

$$W_{\mathfrak{s}} = \mathrm{CO}_{L_{\mathfrak{s}}}(\mathcal{BS}_{\mathfrak{s}})$$

as a definition rather than proving it as a theorem (since a global Landau-Ginzburg potential $W \in \mathcal{O}(X^\vee)$ such that $W_{|T_{\mathfrak{s}}} = W_{\mathfrak{s}}$ is not known in this generality).

Chapter 2

PREPARATION

In this chapter, we introduce some notations and conventions used in the rest of the thesis. After reviewing Young diagrams and Schur polynomials, we recall some classical facts about complex Grassmannians and describe a Landau-Ginzburg model proposed by Marsh-Rietsch [53].

2.1. Young diagrams and their relatives

Throughout this document, k and n are integers with $1 \leqslant k < n$, and $N = k(n-k)$.

Definition 2.1.1. *The symbol $d = (d_1, \ldots, d_k)$ denotes a Young diagram in the $k \times (n-k)$ grid, obtained by placing d_i consecutive boxes in the i-th row for all $1 \leqslant i \leqslant k$, starting from the left in each row and with $d_1 \geqslant d_2 \geqslant \cdots \geqslant d_k$.*

Example 2.1.2. If $k = 2$ and $n = 5$, the diagrams $d \subseteq 2 \times 3$ are:

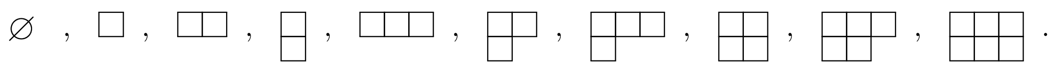

Sometimes it is useful to think of d as a subset of $\{1, \ldots, n\} = [n]$, in which case $d^{|}$ denotes the size k set of the vertical steps, and d^{-} the size $n-k$ set of horizontal steps. The steps of a diagram are counted from the top-right corner of the grid to the bottom-left, following the part of the border of d in the interior of the grid.

Example 2.1.3. Let $k = 3$ and $n = 8$. Then $d = (3, 2, 0)$ denotes a Young diagram. The vertical steps are $d^{|} = \{3, 5, 8\}$, and the horizontal steps are $d^{-} = \{1, 2, 4, 6, 7\}$. These sets are computed by placing d in the 3×5 grid as follows:

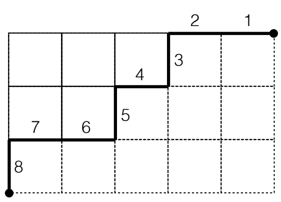

The transpose d^T of Young diagram d is a diagram in the $(n-k)\times k$ grid, obtained by transposing d. The Poincaré dual $PD(d)$ is a diagram in the $k\times(n-k)$ grid obtained by taking the complement of d and rotating by π to place it in the top left corner.

Example 2.1.4. Let $k=3$ and $n=7$. An example of Young diagram and its Poincaré dual in the 3×4 grid is given by

$$d = \begin{array}{|c|c|c|c|}\hline & & & \\ \hline & & & \multicolumn{1}{c}{} \\ \cline{1-3} \end{array} \quad \text{and} \quad \mathrm{PD}(d) = \begin{array}{|c|c|c|c|}\hline & & & \\ \hline & \multicolumn{3}{c}{} \\ \cline{1-1} \end{array} \quad .$$

Definition 2.1.5. *To each d in $k\times(n-k)$ associate a symmetric polynomial in k variables, called Schur polynomial of d, and defined as*

$$S_d(z_1,\dots,z_k) = \sum_{T_d} z_1^{t_1}\cdots z_k^{t_k} \quad .$$

The sum is over semi-standard Young tableau on the diagram d, obtained by filling d with labels $\{1,\dots,k\}$ in such a way that rows are weakly increasing and columns are strictly increasing. The exponent t_i of z_i records the number of occurrences of the label i.

Example 2.1.6. The following is an example with $k=2$:

$$d = \begin{array}{|c|c|c|}\hline & & \\ \hline & \multicolumn{2}{c}{} \\ \cline{1-1} \end{array} \quad ; \quad T_d = \begin{array}{|c|c|c|}\hline 1 & 1 & 1 \\ \hline 2 & \multicolumn{2}{c}{} \\ \cline{1-1} \end{array} \quad , \quad \begin{array}{|c|c|c|}\hline 1 & 1 & 2 \\ \hline 2 & \multicolumn{2}{c}{} \\ \cline{1-1} \end{array} \quad , \quad \begin{array}{|c|c|c|}\hline 1 & 2 & 2 \\ \hline 2 & \multicolumn{2}{c}{} \\ \cline{1-1} \end{array} \quad .$$

The corresponding Schur polynomial is $S_{\tiny\yng(3,1)}(z_1,z_2) = z_1^3 z_2 + z_1^2 z_2^2 + z_1 z_2^3$.

Definition 2.1.7. *If u is a box of the Young diagram d at entry (s,t) of the $k\times(n-k)$, define its content as $c(u)=t-s$ and its hook length $h(u)$ as the number of boxes of d below and to the right of u (with u itself counted once).*

Example 2.1.8. For $k=4$ and $n=8$, consider the Young diagram $d=(4,4,3,1)$ in the 4×4 grid. A box $u\in d$ has coordinates $u=(s,t)$, with $1\leqslant s\leqslant 4$ counting the row of the grid (from the top) and $1\leqslant t\leqslant 4$ counting the column (from the left). In the following pictures, each box $u\in d$ is filled with the corresponding values of $c(u)$ and $h(u)$ respectively:

$$c(u) = \begin{array}{|c|c|c|c|} \hline 0 & 1 & 2 & 3 \\ \hline -1 & 0 & 1 & 2 \\ \hline -2 & -1 & 0 & \\ \cline{1-3} -3 & & & \\ \cline{1-1} \end{array} \quad , \quad h(u) = \begin{array}{|c|c|c|c|} \hline 7 & 5 & 4 & 2 \\ \hline 6 & 4 & 3 & 1 \\ \hline 4 & 2 & 1 & \\ \cline{1-3} 1 & & & \\ \cline{1-1} \end{array} \quad .$$

Fixing d, one has an explicit formula for the number of semi-standard tableaux T_d on the diagram d, known as hook-content formula.

Theorem 2.1.9. *(Stanley [79, Theorem 15.3])*

$$\#\{T_d\} = \prod_{u \in d} \frac{k + c(u)}{h(u)} \quad .$$

Remark 2.1.10. The hook-content formula above can be obtained from [79, Theorem 15.3] by setting $x = 1$ in the generating function $H_m(\lambda)(x)$ of column-strict plane partitions of shape λ and largest part $\leqslant m$. In our notation λ is the Young diagram d in the $k \times (n-k)$ grid and $m = k$. In Stanley's terminology, what we call semi-standard Young tableau corresponds to a column-strict plane partition with shape λ and parts (or labels) in $S = \{1, \ldots, k\}$. The correspondence is given by converting each label l in the Young tableau to the label $k+1-l$ of the corresponding plane partition, so that the result has strictly decreasing columns and weakly decreasing rows. Also observe that Stanley's definiton of Schur function $e_\lambda(z_1, \ldots, z_k)$ in terms of plane partitions with shape λ agrees with our $S_\lambda(z_1, \ldots, z_k)$ defined in terms of tableaux on λ because

$$S_\lambda(z_1, \ldots, z_k) = e_\lambda(z_k, \ldots, z_1) = e_\lambda(z_1, \ldots, z_k) \quad ,$$

where the last equality holds because Schur polynomials are symmetric.

The following algebraic equation depending on k and n will often appear in this document:

$$\zeta^n = (-1)^{k+1} \ , \quad \zeta \in \mathbb{C} \quad .$$

If I is any of the $\binom{n}{k}$ sets of k distinct roots of the equation, denote I^c the set of $n-k$ roots not in I, and observe that $I^\vee = e^{\pi i} I^c$ is a set of $n-k$ distinct roots of the equation $\zeta^n = (-1)^{n-k+1}$ obtained by replacing k with $n-k$ in the one above. Denote I_0 the set of k roots closest to 1. Since the Schur polynomials S_d are symmetric functions, it makes sense to evaluate them at sets I in any order, so denote $S_d(I) \in \mathbb{C}$ the corresponding number. If $I = \{\zeta_1, \dots, \zeta_k\}$ denote $|\operatorname{Van}(I)| = \prod_{i<j} |\zeta_i - \zeta_j|$.

We collect here some useful facts about Schur polynomials evaluated at roots of unity.

Proposition 2.1.11. *(Rietsch [67, Proposition 4.3, Lemma 4.4, Proposition 11.1])*

1. $S_{PD(d)}(I) = \overline{S_d(I)} S_{k\times(n-k)}(I)$;
2. $\sum_d S_d(I_1)\overline{S_d(I_2)} = \frac{n^k}{\operatorname{Van}(I_1)} \delta_{I_1,I_2}$;
3. $S_d(I) = S_{d^T}(I^\vee)$;
4. $|S_d(I)| \leqslant |S_d(I_0)|$.

2.2. Classical facts about Grassmannians

A full rank $k \times n$ matrix M determines an k-dimensional linear subspace of $\mathbb{C}^n$ by taking its row-span. Denote $[M]$ the equivalence class of M modulo row operations. This defines a point in the complex Grassmannian $[M] \in \operatorname{Gr}_k(n)$. Similarly, a full rank $n \times (n-k)$ matrix $M^\vee$ defines a point of the dual Grassmannian $[M^\vee] \in \operatorname{Gr}_k^\vee(n) = \operatorname{Gr}_{n-k}(n)$.

Definition 2.2.1. *If d is a Young diagram in the $k \times (n-k)$ grid, the determinant of M at columns $d^|$ is denoted $x_d(M)$ and called Plücker coordinate corresponding to d. Analogously, $x_d(M^\vee)$ is the determinant of $M^\vee$ at rows d^-.*

After choosing an order on the set of Young diagrams, the Plücker coordinates define projective embeddings of $\operatorname{Gr}_k(n)$ and $\operatorname{Gr}_k^\vee(n)$ in $\mathbb{P}^{\binom{n}{k}-1}$. Denote $\mathcal{I}_{k,n} \subset \mathbb{C}[x_d \ : \ d \subseteq k \times (n-k)]$ the homogeneous ideal of $\operatorname{Gr}_k^\vee(n)$, and think of each x_d as an element of the algebra $\mathcal{A}_{k,n} = \mathbb{C}[x_d \ : \ d \subseteq k \times (n-k)]/\mathcal{I}_{k,n}$ of regular functions of the affine cone over $\operatorname{Gr}_k^\vee(n)$.

Grassmannians have a stratification indexed by Young diagrams $\operatorname{Gr}_k(n) = \bigsqcup_d \Omega_d$, where Ω_d is the set of $[M] \in \operatorname{Gr}_k(n)$ whose reduced echelon form, computed by Gaussian elimination, has the $k \times k$ identity matrix at columns $d^|$.

Definition 2.2.2. *These sets Ω_d are Zariski locally closed and, since $\Omega_d \cong \mathbb{C}^{N-|d|}$, they are called Schubert cells. Zariski closure produces a collection of (generally singular) algebraic cycles $X_d = \overline{\Omega_d}$ whose Poincaré dual classes $\sigma_d \in H^{2|d|}(\operatorname{Gr}_k(n))$, called Schubert* *classes, form a basis of cohomology.*

2.3. A gift from representation theory

Definition 2.3.1. *For $1 \leqslant i \leqslant n$ denote d_i the Young diagram whose vertical steps $d_i^{|}$ are cyclic shifts by i (modulo n) of $\{1, \dots, k\}$. These diagrams are called frozen.*

Example 2.3.2. The frozen diagrams for $k = 2$ and $n = 5$ are:

$$d_1 = \ydiagram{2,2} \quad , \quad d_2 = \ydiagram{1,1} \quad , \quad d_3 = \varnothing \quad , \quad d_4 = \ydiagram{3} \quad , \quad d_5 = \ydiagram{3,3} \quad ;$$

their vertical steps are $d_1^{|} = \{2,3\}$, $d_2^{|} = \{3,4\}$, $d_3^{|} = \{4,5\}$, $d_4^{|} = \{1,5\}$, $d_5^{|} = \{1,2\}$.

The divisor

$$D_{FZ} = \{ \, [M] \in \mathrm{Gr}_k(n) \; : \; x_{d_1}(M) \cdots x_{d_n}(M) = 0 \, \}$$

is called frozen, and it is anti-canonical; see e.g. [48, Lemma 5.4]. Denote $D_{FZ}^{\vee} \subset \mathrm{Gr}_k^{\vee}(n)$ the analogous divisor in the dual Grassmannian. The Zariski open set $\mathcal{U}_{k,n} = \mathrm{Gr}_k(n) \backslash D_{FZ}$ is called the (maximal) open positroid variety, and $\mathcal{U}_{k,n}^{\vee} \subset \mathrm{Gr}_k^{\vee}(n)$ is the corresponding variety in the dual Grassmannian.

Following Marsh-Rietsch [53], we define a Landau-Ginzburg model as follows.

Definition 2.3.3. *The Landau-Ginzburg model of $\mathrm{Gr}_k(n)$ is defined to be the pair $(\mathcal{U}_{k,n}^{\vee}, W)$, with W regular function given by*

$$W = \frac{x_{d_1^{\square}}}{x_{d_1}} + \ldots + \frac{x_{d_n^{\square}}}{x_{d_n}} \quad .$$

Here $x_{d_i^{\square}}$ denotes the Plücker coordinate of the Young diagram $d_i^{\square}$ obtained by augmenting d_i by one box, or removing a rim-hook if the new box exceeds the $k \times (n-k)$ grid.

Example 2.3.4. The Landau-Ginzburg model for $\mathrm{Gr}_2(5)$ is given by $(\mathcal{U}_{2,5}^{\vee}, W)$ with

$$\mathcal{U}_{2,5}^{\vee} = \mathrm{Gr}_3(5) \setminus \{ \, x_{\ydiagram{2,2}} x_{\ydiagram{1,1}} x_{\varnothing} x_{\ydiagram{3}} x_{\ydiagram{3,3}} = 0 \, \} \quad ,$$

with

$$W \quad = \quad \frac{x_{\ydiagram{3,2}}}{x_{\ydiagram{2,2}}} + \frac{x_{\ydiagram{2,1}}}{x_{\ydiagram{1,1}}} + \frac{x_{\ydiagram{1}}}{x_{\varnothing}} + \frac{x_{\ydiagram{3,1}}}{x_{\ydiagram{3}}} + \frac{x_{\ydiagram{2}}}{x_{\ydiagram{3,3}}} \quad .$$

The following result says that this Landau-Ginzburg model is a correct mirror for $\mathrm{Gr}_k(n)$ in the sense of closed-string mirror symmetry.

Theorem 2.3.5. *(Rietsch [69, Theorem 4.1]) There is an isomorphism of* $\mathbb{C}$*-algebras*

$$\mathrm{QH}(\mathrm{Gr}_k(n)) \cong \mathrm{Jac}(W) \quad ,$$

where QH *denotes the small quantum cohomology ring evaluated at* $q = 1$*, and the Jacobian ring of* W *on the right is given by* $\mathrm{Jac}(W) = \mathbb{C}[\mathcal{U}_{k,n}^{\vee}]/(\partial_{x_d} W, \forall d)$.

Chapter 3

GENERATION BY THE GELFAND-ZETLIN TORUS

In this chapter, we show that the monotone Lagrangian torus fiber of an integrable system on the complex Grassmannian $\mathrm{Gr}(k,n)$ introduced by Guillemin-Sternberg [40] supports generators for all maximum modulus summands in the spectral decomposition of the Fukaya category over $\mathbb{C}$. We introduce an action of the dihedral group D_n on the Landau-Ginzburg mirror proposed by Marsh-Rietsch [53] that makes it equivariant and use it to show that, given a lower modulus, the torus supports nonzero objects in none or many summands of the Fukaya category with that modulus. The alternative is controlled by the vanishing of rectangular Schur polynomials at the n-th roots of unity, and for $n = p$ prime this suffices to give a complete set of generators and prove Homological Mirror Symmetry for $\mathrm{Gr}(k,p)$.

3.1. Quantum spectrum of Grassmannians

In this section, we describe the spectrum of the operator $c_1\star$ acting on the quantum cohomology $\mathrm{QH}(\mathrm{Gr}_k(n))$ of Grassmannians (evaluated at $q = 1$). This is the first step in the study of the Fukaya category $\mathcal{F}(\mathrm{Gr}_k(n))$, as the eigenvalues of this operator label the summands of the category; see Appendix B. Explicit formulas for quantum products of Schubert classes were first computed by Bertram [9]. In particular, the product by $c_1 = n\sigma_{\square}$ is determined by the quantum Pieri rule:

$$\sigma_{\square} \star \sigma_d = \sigma_{\square} \cdot \sigma_d + q\sigma_{\widehat{d}} \quad .$$

The first term in this formula is the cup product, while the second is a quantum correction. The classical part $\sigma_{\square} \cdot \sigma_d$ is a sum of Schubert classes obtained by adding one box to d in all possible ways. The quantum part $\sigma_{\widehat{d}}$ is a single Schubert class, with diagram $\widehat{d}$ obtained by erasing the full first row and the full first column from d, or 0 otherwise (i.e. if d has less than $n-k$ boxes in first row or less than k boxes in first column).

Example 3.1.1. Let $k = 2$ and $n = 5$. Some sample classical/quantum contributions are:

$$\sigma_{\ydiagram{1}} \cdot \sigma_{\ydiagram{2,1}} = \sigma_{\ydiagram{3,1}} + \sigma_{\ydiagram{2,2}} \quad , \quad \sigma_{\widehat{\ydiagram{3,2}}} = \sigma_{\ydiagram{1}} \quad , \quad \sigma_{\widehat{\ydiagram{2,2}}} = 0 \quad .$$

The eigenvalues with maximum modulus in the spectrum of $c_1\star$ have been studied before. In fact, for general Fano manifolds they are expected to satisfy the following conjecture.

Conjecture 3.1.2. *(Galkin-Golyshev-Iritani [31, Conjecture 3.1.2]) If X is a smooth projective Fano variety, denote*

$$T = \max\{\ |\lambda|\ :\ \lambda \textit{ eigenvalue of } c_1\star\ \}$$

and r its Fano index. Then:

1. *T is an eigenvalue of $c_1\star$;*
2. *if λ is an eigenvalue of $c_1\star$ with $|\lambda| = T$, then $u = T\zeta$ for some r-th root of unity $\zeta \in \mathbb{C}$;*
3. *the multiplicity of T is 1 .*

The conjecture above is known to hold for Grassmannians and more general homogeneous varieties G/P; see Galkin-Golyshev-Iritani [31] and Cheong-Li [16]. Since we are interested in the full spectrum of $c_1\star$, it is in principle possible to use the quantum Pieri rule to compute it in specific cases. However, in Proposition 3.1.4 we use a different approach, relying on the existence of a particular basis for $\mathrm{QH}(\mathrm{Gr}_k(n))$: the Schur basis. The author learned of this basis from the work of Rietsch [67]. The Schur basis σ_I is indexed by sets I as in 2.1 and given by

$$\sigma_I = \sum_d \overline{S_d(I)}\sigma_d \quad .$$

The elements of the Schur basis are eigenvectors for $c_1\star$, and in fact for any operator $\sigma_d\star$. For the reader's convenience, we give a proof below.

Lemma 3.1.3. *(Rietsch [67]) For any $d \subseteq k \times (n-k)$ and any set I of distinct roots* *of* $x^n = (-1)^{k+1}$*, the following identity holds:*

$$\sigma_d \star \sigma_I = S_d(I)\sigma_I \quad .$$

Proof. By definition of Schur basis

$$\sigma_d \star \sigma_I = \sum_{\nu} \overline{S_\nu(I)} \sigma_d \star \sigma_\nu \quad ,$$

where $\nu \subseteq k \times (n-k)$ runs among all Young diagrams. The product of two Schubert classes in $\mathrm{QH}(\mathrm{Gr}_k(n))$ is given by

$$\sigma_d \star \sigma_\nu = \sum_{\mu} \left(\sum_{h \in \mathbb{N}} \langle \sigma_d, \sigma_\nu, \sigma_{PD(\mu)} \rangle_h q^h \right) \sigma_\mu \quad ,$$

where $PD(\mu)$ denotes the Poincaré dual Young diagram of μ, and $\langle \sigma_d, \sigma_\nu, \sigma_{PD(\mu)} \rangle_h$ is the Gromov-Witten invariant counting genus 0 curves of degree h through the Schubert cycles $X_d, X_\nu, X_{PD(\mu)} \subseteq \mathrm{Gr}_k(n)$. This number is 0 unless $|d| + |\nu| + |PD(\mu)| = k(n-k) + hn$, so that calling

$$h(\mu) = \frac{|d| + |\nu| + |PD(\mu)| - k(n-k)}{n}$$

we get

$$\sigma_d \star \sigma_\nu = \sum_{\mu} \langle \sigma_d, \sigma_\nu, \sigma_{PD(\mu)} \rangle_{h(\mu)} q^{h(\mu)} \sigma_\mu \quad .$$

The Gromov-Witten invariant above has an explicit expression, known as Bertram-Vafa-Intriligator formula:

$$\langle \sigma_d, \sigma_\nu, \sigma_{PD(\mu)} \rangle_{h(\mu)} = \frac{1}{n^k} \sum_{J} \frac{S_d(J) S_\nu(J) S_{PD(\mu)}(J)}{S_{k \times (n-k)}(J)} |\operatorname{Van}(J)|^2 \quad ;$$

see [67, Theorem 10.3] (also [9], [78]). In the formula, the sum runs over J size k sets of roots of $x^n = (-1)^{k+1}$, and if $J = \{\zeta_1, \ldots, \zeta_k\}$

$$|\operatorname{Van}(J)| = \prod_{i<j} |\zeta_i - \zeta_j| \quad .$$

Rearranging the sums in the product $\sigma_d \star \sigma_I$, and using the fact (Proposition 2.1.11)

that
$$\frac{S_{PD(\mu)}(J)}{S_{k\times(n-k)}(J)} = \overline{S_\mu(J)} \quad ,$$
we find that
$$\sigma_d \star \sigma_I = \frac{1}{n^k}\sum_\mu q^{h(\mu)}\sigma_\mu \left(\sum_J S_d(J)\overline{S_\mu(J)}|\operatorname{Van}(J)|^2 \left(\sum_\nu S_\nu(J)\overline{S_\nu(I)}\right)\right) \quad .$$
Now by Proposition 2.1.11
$$\sum_\nu S_\nu(J)\overline{S_\nu(I)} = \frac{n^k}{|\operatorname{Van}(J)|^2}\delta_{J,I} \quad ,$$
so we arrive at
$$\sigma_d \star \sigma_I = S_d(I)\left(\sum_\mu q^{h(\mu)}\overline{S_\mu(I)}\sigma_\mu\right) \quad .$$
Evaluating at $q = 1$ gives the desired formula. □

We are now ready to prove the following.

Proposition 3.1.4. *The following properties hold:*

1. *The eigenvalues of $c_1\star$ acting on $\operatorname{QH}(\operatorname{Gr}_k(n))$ (evaluated at $q = 1$) are given by $n(\zeta_1 + \ldots + \zeta_k)$, with $\{\zeta_1, \ldots \zeta_k\}$ varying among the size k sets of roots of $x^n = (-1)^{k+1}$.*

2. *Let $O(2)$ act on the complex plane by linear isometries of the Euclidean metric. The subgroup that maps the set of eigenvalues of $c_1\star$ to itself is isomorphic to the dihedral group D_n.*

3. *If $n = p$ prime, then all eigenvalues of $c_1\star$ have multiplicity one.*

Proof. 1) Follows from $c_1 = n\sigma_\square$ and the fact that a single box Young diagram supports exactly k tableaux, obtained by labelling it with any of the labels in $\{1, \ldots, k\}$, so that
$$S_\square(x_1, \ldots, x_k) = x_1 + \ldots + x_k \quad .$$

2) If $I = \{\zeta_1, \ldots, \zeta_k\}$, rotation of $2\pi/n$ and conjugation give
$$e^{2\pi i/n} nS_\square(I) = n(e^{2\pi i/n}\zeta_1 + \ldots + e^{2\pi i/n}\zeta_k) = nS_\square(e^{2\pi i/n} I)$$

$$\overline{nS_{\square}(I)} = n(\overline{\zeta_1} + \ldots + \overline{\zeta_k}) = nS_{\square}(\overline{I})$$

and these two transformations generate a copy of D_n in the subgroup of $O(2)$ that preserves the eigenvalues. There are no other transformations with this property because the subgroup is finite, and the only finite subgroups of $O(2)$ are cyclic or dihedral; therefore it must be contained in a dihedral group, possibly larger than D_n. On the other hand, it cannot be larger than D_n because there are n eigenvalues with maximum modulus: this follows from the fact that n is the Fano index of $\mathrm{Gr}_k(n)$, and the Grassmannians have property $\mathcal{O}$ introduced by Galkin-Golyshev-Iritani [31] (see also [16, Proposition 3.3 and Corollary 4.11]), so that any element in our subgroup must be in particular a symmetry of the n-gon formed by the eigenvalues of maximum modulus.

3) For $p = 2$ we must have $k = 1$, and the statement is true. If $p > 2$ prime, observe that the statement for $\mathrm{Gr}_k(p)$ is equivalent to the one for $\mathrm{Gr}_{p-k}(p)$ because the two Grassmannians are isomorphic. We can use this to assume without loss of generality that k is odd, since when it is even we can replace k with $p - k$. Let now $\{\xi_1, \ldots, \xi_k\}$ and $\{\zeta_1, \ldots, \zeta_k\}$ be two size k sets of p-th roots of

$$x^p = (-1)^{k+1} = 1$$

and call $z = e^{2\pi i/p}$. Rewrite

$$\xi_1 + \ldots + \xi_k = z^{i_1} + \ldots + z^{i_k} \quad , \quad \zeta_1 + \ldots + \zeta_k = z^{j_1} + \ldots + z^{j_k}$$

with $0 \leqslant i_1 < \ldots < i_k < p$ and $0 \leqslant j_1 < \ldots < j_k < p$. Denote $\langle z \rangle$ the subgroup of $\mathbb{C}^\times$ generated by z. The map $\phi(1) = z$ extends to a morphism of group rings

$$\phi : \mathbb{Z}[\mathbb{Z}/p\mathbb{Z}] \to \mathbb{Z}[\langle z \rangle] \quad .$$

Think now of the sums above as elements of a group ring

$$z^{i_1} + \ldots + z^{i_k} = \phi\left(\sum_{u \in \mathbb{Z}/p\mathbb{Z}} a_u t^u\right) = \phi(a) \quad , \quad z^{j_1} + \ldots + z^{j_k} = \phi\left(\sum_{u \in \mathbb{Z}/p\mathbb{Z}} b_u t^u\right) = \phi(b)$$

where $a, b \in \mathbb{Z}[\mathbb{Z}/p\mathbb{Z}]$ have coefficients

$$a_u = \begin{cases} 1 & \text{if } u \in \{i_1, \ldots, i_k\} \\ 0 & \text{otherwise} \end{cases} \quad , \quad b_u = \begin{cases} 1 & \text{if } u \in \{j_1, \ldots, j_k\} \\ 0 & \text{otherwise} \end{cases} \quad .$$

Now the two eigenvalues of $c_1\star$ corresponding to $\{i_1, \ldots, i_k\}$ and $\{j_1, \ldots, j_k\}$ are equal whenever $\phi(a) = \phi(b)$, or equivalently $\phi(a - b) = 0$. The kernel of the morphism ϕ is known (de Bruijn [21, Theorem 1]; see also Lam-Leung [50, Theorem 2.2]) and it is

$$\ker \phi = \{l(1 + t + \ldots + t^{p-1}) \,:\, l \in \mathbb{Z}\} \quad .$$

Therefore there exists $l \in \mathbb{Z}$ such that

$$\sum_{u \in \mathbb{Z}/p\mathbb{Z}} (a_u - b_u)t^u = l + lt + \ldots + lt^{p-1}$$

so that $a_u - b_u = l$ for every $u \in \mathbb{Z}/p\mathbb{Z}$. Observe that for every u we have $a_u - b_u \in \{-1, 0, 1\}$, and moreover we can't have $l = \pm 1$ because both a and b have exactly k of their coefficients (a_u and b_u respectively) different from 0. We conclude that $l = 0$, so that $a = b$ and therefore $\{i_1, \ldots, i_k\} = \{j_1, \ldots, j_k\}$. □

3.2. Disk potential of a Gelfand-Zetlin fiber

From the point of view of symplectic topology, $\mathrm{Gr}_k(n)$ fits naturally in the class of coadjoint orbits. We denote $\mathfrak{u}(n)^\vee$ the dual Lie algebra of the unitary group $U(n)$ and recall that the Lie bracket induces a symplectic structure on coadjoint orbits given by

$$\omega_\phi(X, Y) = \phi([X, Y]) \qquad \phi \in \mathfrak{u}(n)^\vee \quad X, Y \in \mathfrak{u}(n) \quad ,$$

and the action of $U(n)$ is Hamiltonian with respect to this structure. It is convenient to identify $\mathfrak{u}(n)^\vee$ with the real vector space $\mathcal{H}_n$ of Hermitian matrices of size n, where the action of $U(n)$ is given by conjugation. Each $H \in \mathcal{H}_n$ has real eigenvalues, labeled $\alpha_1 \geqslant \ldots \geqslant \alpha_n$. By the spectral theorem, the tuple $\alpha = (\alpha_1, \ldots, \alpha_n)$ is a complete invariant for the orbits of the $U(n)$ action, so that we can denote them $\mathcal{O}_\alpha \subset \mathcal{H}_n$. We are interested in the case where

$$\alpha_1 = \ldots = \alpha_k > \alpha_{k+1} = \ldots = \alpha_n$$

because in this case $\mathcal{O}_\alpha \cong \mathrm{Gr}_k(n)$. Therefore, in this section we think $\mathrm{Gr}_k(n) \subset \mathcal{H}_n$ as Hermitian matrices with k equal big eigenvalues and $n-k$ equal small eigenvalues.

For each $H \in \mathrm{Gr}_k(n)$ and $1 \leqslant s \leqslant n-1$ one can consider the size s minor H_s of H consisting of the first s rows and columns, so that $H_s \in \mathcal{H}_s$ and in analogy with what was done above one can label its eigenvalues

$$\Phi_{1,s} \geqslant \Phi_{2,s-1} \geqslant \ldots \geqslant \Phi_{s-1,2} \geqslant \Phi_{s,1} \quad .$$

As a consequence of the min-max characterization of the eigenvalues, for each $s \geqslant 2$ the eigenvalues of H_s interlace with those of H_{s-1}:

$$\begin{array}{ccccccccc}
\Phi_{1,s} & & & & \Phi_{2,s-1} \quad \ldots \quad \Phi_{s-1,2} & & & & \Phi_{s,1} \\
& \rotatebox{-45}{$\geqslant$} & & \rotatebox{45}{$\leqslant$} & & \rotatebox{-45}{$\geqslant$} & & \rotatebox{45}{$\leqslant$} & \\
& & \Phi_{1,s-1} & & \ldots & & \Phi_{s-1,1} & &
\end{array} \quad .$$

This implies, together with the assumption that $\alpha_1 = \ldots = \alpha_k$ and $\alpha_{k+1} = \ldots = \alpha_n$, the inequalities of Figure 3.1.

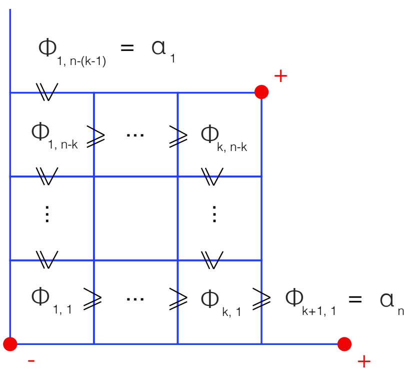

Figure 3.1: Inequalities for the Gelfand-Zetlin polytope Δ_α and ladder diagram Γ_α.

Therefore we are left with $k(n-k)$ non-constant functions on $\mathrm{Gr}_k(n)$, and ordering them by lexicographic order on the subscripts they become the entries of a map

$$\Phi : \mathrm{Gr}_k(n) \to \mathbb{R}^{k(n-k)} \quad .$$

The image Δ_α of this map is a convex polytope cut out by the inequalities of Figure 3.1. In fact, the following holds.

Theorem 3.2.1. *(Guillemin-Sternberg [40, Section 5]) The map Φ is a completely integrable system on $\mathrm{Gr}_k(n)$: on the open dense subset $\Phi^{-1}(\Delta_\alpha \backslash \partial\Delta_\alpha) \subset \mathrm{Gr}_k(n)$ its entries are smooth functions, they pairwise Poisson commute, and their differentials are linearly independent.*

It follows from general properties of completely integrable systems that the fibers of Φ over the interior of Δ_α must be Lagrangian tori (see for example Duistermaat [22, Theorem 1.1]). Moreover, the following result allows to locate the unique monotone fiber among these tori (see Appendix A for a discussion of monotonicity).

Theorem 3.2.2. *(Cho-Kim [19, Section 5 and Theorem 5.2]) If $\alpha_1 = \cdots = \alpha_k = n-k$ and $\alpha_{k+1} = \cdots = \alpha_n = -k$, the symplectic structure ω on $\mathcal{O}_\alpha \cong \mathrm{Gr}_k(n)$ satisfies $[\omega] = c_1$ and the interior of Δ_α contains a unique lattice point $\mathbf{u}$ such that $\Phi^{-1}(\mathbf{u})$ is monotone. The coordinates of this lattice point are $\mathbf{u}_{i,j} = j - i$.*

More generally, Cho-Kim [19] classify all the monotone Lagrangian fibers of the Gelfand-Zetlin system for arbitrary partial flag manifolds.

Definition 3.2.3. *Denote the monotone torus fiber of Φ by $L_{GZ} \subset \mathrm{Gr}_k(n)$, and call it the Gelfand-Zetlin torus.*

Being a regular Lagrangian fibration over the interior of Δ_α, the integrable system Φ induces a basis $\gamma_{i,j} \in H_1(L_{GZ};\mathbb{Z})$. Denote

$$W_{L_{GZ}} \in \mathbb{C}[x_{i,j}^{\pm 1}] \qquad 1 \leqslant i \leqslant k, \quad 1 \leqslant j \leqslant n-k$$

the Gromov-Witten disk potential written in the coordinates induced by this basis, as explained in Appendix B. Our goal now is to compute this Laurent polynomial explicitly.

The two key ingredients of this calculation are a correspondence between Maslov 2 J-holomorphic disks and codimension 1 faces of Δ_α due to Nishinou-Nohara-Ueda [58], and a combinatorial description of boundary faces of Δ_α due to An-Cho-Kim [5].

Theorem 3.2.4. *(Nishinou-Nohara-Ueda [58, Theorem 10.1]) The Maslov 2 disk potential $W_{L_{GZ}}$ has one monomial with coefficient one for each codimension 1 face of Δ_α, with exponents the coordinates of the corresponding inward primitive normal vector.*

The idea of the theorem above is to consider a toric degeneration of $\mathrm{Gr}_k(n)$ to a (generally singular) toric variety $X(\Delta_\alpha)$ whose polytope is Δ_α, and to construct a small toric resolution of singularities for it. Small here means that the exceptional locus has codimension at least two. Such degenerations have been found by Gonciuela-Lakshmibai [33]. One then uses the degeneration to construct a cobordism between the moduli space of Maslov 2 disks bounding $L_{GZ} \subset \mathrm{Gr}_k(n)$ and the moduli space of Maslov 2 disks bounding a toric Lagrangian fiber of the resolution of $X(\Delta_\alpha)$. Smallness of the resolution guarantees that disks intersecting the singular locus in the central fiber of the degeneration don't contribute to the potential, because they correspond to disks of Maslov index at least 4 in the resolution. One then concludes by using the calculation of Cho [14] of the disk potential of toric Lagrangian fibers.

In the proof of Proposition 3.2.6 we also make use of the following result.

Theorem 3.2.5. *(An-Cho-Kim [5, Theorem 1.11]) There is a bijection between faces $\Delta_f \subset \Delta_\alpha$ and face graphs $\Gamma_f \subset \Gamma_\alpha$ in the ladder diagram, such that the dimension of Δ_f matches the number of loops in Γ_f.*

The ladder diagram Γ_α is a $k \times (n-k)$ grid with two extra edges; the bottom left corner is labelled by $-$ and there are two nodes labelled by $+$, see Figure 3.1. A positive path is a sequence of edges in Γ_α that connects the $-$ node with one of the two $+$ nodes and only goes up or right. A face graph $\Gamma_f \subset \Gamma_\alpha$ is any union of positive paths that covers both $+$ nodes. A loop of Γ_f is a minimal unoriented cycle of Γ_f thought as a graph.

Figure 3.2 gives a complete list of face graphs with five loops for $k = 2$ and $n = 5$, and the bijection mentioned in the theorem above is obtained by setting to $=$ those inequalities defining the polytope Δ_α that do not cross an edge when we put Γ_f on top of the grid of inequalities as done in Figure 3.1.

We use the above mentioned toric degeneration result of Nishinou-Nohara-Ueda [58] to work out an explicit formula in terms of k and n for the disk potential of the Gelfand-

Zetlin torus. This formula will be used in the proof of Theorem 3.4.4.

Proposition 3.2.6. *If $L_{GZ} \subset \mathrm{Gr}_k(n)$ is the Gelfand-Zetlin torus:*

1. *There are $(k-1)(n-k) + k(n-k-1) + 2$ Maslov 2 J-holomorphic disks through a generic point of the torus.*

2. *The disk potential is given by*

$$W_{L_{GZ}} = \sum_{i=1}^{k-1}\sum_{j=1}^{n-k} \frac{x_{i,j}}{x_{i+1,j}} + \sum_{i=1}^{k}\sum_{j=1}^{n-k-1} \frac{x_{i,j+1}}{x_{i,j}} + \frac{1}{x_{1,n-k}} + x_{k,1} \quad .$$

Proof. 1) Combining Theorems 3.2.4 and 3.2.5 we know that through a generic point of L_{GZ} there must be exactly one Maslov 2 J-holomorphic disk for each codimension one face $\Delta_f \subset \Delta_\alpha$, and these in turn correspond to face graphs $\Gamma_f \subset \Gamma_\alpha$ with $k(n-k)-1$ loops, where $k(n-k) = \dim \Delta_\alpha$. The ambient ladder diagram Γ_α is a grid with $k(n-k)$ cells, therefore Δ_f falls in one of the following three types (see Figure 3.2):

- **Type** $\square\square$ - the full Γ_α minus an interior vertical edge ;
- **Type** $\genfrac{}{}{0pt}{}{\square}{\square}$ - the full Γ_α minus an interior horizontal edge ;
- **Type** $\square$ - one of two exceptional cases consisting of the full Γ_α minus a loop at a corner .

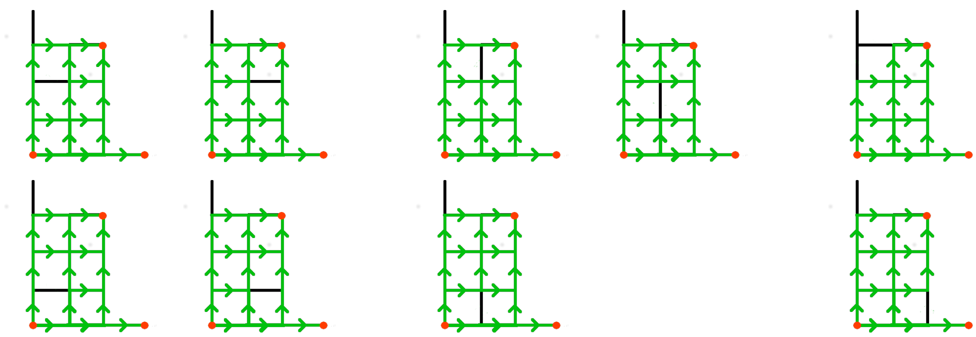

(a) Type $\genfrac{}{}{0pt}{}{\square}{\square}$ (b) Type $\square\square$ (c) Type $\square$

Figure 3.2: Face diagrams $\Gamma_f \subset \Gamma_\alpha$ of codimension 1 faces for the Gelfand-Zetlin polytope of Δ_α of the Grassmannian $\mathrm{Gr}_2(5)$.

There are $(k-1)(n-k)$ ways to remove an interior vertical edge from the $k \times (n-k)$ grid Γ_α: they correspond to the ways of placing a horizontal brick $\square\square$ in it, where we think at the central vertical edge as the one to be removed from Γ_α to obtain Γ_f. Similarly, there are $k(n-k-1)$ ways to remove an interior horizontal edge from the $k \times (n-k)$ grid

Γ_α: they correspond to the ways of placing a vertical brick $\begin{smallmatrix}\square\\\square\end{smallmatrix}$ in it, where we think at the central horizontal edge as the one to be removed from Γ_α to obtain Γ_f. Finally, the two exceptional cases are best described by Figure 3.2. Note that one cannot get any face graph Γ_f by removing boundary edges at the top right and bottom left corners of Γ_α without violating the condition on Γ_f of being union of positive paths and covering both the + nodes.

2) We write down inequalities for the codimension one faces $\Delta_f \subset \Delta_\alpha$ corresponding to the face graphs Γ_f above, and work out the coordinates of the corresponding inward primitive normal vectors $n_f \in \mathbb{Z}^{k(n-k)} \subset \mathbb{R}^{k(n-k)}$; these coordinates will be the exponents of the Laurent monomials of W_{LGZ}, where the variables $x_{i,j}$ correspond to the coordinates $\Phi_{i,j}$ of the Gelfand-Zetlin integrable system as explained at the beginning of this section.

By putting different types of face graphs Γ_f on top of the grid of inequalities of Δ_α as in Figure 3.1, one finds:

- **Type** $\square\square$ $\Phi_{i,j} = \Phi_{i+1,j}$ for $1 \leqslant i \leqslant k-1$ and $1 \leqslant j \leqslant n-k$;
- **Type** $\begin{smallmatrix}\square\\\square\end{smallmatrix}$ $\Phi_{i,j} = \Phi_{i,j+1}$ for $1 \leqslant i \leqslant k$ and $1 \leqslant j \leqslant n-k-1$;
- **Type** $\square$ $\Phi_{1,n-k} = \alpha_1$ and $\Phi_{k,1} = \alpha_n$.

Any of the codimension 1 faces $\Delta_f \subset \Delta_\alpha$ above is obtained by setting one $\geqslant$ to $=$ in the facet presentation of the Gelfand-Zetlin polytope:

$$\Delta_\alpha = \{\, \Phi \in \mathbb{R}^{k(n-k)} \ : \ n_f \cdot \Phi \geqslant -c_f \ \forall \Delta_f \subset \Delta_\alpha \text{ such that } \operatorname{codim} \Delta_f = 1 \,\} \quad .$$

Here $\cdot$ denotes the inner product with the unique vector $n_f \in \mathbb{Z}^{k(n-k)} \subset \mathbb{R}^{k(n-k)}$ that generates the semigroup of integral vectors satisfying the inequality. In our case the inward primitive normal vectors are:

- **Type** $\square\square$ for $1 \leqslant i \leqslant k-1$ and $1 \leqslant j \leqslant n-k$

$$n_f = \begin{cases} 1 & \text{in entry } \Phi_{i,j} \\ -1 & \text{in entry } \Phi_{i+1,j} \\ 0 & \text{in other entries} \end{cases} \quad ;$$

- **Type** $\begin{smallmatrix}\square\\ \square\end{smallmatrix}$ for $1 \leqslant i \leqslant k$ and $1 \leqslant j \leqslant n-k-1$

$$n_f = \begin{cases} -1 & \text{in entry } \Phi_{i,j} \\ 1 & \text{in entry } \Phi_{i,j+1} \\ 0 & \text{in other entries} \end{cases} ;$$

- **Type** $\square$ for $\Phi_{1,n-k} = \alpha_1$ and $\Phi_{k,1} = \alpha_n$ respectively

$$n_f = \begin{cases} -1 & \text{in entry } \Phi_{1,n-k} \\ 0 & \text{in other entries} \end{cases} \quad \text{and} \quad n_f = \begin{cases} 1 & \text{in entry } \Phi_{k,1} \\ 0 & \text{in other entries} \end{cases} .$$

We conclude that $W_{L_{GZ}}$ is a sum of monomials whose exponents are given by the coordinates of the inward primitive normal vectors, giving the formula of the statement.

$\square$

3.3. Guessing the mirror chart

According to mirror symmetry heuristic, a Landau-Ginzburg model $X^\vee$ for a symplectic manifold X should be thought of as moduli space of Lagrangians $L \subset X$, with the potential $W : X^\vee \to \mathbb{C}$ matching, in a suitable local chart corresponding to L, the Gromov-Witten disk potential W_L. Specialize this heuristic to $X = \mathrm{Gr}_k(n)$ and $X^\vee = \mathcal{U}_{k,n}$, where W is defined as in Section 2.3. Recall from Section 3.2 that we have an explicit formula for the Gromov-Witten disk potential W_L of the Gelfand-Zetlin torus $L = L_{GZ}$. In this Section, we give a guess for what the corresponding chart $T_{GZ} \subset \mathcal{U}_{k,n}$ is, and characterize the critical points of W that belong to this chart. Section 3.4 verifies that the guess is correct, i.e. it satisfies the heuristic explained above.

According to Scott [74], $\mathcal{U}_{k,n}$ contains open subschemes that are algebraic tori of the form

$$T_{\mathcal{C}} = \{\, [M^\vee] \in \mathcal{U}_{k,n} \;:\; x_d(M^\vee) \neq 0 \, \forall d \in \mathcal{C} \,\}$$

labeled by certain collections of Young diagrams $\mathcal{C}$ in a $k \times (n-k)$ grid such that $\{d_1, \ldots, d_n\} \subseteq \mathcal{C}$. Each collection $\mathcal{C}$ is such that the Plücker coordinates x_d with $d \in \mathcal{C}$ form a transcendence basis of the function field of the affine cone over $\mathrm{Gr}_k^\vee(n)$, and these can be thought of as coordinates for the torus chart $T_{\mathcal{C}} \cong (\mathbb{C}^{\times})^{k(n-k)}$ after setting $x_{\varnothing} = 1$. Restricting the potential W to each torus chart, we get Laurent polynomials

$$W_{\mathcal{C}} = W_{|T_{\mathcal{C}}} \in \mathbb{C}[\, x_d^{\pm 1} \,:\, d \in \mathcal{C}\,] \quad .$$

If $\mathcal{C}$ and $\mathcal{C}'$ are different collections of Plücker coordinates, the corresponding Laurent polynomials $W_{\mathcal{C}}$ and $W_{\mathcal{C}'}$ involve different sets of variables x_d: for $W_{\mathcal{C}}$ the variables are Plücker coordinates parametrized by Young diagrams $d \in \mathcal{C}$, while for $W_{\mathcal{C}'}$ by diagrams $d \in \mathcal{C}'$.

Definition 3.3.1. *The complex torus chart $T_{\mathcal{C}^R} \subset \mathcal{U}_{k,n}$ corresponding to the collection $\mathcal{C}^R$ of rectangular Young diagrams in the $k \times (n-k)$ grid is called the rectangular chart.*

This chart has the property that it always exists in $\mathrm{Gr}_k^{\vee}(n)$, no matter what k and n are; instead an arbitrary collection of $k(n-k)$ Young diagrams in a $k \times (n-k)$ grid does not in general give a transcendence basis for the function field of the affine cone over $\mathrm{Gr}_k^{\vee}(n)$; see Chapter 4 for a more accurate description of this phenomenon. One more consideration about the rectangular torus chart $T_{\mathcal{C}^R}$ is that when $k = 1$, i.e. for $\mathrm{Gr}(1,n) = \mathbb{P}^{n-1}$, $\mathrm{Gr}^{\vee}(1,n) = (\mathbb{C}^{\star})^{n-1}$ is a single torus, and there is only one possible way to choose $1 \cdot (n-1) = n-1$ nonempty Young diagrams in a $1 \times (n-1)$ grid, and they are forced to be all rectangles. All this suggests that the rectangular torus chart $T_{\mathcal{C}^R}$ should be the analogue of the chart of the Landau-Ginzburg mirror corresponding to local systems on the Lagrangian Clifford torus in the projective space. Since the Gelfand-Zetlin torus $L_{GZ} \subset \mathrm{Gr}_k(n)$ generalizes the Clifford torus to arbitrary Grassmannians, it is natural to guess that its mirror chart should be $T_{GZ} = T_{\mathcal{C}^R}$. The restriction of the potential W to the rectangular chart $T_{\mathcal{C}^R}$ has been computed explicitly by Marsh-Rietsch. We record their formula here for later use in Theorem 3.4.4.

Theorem 3.3.2. *(Marsh-Rietsch [53, Section 6.3]; see also Rietsch-Williams [70, Proposition 9.5]) If $W : \mathcal{U}_{k,n} \to \mathbb{C}$ is the Landau-Ginzburg potential, using the notation $x_{i\times j}$ for $x_{d_{i\times j}}$ its restriction to the rectangular chart $T_{\mathcal{C}^R}$ is given by*

$$W \restriction_{T_{\mathcal{C}^R}} = x_{1\times 1} + \sum_{i=2}^{k}\sum_{j=1}^{n-k} \frac{x_{i\times j}\, x_{(i-2)\times(j-1)}}{x_{(i-1)\times(j-1)}\, x_{(i-1)\times j}} + \frac{x_{(k-1)\times(n-k-1)}}{x_{k\times(n-k)}} + \sum_{i=1}^{k}\sum_{j=2}^{n-k} \frac{x_{i\times j}\, x_{(i-1)\times(j-2)}}{x_{(i-1)\times(j-1)}\, x_{i\times(j-1)}} \quad .$$

The critical locus of W has been studied by Rietsch, and it consists of $\binom{n}{k}$ non-degenerate critical points. These points have the following explicit description.

Theorem 3.3.3. *(Marsh-Rietsch [53, Proposition 9.3], Rietsch [67, Theorem 3.4 and Lemma 3.7]; see also Karp [42, Theorem 1.1 and Corollary 3.12]) The critical points of* $W : \mathcal{U}_{k,n} \to \mathbb{C}$ *are given by*

$$[M_{I^\vee}^\vee] = \begin{bmatrix} 1 & 1 & 1 & \dots & 1 \\ \zeta_1 & \zeta_2 & \zeta_3 & \dots & \zeta_{n-k} \\ \zeta_1^2 & \zeta_2^2 & \zeta_3^2 & \dots & \zeta_{n-k}^2 \\ \vdots & \vdots & \vdots & & \vdots \\ \zeta_1^{n-1} & \zeta_2^{n-1} & \zeta_3^{n-1} & \dots & \zeta_{n-k}^{n-1} \end{bmatrix}$$

where $I^\vee = \{\zeta_1, \dots, \zeta_{n-k}\}$ *is a set of* $n-k$ *distinct roots of* $x^n = (-1)^{n-k+1}$.

We conclude this section with a criterion to decide when a critical point of W belongs to the rectangular chart $T_{\mathcal{C}^R}$, formulated in terms of zeros of Schur polynomials at roots of unity.

Proposition 3.3.4. *Let* $I^\vee$ *be a size* $n-k$ *subset of roots of* $x^n = (-1)^{n-k+1}$ *and denote* $[M_{I^\vee}^\vee] \in \mathcal{U}_{k,n}$ *the corresponding critical point of* W*; then the following properties hold:*

1. $$[M_{I^\vee}^\vee] \in T_{\mathcal{C}^R} \iff S_{d^T}(I^\vee) \neq 0 \quad \forall d \text{ rectangular}$$

   .

2. *The dihedral group* D_n *acts on the sets* $I^\vee$ *via* $rI^\vee = e^{2\pi i/n} I^\vee$ *and* $sI^\vee = \overline{I^\vee}$ *and*

$$S_{d^T}(I^\vee) \neq 0 \iff S_{d^T}(gI^\vee) \neq 0 \quad \forall g \in D_n \quad .$$

Proof. 1) From the definition of rectangular chart $T_{\mathcal{C}^R}$

$$[M_{I^\vee}^\vee] \in T_{\mathcal{C}^R} \iff x_d(M_{I^\vee}^\vee) \neq 0 \quad \forall d \quad \text{rectangular Young diagram} \quad ,$$

and from the description of the critical points of W (Theorem 3.3.3)

$$[M^{\vee}_{I^{\vee}}] = \begin{bmatrix} 1 & 1 & 1 & \dots & 1 \\ \zeta_1 & \zeta_2 & \zeta_3 & \dots & \zeta_{n-k} \\ \zeta_1^2 & \zeta_2^2 & \zeta_3^2 & \dots & \zeta_{n-k}^2 \\ \vdots & \vdots & \vdots & & \vdots \\ \zeta_1^{n-1} & \zeta_2^{n-1} & \zeta_3^{n-1} & \dots & \zeta_{n-k}^{n-1} \end{bmatrix}$$

where $I^{\vee} = \{\zeta_1, \dots, \zeta_{n-k}\}$ is a set of $n-k$ distinct roots of $x^n = (-1)^{n-k+1}$. The horizontal steps of the empty diagram $d = \varnothing$ are $d^- = \varnothing^- = \{1, \dots, n-k\}$, so that by the Vandermonde formula and the definition of x_d as determinant of minor at rows d^-

$$x_{\varnothing}(M^{\vee}_{I^{\vee}}) = \prod_{1 \leqslant i < j \leqslant n-k} (\zeta_j - \zeta_i) \neq 0 \quad .$$

Therefore

$$[M^{\vee}_{I^{\vee}}] \in T_{\mathcal{C}^R} \iff \frac{x_d(M^{\vee}_{I^{\vee}})}{x_{\varnothing}(M^{\vee}_{I^{\vee}})} \neq 0 \quad \forall d \quad \text{rectangular Young diagram} \quad .$$

The claim follows from the fact that

$$\frac{x_d(M^{\vee}_{I^{\vee}})}{x_{\varnothing}(M^{\vee}_{I^{\vee}})} = S_{d^T}(I^{\vee}) \quad .$$

This holds because when we write the diagram d^T in partition form $d^T = (d_1^T, \dots, d_{n-k}^T)$, i.e. as a tuple where d_i^T is the number of boxes at row i, one of the many equivalent ways of defining the Schur polynomial of d^T is

$$S_{d^T}(x_1,\dots,x_{n-k}) = \frac{\det\begin{pmatrix} x_1^{d^T_{n-k}} & \dots & x_{n-k}^{d^T_{n-k}} \\ x_1^{d^T_{n-k-1}+1} & \dots & x_{n-k}^{d^T_{n-k-1}+1} \\ \vdots & & \vdots \\ x_1^{d^T_1+n-k-1} & \dots & x_{n-k}^{d^T_1+n-k-1} \end{pmatrix}}{\det\begin{pmatrix} 1 & \dots & 1 \\ x_1 & \dots & x_{n-k} \\ \vdots & & \vdots \\ x_1^{n-k-1} & \dots & x_{n-k}^{n-k-1} \end{pmatrix}} \quad .$$

Once evaluated at $I^\vee$, the denominator is $x_\varnothing(M^\vee_{I^\vee})$ and the numerator equals $x_d(M^\vee_{I^\vee})$ because the horizontal steps of d and the number of boxes in each row of d^T are related by

$$d^- = \{d^T_{n-k}+1,\dots,d^T_1+n-k\} \quad .$$

2) Observe that for every d

$$S_{d^T}(rI^\vee) = (e^{2\pi i/n})^{|d^T|}S_d(I^\vee) \quad , \quad S_{d^T}(sI^\vee) = \overline{S_{d^T}(I^\vee)}$$

because S_{d^T} is a homogeneous polynomial of degree the number of boxes $|d^T|$ of d^T. $\square$

3.4. Matching things up and the $n = p$ prime case

The key diagram to have in mind for this section is the following:

$$\begin{tikzcd} D_n \circlearrowleft (\mathbb{C}^\times)^{k(n-k)} \arrow[r, hook, "\theta_R"] \arrow[dr, "W_{LGZ}"'] & \mathcal{U}_{k,n}^{\circlearrowleft D_n} \arrow[d, "W"] \\ & \mathbb{C}^{\circlearrowleft D_n} \end{tikzcd} \tag{3.1}$$

Recall that W is the potential of the Landau-Ginzburg model described in Section 2.3:

$$W = \frac{x_{d_1\square}}{x_{d_1}} + \dots + \frac{x_{d_n\square}}{x_{d_n}} \quad .$$

$W_{L_{GZ}}$ is the disk potential of the Gelfand-Zetlin torus, thought of as an algebraic function on the space of local systems $(\mathbb{C}^\times)^{k(n-k)}$ and computed in Section 3.2:

$$W_{L_{GZ}} = \sum_{i=1}^{k-1}\sum_{j=1}^{n-k} \frac{x_{i,j}}{x_{i+1,j}} + \sum_{i=1}^{k}\sum_{j=1}^{n-k-1} \frac{x_{i,j+1}}{x_{i,j}} + \frac{1}{x_{1,n-k}} + x_{k,1} \quad .$$

The target of both maps is $\mathbb{C}$, and it carries an action of the dihedral group D_n by $2\pi/n$ counter-clockwise rotation and conjugation, which encodes the symmetries of the eigenvalues of $c_1\star$ on $\mathrm{QH}(\mathrm{Gr}_k(n))$ observed in Figure 1.1.

We introduce an open embedding identifying the local systems of the Gelfand-Zetlin torus with the rectangular chart $T_{\mathcal{C}^R} \subset \mathcal{U}_{k,n}$. The embedding $\theta_R : (\mathbb{C}^\times)^{k(n-k)} \to \mathcal{U}_{k,n}$ is defined by the equations

$$x_{i,j} = \frac{x_{(k+1-i)\times j}}{x_{(k-i)\times(j-1)}} \quad 1 \leqslant i \leqslant k \quad 1 \leqslant j \leqslant n-k \quad ,$$

with $x_{i\times j} = x_{d_{i\times j}}$ denoting the Plücker coordinate corresponding to the $i \times j$ rectangular Young diagram.

The formula above is phrased to be efficient for the purposes of Theorem 3.4.4. One can use the equations to write the coordinates $x_{i\times j}$ in terms of the coordinates $x_{i,j}$ on the space of local systems, proceeding by lexicographic order on i, j. Since the $k(n-k)$ functions $x_{i\times j}$ give a transcendence basis for the function field $\mathbb{C}(\mathcal{U}_{k,n})$, the other entries x_d of this map for d non-rectangular Young diagram are determined by the Plücker relations. The image of this embedding is the rectangular chart $T_{\mathcal{C}^R}$ of Section 3.3. A new ingredient in the diagram above is the action of the dihedral group D_n on $\mathcal{U}_{k,n}$ (the action on the space of local systems $(\mathbb{C}^\times)^{k(n-k)}$ will be defined as pull-back along θ_R, see proof of Theorem 3.4.6).

Definition 3.4.1. *Indexing the standard basis v_d of $\mathbb{C}^{\binom{n}{k}}$ with Young diagrams $d \subseteq k \times (n-k)$, call dihedral projective representation the group morphism $D_n \to \mathrm{PGL}(\binom{n}{n-k}, \mathbb{C})$ given on the generators r, s of D_n by*

$$r \cdot v_d = (e^{2\pi i/n})^{|d|} v_d \quad , \quad s \cdot v_d = v_{\mathrm{PD}(d)}$$

where $|d|$ denotes the number of boxes in d and $\mathrm{PD}(d)$ is the Poincaré dual Young *diagram of d.*

Observe that $r^n = s^2 = 1$ in the definition above because $e^{2\pi i/n}$ is an n-th root of unity and $\mathrm{PD}(\mathrm{PD}(d)) = d$. Moreover, the relation $rs = sr^{-1}$ holds in $\mathrm{PGL}(\binom{n}{n-k}, \mathbb{C})$ because

$$rs \cdot v_d = (e^{2\pi i/n})^{|\,\mathrm{PD}(d)|} v_{\mathrm{PD}(d)} \quad , \quad sr^{-1} \cdot v_d = (e^{2\pi i/n})^{-|d|} v_{\mathrm{PD}(d)}$$

and $|\,\mathrm{PD}(d)| = k(n-k) - |d|$, so that $rs = e^{2\pi i k(n-k)/n} sr^{-1}$ with the scaling factor independent of d. The dihedral projective representation induces an algebraic action of D_n on $\mathbb{P}^{\binom{n}{k}-1}$, and the following holds.

Lemma 3.4.2. *The dual Grassmannian $\mathrm{Gr}_k^\vee(n) \subset \mathbb{P}^{\binom{n}{k}-1}$ is invariant under the action of D_n induced by the dihedral projective representation.*

Proof. Write the full rank $n \times (n-k)$ matrix $M^\vee$ as a list of rows

$$M^\vee = (m_1, \ldots, m_n) \quad m_i \in \mathbb{C}^{n-k} \; 1 \leqslant i \leqslant n \quad .$$

If $d \subseteq k \times (n-k)$, and $d^- = \{i_1, \ldots, i_{n-k}\}$ are its horizontal steps, the corresponding dual Plücker coordinate of $[M^\vee] \in \mathrm{Gr}_k^\vee(n)$ is

$$x_d(M^\vee) = \det(m_{i_1}, \ldots, m_{i_{n-k}}) \quad .$$

If $\zeta = e^{2\pi i/n}$, one can define a D_n-action on $\mathrm{Gr}_k^\vee(n)$ via

$$r \cdot [M^\vee] = [\zeta m_1, \zeta^2 m_2, \ldots, \zeta^n m_n] \quad \text{and} \quad s \cdot [M^\vee] = [m_n, m_{n-1}, \ldots, m_1] \quad ,$$

and observe that

$$x_d(r \cdot [M^\vee]) = \zeta^{i_1 + \cdots + i_{n-k}} x_d([M^\vee]) \quad , \quad x_d(s \cdot [M^\vee]) = x_{PD(d)}([M^\vee]) \quad .$$

We claim that these agree with the homogeneous coordinates of $[M^\vee]$ under the projective action D_n coming from the dihedral projective representation. For the s action there is nothing to check. Regarding r, the claim follows from the existence of a constant $C_{k,n}$ independent of d such that $|d| = C_{k,n} + i_1 + \ldots + i_{n-k}$. To see that this constant exists, write the Young diagram as a partition $d = (d_1, \ldots d_k)$, with d_i number of boxes in the i-th row of d. If $d^{|} = \{j_1, \dots j_k\}$ are the vertical steps of d, one has

$$d_1 = n-k-(j_1-1) \quad , \quad d_2 = d_1-(j_2-j_1-1) \quad , \quad \dots \quad , \quad d_k = d_{k-1}-(j_k-j_{k-1}-1) \quad .$$

It follows that

$$|d| = d_1 + \cdots + d_k = k(n-k) + \frac{k(k+1)}{2} - (j_1 + \cdots + j_k) \quad ;$$

moreover $[n] = d^{-} \sqcup d^{|}$ implies

$$i_1 + \cdots + i_{n-k} = \frac{n(n+1)}{2} - (j_1 + \cdots + j_k) \quad ,$$

from which one finds

$$C_{k,n} = k(n-k) + \frac{k(k+1)}{2} - \frac{n(n+1)}{2} \quad .$$

□

Recall that

$$\mathcal{U}_{k,n} = \mathrm{Gr}_k^{\vee}(n) \setminus D_{FZ}^{\vee} \quad ,$$

where $D_{FZ}^{\vee}$ is the divisor cut out by $x_{d_1} \cdots x_{d_n} = 0$. Since the collection of diagrams $d_1, \dots, d_n$ is closed under Poincaré duality, the divisor $D_{FZ}^{\vee}$ is D_n-invariant and one gets an action of D_n on $\mathcal{U}_{k,n}$.

Definition 3.4.3. *Call Young action the algebraic D_n-action on $\mathcal{U}_{k,n}$ induced by the dihedral projective representation of Definition 3.4.1.*

For notational convenience, we introduce a D_n-action on the sets I of k distinct roots of $x^n = (-1)^{k+1}$ that extends the one on $\mathbb{C}$ element-wise

$$r \cdot I = e^{2\pi i/n} I \quad , \quad s \cdot I = \overline{I} \quad .$$

In the theorems below, I will parametrize objects of the Fukaya category $\mathcal{F}(\mathrm{Gr}_k(n))$ supported on the Gelfand-Zetlin torus $L_{GZ} \subset \mathrm{Gr}_k(n)$, whereas $I^{\vee}$ will parametrize critical points of the Landau-Ginzburg potential $W : \mathcal{U}_{k,n} \to \mathbb{C}$. See Appendix B for the setup of the monotone Fukaya category. Let $L_{GZ} \subset \mathrm{Gr}_k(n)$ be the Gelfand-Zetlin torus, and $\gamma_{ij} \in H_1(L_{GZ};\mathbb{Z})$ for $1 \leqslant i \leqslant k$, $1 \leqslant j \leqslant n-k$ is the basis of cycles induced by the integrable system. For each set I of k distinct roots of $x^n = (-1)^{k+1}$, define a local system on the torus whose holonomy is given by

$$\mathrm{hol}_I(\gamma_{ij}) = \frac{S_{(k+1-i)\times j}(I)}{S_{(k-i)\times(j-1)}(I)} \quad .$$

The definition above makes sense only when the denominator is nonzero, in which case $(L_{GZ})_I$ denotes the corresponding object of the Fukaya category. When the denominator is zero the object is not defined.

Theorem 3.4.4. *The objects*

$$(L_{GZ})_{I_0}\ ,\ (L_{GZ})_{rI_0}\ ,\ (L_{GZ})_{r^2 I_0}\ ,\ \dots\ ,\ (L_{GZ})_{r^{n-1}I_0}$$

are defined and split-generate the n summands $\mathcal{F}_\lambda(\mathrm{Gr}_k(n))$ of the monotone Fukaya category with maximum $|\lambda|$.

Proof. As a first step we prove that diagram (3.1) commutes, or in other words $\theta_R^* W = W_{L_{GZ}}$. The image of θ_R is the rectangular torus chart $T_{\mathcal{C}^R} \subset \mathrm{Gr}_k^\vee(n)$ and by Theorem 3.3.2

$$W \restriction_{T_{\mathcal{C}^R}} = x_{1\times 1} + \sum_{i=2}^{k}\sum_{j=1}^{n-k} \frac{x_{i\times j}\, x_{(i-2)\times(j-1)}}{x_{(i-1)\times(j-1)}\, x_{(i-1)\times j}} + \frac{x_{(k-1)\times(n-k-1)}}{x_{k\times(n-k)}} + \sum_{i=1}^{k}\sum_{j=2}^{n-k} \frac{x_{i\times j}\, x_{(i-1)\times(j-2)}}{x_{(i-1)\times(j-1)}\, x_{i\times(j-1)}} \quad .$$

From the definition of θ_R

$$x_{i,j} = \frac{x_{(k+1-i)\times j}}{x_{(k-i)\times(j-1)}} \qquad 1 \leqslant i \leqslant k \quad 1 \leqslant j \leqslant n-k$$

so that

$$\theta_R^* W = x_{k,1} + \sum_{i=2}^{k}\sum_{j=1}^{n-k} \frac{x_{k+1-i,j}}{x_{k+2-i,j}} + \frac{1}{x_{1,n-k}} + \sum_{i=1}^{k}\sum_{j=2}^{n-k} \frac{x_{k+1-i,j}}{x_{k+1-i,j-1}} \quad .$$

The last expression matches the Maslov 2 disk potential $W_{L_{GZ}}$ computed in Proposition 3.2.6 (re-index the first sum with $l = k+1-i$, and the second sum with $l = k+1-i$ and $h = j-1$).

Because of Theorem B.3.3, critical points $\mathrm{hol}_I \in (\mathbb{C}^\times)^{k(n-k)}$ of $W_{L_{GZ}}$ correspond to holonomies of local systems on the Gelfand-Zetlin torus such that

$$\mathrm{HF}((L_{GZ})_I,(L_{GZ})_I)\neq 0 \quad ,$$

and by commutativity of diagram (3.1) these are the same as critical points of $W : \mathrm{Gr}_k^\vee(n)\to\mathbb{C}$ that are contained in the rectangular chart $T_{\mathcal{C}^R}$. By Theorem 3.3.3 and Proposition 2.1.11, critical points of W are of the form $[M_{I^\vee}^\vee]\in\mathrm{Gr}_k^\vee(n)$ for I set of k distinct roots of $x^n=(-1)^{k+1}$, and by Proposition 3.3.4 $[M_{I^\vee}^\vee]\in T_{\mathcal{C}^R}$ if and only if the following nonvanishing condition on Schur polynomials holds:

$$S_{d^T}(I^\vee)=S_d(I)\neq 0 \quad \forall d \quad \text{rectangular} \quad .$$

This allows us to define for any $[M_{I^\vee}^\vee]\in T_{\mathcal{C}^R}$ a local system on the Gelfand-Zetlin torus with

$$\mathrm{hol}_I(\gamma_{ij})=\frac{S_{(k+1-i)\times j}(I)}{S_{(k-i)\times(j-1)}(I)} \quad .$$

Observe that arguing as in Proposition 3.3.4

$$\frac{x_{(k+1-i)\times j}([M_{I^\vee}^\vee])}{x_{(k-i)\times(j-1)}([M_{I^\vee}^\vee])}=\frac{S_{((k+1-i)\times j)^T}(I^\vee)}{S_{((k-i)\times(j-1))^T}(I^\vee)}=\frac{S_{(k+1-i)\times j}(I)}{S_{(k-i)\times(j-1)}(I)} \quad .$$

We conclude that $\theta_R(\mathrm{hol}_I)=[M_{I^\vee}^\vee]$, meaning that $\mathrm{HF}((L_{GZ})_I,(L_{GZ})_I)\neq 0$.

To decide in which summand $\mathcal{F}_\lambda(\mathrm{Gr}_k(n))$ of the Fukaya category the object $(L_{GZ})_I$ lives, we compute

$$\lambda=W_{L_{GZ}}(\mathrm{hol}_I)=W([M_{I^\vee}^\vee])=\left(\frac{x_1^\square}{x_1}+\ldots+\frac{x_n^\square}{x_n}\right)([M_{I^\vee}^\vee]) \quad .$$

Dividing numerator and denominator by $x_\varnothing$, one finds for every $1\leqslant t\leqslant n$

$$\frac{x_t^\square}{x_t}([M_{I^\vee}^\vee])=\frac{S_{(\square\star d_t)^T}(I^\vee)}{S_{(d_t)^T}(I^\vee)}=\frac{S_{\square\star d_t}(I)}{S_{d_t}(I)} \quad ,$$

where d_t is the t-th frozen Young diagram.

Calling $\sigma_{d_t}\in\mathrm{QH}(\mathrm{Gr}_k(n))$ the Schubert class of the Young diagram d_t, Lemma 3.1.3

says that the action of $\sigma_t\star$ on the Schur basis σ_I is given by

$$\sigma_{d_t} \star \sigma_I = S_{d_t}(I)\sigma_I \quad .$$

Since $d_t^{\square} = \square \star d_t$ is a single Schubert class due to the special rectangular shape of d_t, we have

$$\sigma_{d_t^{\square}} \star \sigma_I = S_{\square}(I) S_{d_t}(I)\sigma_I$$

and therefore $S_{d_t^{\square}}(I) = S_{\square}(I)S_{d_t}(I)$. We conclude that $\lambda = nS_{\square}(I)$.

Choosing now $I = I_0$ set of k roots closest to 1, the set $I_0^{\vee}$ contains the $n-k$ roots of $x^n = (-1)^{n-k+1}$ closest to 1, and the corresponding critical point $[M_{I_0^{\vee}}]$ lies in the totally positive part of the Grassmannian; see [42, Theorem 1.1]. This means that all the Plücker coordinates of $[M_{I_0^{\vee}}]$ are real, non-vanishing, and have the same sign. In particular, $[M_{I_0^{\vee}}]$ is in the rectangular chart $T_{\mathcal{C}^R}$ and this gives a nonzero object

$$(L_{GZ})_{I_0} \text{ in } \mathcal{F}_{\lambda}(\mathrm{Gr}_k(n)) \quad , \quad \lambda = W([M_{I_0^{\vee}}]) = nS_{\square}(I_0) \in \mathbb{R}^+ \quad .$$

Moreover, using the inequalities of Schur polynomials at roots of unity of 2.1.11

$$|S_{\square}(I)| \leqslant S_{\square}(I_0) \quad \forall I$$

and this says that $(L_{GZ})_{I_0}$ lives in a summand of the Fukaya category labelled by an eigenvalue of $c_1\star$ with maximum modulus. It is known [16, Proposition 3.3 and Corollary 4.11] that there are n eigenvalues of $c_1\star$ with maximum modulus, all of multiplicity one, and they are given by rotations of multiples of $2\pi/n$ of $nS_{\square}(I_0) \in \mathbb{R}^+$. One can get nonzero objects in each of them by considering

$$(L_{GZ})_{I_0}, \, (L_{GZ})_{rI_0}, \, (L_{GZ})_{r^2I_0}, \, \ldots, \, (L_{GZ})_{r^{n-1}I_0}$$

and observing that for all $0 \leqslant s < n$ the critical point $[M_{(r^sI_0)^{\vee}}]$ of W still belongs to the rectangular chart $T_{\mathcal{C}^R}$, thanks to Proposition 3.3.4 (see also proof of Theorem 3.4.6), with

$$W([M_{(r^sI_0)^{\vee}}]) = nS_{\square}(r^sI_0) = r^s nS_{\square}(I_0) \quad ,$$

where in the last step we used that the Schur polynomial of $\square$ is linear. The fact that these summands are indexed by eigenvalues of multiplicity one guarantees that a single nonzero object generates, thanks to Theorem B.3.4. $\square$

Remark 3.4.5. In fact, the theorem above shows that whenever a critical point $[M^\vee_{I^\vee}]$ of the Landau-Ginzburg potential belongs to the rectangular torus chart $T_{\mathcal{C}^R} \subset \mathrm{Gr}^\vee_k(n)$ the object $(L_{GZ})_I$ is defined and nonzero in the summand of the Fukaya category $\mathcal{F}_\lambda(\mathrm{Gr}_k(n))$ with

$$\lambda = W([M^\vee_{I^\vee}]) = nS_\square(I)$$

even when $|\lambda|$ has not maximum modulus. The difference in this case is that the summand $\mathrm{QH}_\lambda(\mathrm{Gr}_k(n))$ of quantum cohomology is not necessarily one-dimensional, therefore one cannot conclude that this object generates $\mathbf{D}\mathcal{F}_\lambda(\mathrm{Gr}_k(n))$.

As Figure 1.2 illustrates, the question of what summands with lower $|\lambda|$ contain nonzero objects supported on the Gelfand-Zetlin torus is related to the arithmetic of k and n. On the other hand, we show in Theorem 3.4.6 that the equivariance of the Landau-Ginzburg model with respect to the action of D_n introduced at the beginning of this section forces a certain dichotomy, for which summands $\mathcal{F}_\lambda(\mathrm{Gr}_k(n))$ in each level $|\lambda|$ contain either none or a full D_n-orbit of nonzero objects.

Theorem 3.4.6. *If $(L_{GZ})_I$ is an object of $\mathcal{F}_\lambda(\mathrm{Gr}_k(n))$, then it is nonzero and the objects*

$$(L_{GZ})_{gI} \quad \text{in} \quad \mathcal{F}_{g\lambda}(\mathrm{Gr}_k(n)) \quad \text{for all} \quad g \in D_n$$

are defined and nonzero as well.

Proof. If $[M^\vee_{I^\vee}] \in \mathrm{Gr}^\vee_k(n)$ is a critical point of the Landau-Ginzburg potential W, the Young action of D_n on $\mathrm{Gr}^\vee_k(n)$ sends it to another critical point

$$g[M^\vee_{I^\vee}] = [M^\vee_{(gI)^\vee}] \qquad \forall g \in D_n \quad .$$

We verify this equality on generators r, s of D_n. Calling $N = \binom{n}{n-k} - 1$, the Plücker coordinates of $[M^\vee_{I^\vee}] \in \mathrm{Gr}^\vee_k(n) \subset \mathbb{P}^N$ are

$$[x_{d_0}(M^\vee_{I^\vee}) : x_{d_1}(M^\vee_{I^\vee}) : \cdots : x_{d_N}(M^\vee_{I^\vee})] \quad .$$

The Young diagrams $d_0, \dots, d_N$ are labelled according to lexicographic order on their sets of horizontal steps. The action of r gives

$$r \cdot [M_{I^\vee}^\vee] = [(e^{2\pi i/n})^{|d_0|} x_{d_0}(M_{I^\vee}^\vee) : (e^{2\pi i/n})^{|d_1|} x_{d_1}(M_{I^\vee}^\vee) : \cdots : (e^{2\pi i/n})^{|d_N|} x_{d_N}(M_{I^\vee}^\vee)]$$

Now observe that $d_0 = \varnothing$ is the empty diagram, whose horizontal steps are $\{1, \dots n-k\}$. Therefore the number of boxes of d_0 is $|d_0| = 0$, and thanks to Proposition 3.3.4 we know that $x_{d_0}(M_{I^\vee}^\vee) \neq 0$. Scaling the homogeneous coordinates by this factor we have

$$r \cdot [M_{I^\vee}^\vee] = [1 : (e^{2\pi i/n})^{|d_1|} S_{d_1}(I) : \cdots : (e^{2\pi i/n})^{|d_N|} S_{d_N}(I)] \quad .$$

The Schur polynomial S_{d_i} is homogeneous of degree $|d_i|$, therefore

$$(e^{2\pi i/n})^{|d_1|} S_{d_i}(I) = S_{d_i}(e^{2\pi i/n} I) = S_{d_i}(rI) \qquad \forall 0 \leqslant i \leqslant N \quad .$$

Scaling back the homogeneous coordinates by a factor $x_{d_0}(M_{(rI)^\vee}^\vee)$ we get

$$r \cdot [M_{I^\vee}^\vee] = [x_{d_0}(M_{(rI)^\vee}^\vee) : x_{d_1}(M_{(rI)^\vee}^\vee) : \cdots : x_{d_N}(M_{(rI)^\vee}^\vee)] = [M_{(rI)^\vee}^\vee] \quad .$$

The verification for the action of the generator s is analogous:

$$s \cdot [M_{I^\vee}^\vee] = [x_{PD(d_0)}(M_{I^\vee}^\vee) : x_{PD(d_1)}(M_{I^\vee}^\vee) : \cdots : x_{PD(d_N)}(M_{I^\vee}^\vee)] \quad .$$

Scaling the homogeneous coordinates by $x_{d_0}(M_{I^\vee}^\vee)$ we have

$$s \cdot [M_{I^\vee}^\vee] = [S_{PD(d_0)}(I) : S_{PD(d_1)}(I) : \cdots : S_{PD(d_N)}(I)] \quad .$$

From Proposition 2.1.11 it follows that

$$S_{PD(d_i)}(I) = \overline{S_{d_i}(I)} c_I \qquad \forall 0 \leqslant i \leqslant N \quad ,$$

where $c_I = S_{d_N}(I) \in \mathbb{C}^\times$ is a constant that depends on I, but not on d_i. Therefore we have

$$s \cdot [M_{I^\vee}^\vee] = [\overline{S_{d_0}(I)} : \overline{S_{d_1}(I)} : \cdots : \overline{S_{d_N}(I)}] = [S_{d_0}(sI) : S_{d_1}(sI) : \cdots : S_{d_N}(sI)] = [M_{(sI)^\vee}^\vee]$$

where the last equality is obtained by scaling the homogeneous coordinates by $x_{d_0}(M^\vee_{(sI)^\vee})$. This concludes the proof that the critical locus of W is D_n-invariant.

We also observe that W is D_n-equivariant when restricted to the singular locus. Indeed, we saw in Theorem 3.4.4 that $W([M^\vee_I]) = nS_\square(I)$ and therefore

$$r \cdot W([M^\vee_{I^\vee}]) = e^{2\pi i/n} nS_\square(I) = nS_\square(rI) = W([M^\vee_{(rI)^\vee}]) = W(r \cdot [M^\vee_{I^\vee}])$$

$$s \cdot W([M^\vee_{I^\vee}]) = \overline{nS_\square(I)} = nS_\square(sI) = W([M^\vee_{(sI)^\vee}]) = W(s \cdot [M^\vee_{I^\vee}]) \quad .$$

Also notice that $W : \mathcal{U}_{k,n} \to \mathbb{C}$ can't be globally D_n-equivariant, because $W(s \cdot -)$ is an algebraic function while $s \cdot W(-)$ is not. On the other hand W is globally $\mathbb{Z}/n\mathbb{Z}$-equivariant, where $\mathbb{Z}/n\mathbb{Z}$ is the subgroup of D_n generated by r. Indeed, by definition we have

$$W = \frac{x_1^\square}{x_1} + \ldots + \frac{x_n^\square}{x_n}$$

and recall that $x_t = x_{d_t}$ Plücker coordinate of the t-th boundary rectangular Young diagram, with $x_t^\square = x_{d_t^\square}$. The fact that $|d_t^\square| \equiv |d_t| + 1 \pmod n$ for every $1 \leqslant t \leqslant n$ implies that

$$\frac{r \cdot x_t^\square}{r \cdot x_t} = \frac{(e^{2\pi i/n})^{|\square\star d_t|} x_n^\square}{(e^{2\pi i/n})^{|d_t|} x_n} = e^{2\pi i/n} \frac{x_n^\square}{x_n}$$

which means that W is globally $\mathbb{Z}/n\mathbb{Z}$-equivariant.

Observe now that the rectangular torus chart $T_{\mathcal{C}^R} \subset \mathrm{Gr}_k^\vee(n)$ is $\mathbb{Z}/n\mathbb{Z}$-invariant because

$$x_d(M^\vee) \neq 0 \iff r \cdot x_d(M^\vee) = (e^{2\pi i/n})^{|d|} x_d(M^\vee) \neq 0 \quad .$$

On the other hand $T_{\mathcal{C}^R}$ is not D_n-invariant, because the Poincaré dual of a general rectangular Young diagram is not necessarily rectangular (as opposed to the case of a frozen Young diagram, see Section 2.1).

Thanks to the fact that the action of s on the critical points matches the action by conjugation, we have

$$[M^\vee_{I^\vee}] \in T_{\mathcal{C}^R} \iff [M^\vee_{I^\vee}] \in V \quad , \quad V = \bigcap_{g \in D_n} g \cdot T_{\mathcal{C}^R}$$

and V is an open D_n-invariant subscheme of $T_{\mathcal{C}^R}$. Defining $U = \theta_R^{-1}(V) \subset (\mathbb{C}^\times)^{k(n-k)}$, this is an open subscheme of the space of rank one $\mathbb{C}$-linear local systems on the Gelfand-Zetlin torus $L_{GZ} \subset \mathrm{Gr}_k(n)$. Since θ_R is an open embedding, we can use it to pull-back the D_n action on U, so that diagram (3.1) becomes fully $\mathbb{Z}/n\mathbb{Z}$-equivariant, and D_n equivariant whenever restricted to critical points and values. □

In Theorem 3.4.7 we show that there are indeed classes of Grassmannians for which the considerations of Theorem 3.4.4 and 3.4.6 suffice to identify a complete set of generators for the Fukaya category, and prove homological mirror symmetry.

Theorem 3.4.7. *When $n = p$ is prime the objects $(L_{GZ})_I$ split-generate the Fukaya category of $\mathrm{Gr}_k(p)$, and for every $\lambda \in \mathbb{C}$ there is an equivalence of triangulated categories*

$$\mathbf{D}\mathcal{F}_\lambda(\mathrm{Gr}_k(p)) \simeq \mathbf{D}\mathcal{S}(W^{-1}(\lambda)) \quad .$$

Proof. By Proposition 3.1.4 and the assumption $n = p$ prime, we have that

$$\dim \mathrm{QH}_\lambda(\mathrm{Gr}_k(p)) = 1 \qquad \forall \lambda \text{ eigenvalue of } c_1 \star \quad .$$

Thanks to Theorem B.3.4, any nonzero object supported on the Gelfand-Zetlin torus will generate the summand of the Fukaya category in which it lives, therefore it suffices to show that the torus supports objects in all summands to have a complete set of generators.

When $n = 2$ we have $\mathrm{Gr}(1,2) = \mathbb{P}^1$, and the objects of the statement are the two local system on the Clifford torus giving objects with nontrivial Floer cohomology investigated by Cho [14]. We will show that when $n = p > 2$ is prime all critical points $[M_{I^\vee}^\vee]$ of $W : \mathcal{U}_{k,p} \to \mathbb{C}$ are contained in the rectangular chart $T_{\mathcal{C}^R}$. By Theorem 3.4.4 and Remark 3.4.5 this will imply that for every $I = \{\zeta_1, \ldots, \zeta_k\}$ size k set of roots of $x^p = (-1)^{k+1}$ the object $(L_{GZ})_I$ is nonzero in the summand $\mathcal{F}_\lambda(\mathrm{Gr}_k(p))$ of the Fukaya category, where $\lambda = pS_\square(I) = p(\zeta_1 + \ldots + \zeta_k)$.

By Proposition 3.3.4 and Proposition 2.1.11 $[M_{I^\vee}^\vee] \in T_{\mathcal{C}^R}$ if and only if

$$S_{i\times j}(I) \neq 0 \quad \forall i \times j \quad \text{ rectangular diagram in } k \times (p-k) \text{ grid} \quad .$$

If by contradiction $S_{i\times j}(I) = 0$ for some I and diagram $i \times j$, then by definition of Schur polynomial this means that

$$S_{i\times j}(I) = \sum_{T_{i\times j}} \zeta_1^{t_1} \cdots \zeta_k^{t_k} = 0 \quad ,$$

where the sum runs over all semi-standard Young tableaux $T_{i\times j}$ of the diagram $i \times j$. Let us assume first that k is odd, so that roots of $x^p = (-1)^{k+1} = 1$ are p-th roots of unity. Then each term in $S_{i\times j}(I)$ above is itself a p-th root of unity, and we have a vanishing sum of a number of p-th roots of unity equal to $S_{i\times j}(1, \dots, 1)$, i.e. the number of semi-standard Young tableaux of $i \times j$. A result of Lam-Leung on vanishing sums of roots of unity [50, Theorem 5.2] implies that $S_{i\times j}(1, \dots, 1)$ must be a multiple of p. On the other hand by Stanley's hook-content formula (Theorem 2.1.9)

$$S_{i\times j}(1, \dots, 1) = \prod_{u\in i\times j} \frac{k + c(u)}{h(u)} \quad .$$

Therefore we must have

$$\prod_{u\in i\times j} \frac{k + c(u)}{h(u)} \equiv 0 \pmod p \quad .$$

By assumption p is prime and $1 \leqslant h(u) \leqslant p - 1$, therefore there exists $u \in i \times j$ such that

$$c(u) \equiv -k \pmod p \quad .$$

Being $u \in i \times j$, it has to be at entry (s, t) of the grid with $1 \leqslant s \leqslant i$ and $1 \leqslant t \leqslant j$. Also notice that being the rectangle $i \times j$ in a $k \times (p - k)$ grid we have $1 \leqslant i \leqslant k$ and $1 \leqslant j \leqslant p - k$. We conclude that

$$-k < 1 - k \leqslant 1 - i \leqslant c(u) = t - s \leqslant j - 1 \leqslant p - k - 1 < p - k$$

in contradiction with $c(u) \equiv -k$ modulo p. This concludes the proof in the case of k odd. When k is even I consists of roots of $x^p = (-1)^{k+1} = -1$ and the argument above doesn't apply; on the other hand by Proposition 2.1.11

$$S_{i\times j}(I) \neq 0 \iff S_{j\times i}(e^{\pi i p} I^c) \neq 0$$

where I^c denotes the roots of $x^p = (-1)^{k+1} = -1$ that are not in I, giving $p-k$ distinct roots of $x^p = (-1)^{p-k+1} = 1$ once rescaled by $e^{\pi i p}$. This reduces the problem to the previous case and thus proves that the collection of $(L_{GZ})_I$ gives generators for all summands of the Fukaya category.

To prove homological mirror symmetry we argue as follows. Denoted $d = k(p-k)$, the assumption of $n = p$ prime guarantees that for every critical value $\lambda \in \mathbb{C}$ there is exactly one critical point $[M^\vee_{I^\vee_\lambda}] \in \mathcal{U}_{k,p}$ of W with critical value λ, and $[M^\vee_{I^\vee_\lambda}] \in T_{\mathcal{C}^R}$ by the argument given earlier. Therefore $[M^\vee_{I^\vee_\lambda}] = \theta_R(\mathrm{hol}_{I_\lambda})$ for a unique $\mathrm{hol}_{I_\lambda} \in (\mathbb{C}^\times)^d$ critical point of W_{T^d} with critical value λ. We denote $m_\lambda \subset \mathbb{C}[x_1^\pm, \dots, x_d^\pm]$ the maximal ideal corresponding to the point hol_{I_λ}, and $T^d_{I_\lambda}$ the generator of $\mathbf{D}\mathcal{F}_\lambda(\mathrm{Gr}_k(p))$.

The critical point hol_{I_λ} is nondegenerate. This condition holds because a degenerate critical point of W_{T^d} would correspond to a non-reduced point in the critical locus scheme $Z \subset \mathrm{Gr}^\vee_k(p)$ of W (see for example [63, Lemma 3.5]), but closed mirror symmetry for Grassmannians (Theorem 2.3.5) says that

$$Z = \mathrm{Spec}(\mathrm{Jac}(W)) \cong \mathrm{Spec}(\mathrm{QH}(\mathrm{Gr}_k(p))) \quad ,$$

and this scheme is reduced because $\mathrm{QH}(\mathrm{Gr}_k(p))$ is semi-simple, being

$$\mathrm{QH}(\mathrm{Gr}_k(p)) = \bigoplus_\lambda \mathrm{QH}_\lambda(\mathrm{Gr}_k(p))$$

an algebra decomposition with one-dimensional summands. From Theorem B.3.5 of the Setup section we conclude that $\mathbf{D}\mathcal{F}_\lambda(\mathrm{Gr}_k(p)) \simeq \mathbf{D}(Cl_d)$, where Cl_d denotes the Clifford algebra of the quadratic form of rank d on $\mathbb{C}^d$. Now combining the locality property of the derived category of singularities established by Orlov [62, Proposition 1.14] and the fact proved above that all the critical points of W are in the rectangular chart $T_{\mathcal{C}^R} \subset \mathrm{Gr}^\vee(k,p)$, we have for any $\lambda \in \mathbb{C}$

$$\mathbf{D}\mathcal{S}(W^{-1}(\lambda)) \simeq \mathbf{D}\mathcal{S}(W^{-1}(\lambda) \cap T_{\mathcal{C}^R})$$

where the intersection on the right is an affine scheme given by

$$W^{-1}(\lambda) \cap T_{\mathcal{C}^R} = \mathrm{Spec}(\mathbb{C}[x_d^\pm : d \text{ rectangular}]/(W \restriction_{T_{\mathcal{C}^R}} - \lambda)) \quad .$$

Matrix factorizations are just another model for the category of singularity in the affine case, so that to conclude the proof of homological mirror symmetry it suffices to establish an equivalence

$$\mathbf{D}(Cl_d) \simeq \mathbf{D}\mathcal{M}(\mathbb{C}[x_d : d \text{ rectangular}], W \restriction_{T_{\mathcal{C}}R} - \lambda) \quad .$$

Dyckerhoff (Theorem 4.11 [23]) shows that the localization ring morphism $\mathbb{C}[x_1^{\pm}, \ldots, x_d^{\pm}] \to \mathbb{C}[x_1^{\pm}, \ldots, x_d^{\pm}]_{m_\lambda}$ induces an equivalence

$$\mathbf{D}\mathcal{M}(\mathbb{C}[x_1^{\pm}, \ldots, x_d^{\pm}], W_{T^d} - \lambda) \simeq \mathbf{D}\mathcal{M}(\mathbb{C}[x_1^{\pm}, \ldots, x_d^{\pm}]_{m_\lambda}, W_{T^d} - \lambda)$$

and explicitly describes a generator [23, Corollary 2.7] of $\mathbf{D}\mathcal{M}(\mathbb{C}[x_1^{\pm}, \ldots, x_d^{\pm}]_{m_\lambda}, W_{T^d} - \lambda)$ whose endomorphism algebra is again the Clifford algebra Cl_d above, so that

$$\mathbf{D}\mathcal{M}(\mathbb{C}[x_1^{\pm}, \ldots, x_d^{\pm}]_{m_\lambda}, W_{T^d} - \lambda) \simeq \mathbf{D}(Cl_d)$$

and this concludes the proof (see also Sheridan [77, Section 6.1] for a discussion of intrinsic formality of Clifford algebras over $\mathbb{C}$). $\square$

Chapter 4

EXAMPLES OF EXOTIC TORI

In this chapter, we describe an iterative construction of Lagrangian tori in the complex Grassmannian $\mathrm{Gr}(k,n)$, based on the cluster algebra structure of the coordinate ring of a mirror Landau-Ginzburg model proposed by Marsh-Rietsch [53]. Each torus comes with a Laurent polynomial, and local systems controlled by the k-variables Schur polynomials at the n-th roots of unity. We use this data to give examples of monotone Lagrangian tori that are neither displaceable nor Hamiltonian isotopic to each other, and that support nonzero objects in different summands of the spectral decomposition of the Fukaya category over $\mathbb{C}$.

4.1. Initial seed and mutation procedure

Definition 4.1.1. *A quiver with potential of type (k,n) is a pair (Q,W), where:*

1. *Q is an oriented connected graph, with no self-edges or oriented 2 loops, and whose nodes are labeled by Plücker coordinates $x_d \in \mathcal{A}_{k,n}$;*
2. *W is a Laurent polynomial in the labels of the nodes of Q .*

As part of the data, the nodes of Q are partitioned in two groups, called frozen and mutable.

The iterative construction we describe in this section begins with a specific quiver with potential.

Definition 4.1.2. *The initial seed of type (k,n) is the quiver with potential (Q_0,W_0), where:*

1. *Q_0 is the oriented labeled graph in Figure 4.1 ;*

2. W_0 *is the Laurent polynomial*

$$x_{1\times 1}+\sum_{i=2}^{k}\sum_{j=1}^{n-k}\frac{x_{i\times j}x_{(i-2)\times(j-1)}}{x_{(i-1)\times(j-1)}x_{(i-1)\times j}}+\frac{x_{(k-1)\times(n-k-1)}}{x_{k\times(n-k)}}+\sum_{i=1}^{k}\sum_{j=2}^{n-k}\frac{x_{i\times j}x_{(i-1)\times(j-2)}}{x_{(i-1)\times(j-1)}x_{i\times(j-1)}}\quad .$$

A node of Q_0 *is frozen if its label is* $x_{i\times j}$ *with* $i\times j=\varnothing$, $i=k$ *or* $j=n-k$*; the remaining nodes are mutable.*

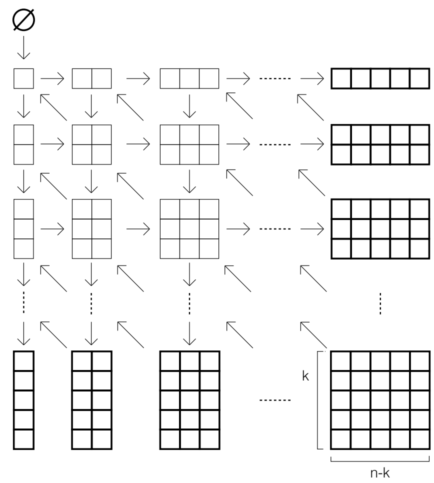

Figure 4.1: Initial quiver Q_0: labels x_d are indicated by d, frozen nodes in bold type.

Observe that the labels on the nodes of Q_0 are precisely the $k(n-k)+1$ variables x_d where d is a rectangular Young diagram, and n of the nodes are frozen.

Given a quiver with potential (Q,W) as in Definition 4.1.1, and fixed a mutable node v of Q, one can form a new labeled quiver Q' as follows:

1. start with $Q'=Q$, and for all length 2 paths $a\to v\to b$ with at least one mutable node among a and b, add to Q' a new edge $a\to b$;
2. modify Q' by reversing all the edges incident to v ;
3. remove all oriented 2-cycles formed in Q', by deleting their arrows .

Calling $l(w)$ the label of a node w in Q, define new labels $l'(w)$ in Q' by declaring $l'(w)=l(w)$ if $w\neq v$, and

$$l'(v)=\frac{\prod_{w\to v}l(w)+\prod_{v\to w}l(w)}{l(v)}\quad .$$

Since Q and Q' have the same nodes, the nodes of Q' inherit the property of being frozen or mutable from Q.

Definition 4.1.3. *The mutation of (Q, W) along v is the pair (Q', W') with Q' constructed as above, and W' obtained from W by substitution $l(v) = (\prod_{w \to v} l'(w) + \prod_{v \to w} l'(w)) l'(v)^{-1}$.*

A priori, mutations of quivers with potentials as in Definition 4.1.1 are not necessarily quivers with potentials, since $l'(v)$ and W' are only rational functions of the Plücker coordinates x_d. The following guarantees that certain iterated mutations of the initial seed of Definition 4.1.2 remain quivers with potentials.

Proposition 4.1.4. *(Scott [74, Theorem 3] and Marsh-Rietsch [53, Section 6.3]) Given a finite sequence of mutations that starts at (Q, W) and ends at (Q', W'):*

1. *if $(Q, W) = (Q_0, W_0)$ is the initial seed of Definition 4.1.2, then W' is a Laurent polynomial in the labels of Q' ;*
2. *if in addition each mutation of the sequence is based at some node with two incoming and two outgoing edges, then the labels of Q' are Plücker coordinates x_d .*

Proof. For the reader's convenience, we explain how the statements follow from the cited results. It suffices to prove them when the sequence of mutations consists of a single mutation, as the general case follows by applying repeatedly the same argument.

1. Marsh-Rietsch [53, Section 6.3] (see also Rietsch-Williams [70, Proposition 9.5]) showed that the potential W_0 of the initial seed is the restriction $W_0 = W_{|T_0}$ of a regular function $W \in \mathcal{A}_{k,n}$ to an algebraic torus $T_0 \subset \mathrm{Gr}_k^\vee(n)$ defined by

$$T_0 = \{[M] \in \mathrm{Gr}_k^\vee(n) \ : \ l(M) \neq 0 \ \forall l \text{ label of } Q_0\} \quad .$$

By Scott [74, Theorem 3] $\mathcal{A}_{k,n}$ is a cluster algebra, and the rational functions labeling the nodes of Q' are cluster variables. Just as with the labels of Q_0, one can use the labels of Q' to define an algebraic torus $T' \subset \mathrm{Gr}_k^\vee(n)$ via

$$T' = \{[M] \in \mathrm{Gr}_k^\vee(n) \ : \ l'(M) \neq 0 \ \forall l' \text{ label of } Q'\} \quad ;$$

this torus is called toric chart in [74, Section 6]. By Definition 4.1.3, W' is obtained from W_0 by substitution $l(v) = (\prod_{w\to v} l'(w) + \prod_{v\to w} l'(w))l'(v)^{-1}$. This means that W' is the pull-back of W_0 along the birational map from T' to T_0 defined by the substitution formula. It is part of the statement that $\mathcal{A}_{k,n}$ is a cluster algebra that the substitution formula gives a relation

$$l(v)l'(v) - \prod_{w\to v} l'(w) - \prod_{v\to w} l'(w) \quad \in \quad \mathcal{I}_{k,n} \quad ,$$

so that $W' = W_{|T'}$ is a restriction of W as well. In particular, W' is a regular function on the algebraic torus T', and hence a Laurent polynomial.

2. If the mutation from (Q, W) to (Q', W') is based at some node v with two incoming and two outgoing edges, denote $\{v_1^+, v_2^+\}$ and $\{v_1^-, v_2^-\}$ the corresponding nodes of Q adjacent to v. The substitution formula of Definition 4.1.3 simplifies to $l(v) = (l'(v_1^+)l(v_2^+) + l'(v_1^-)l(v_2^-))l'(v)^{-1}$. By definition of mutation $l'(v_i^+) = l(v_i^+)$ and $l'(v_i^-) = l(v_i^-)$ for $i = 1, 2$. Moreover, by assumption the l labels are Plücker coordinates, meaning that $l(v_i^+) = x_{d_i^+}$ and $l(v_i^-) = x_{d_i^-}$ for $i = 1, 2$ and $l(v) = x_d$ for some Young diagrams $d, d_1^+, d_2^+, d_1^-, d_2^- \subseteq k \times (n-k)$. Scott [74, proof of Theorem 3] proves that this implies $l'(v) = x_{d'}$ for some Young diagram $d' \subseteq k \times (n-k)$ too, using combinatorial objects called wiring arrangements. The same phenomenon is discussed in Rietsch-Williams [70, Lemma 5.6] in the combinatorial framework of plabic graphs; see also the proof of Proposition 4.2.2 for a comparison between plabic graphs and quivers.

□

Definition 4.1.5. *A length l Plücker sequence of mutations of type (k, n), denoted $\mathfrak{s}$, is a finite sequence of pairs (Q_i, W_i) with $0 \leqslant i \leqslant l$ such that:*

1. *(Q_0, W_0) is the initial seed of type (k, n) of Definition 4.1.2 ;*
2. *(Q_{i+1}, W_{i+1}) is obtained from (Q_i, W_i) by mutation along a mutable node with two incoming and outgoing edges, as in Definition 4.1.3 .*

If we want to suppress the length l, we denote $(Q_l, W_l) = (Q_{\mathfrak{s}}, W_{\mathfrak{s}})$ and call it the final quiver with potential of $\mathfrak{s}$.

4.2. Lagrangian tori from Plücker seeds

In this section, Σ denotes a complete fan in $\mathbb{R}^{k(n-k)}$, and $X(\Sigma)$ its associated proper toric variety; see for example Fulton [30] for background material on toric geometry. The reader familiar with symplectic manifolds and Hamiltonian torus actions can think of Σ as the normal fan $\Sigma = \Sigma^n\Delta$ of a moment polytope Δ, with the important caveat that $X(\Sigma)$ is typically singular, and not even an orbifold; in this case Δ should be thought as the closure of the open convex region obtained from the moment map of the maximal torus orbit.

We will assume that the primitive generators of the rays of Σ in the lattice $\mathbb{Z}^{k(n-k)} \subset \mathbb{R}^{k(n-k)}$ are the vertices of a convex polytope P, and alternatively think of Σ as its face fan $\Sigma = \Sigma^f P$. This condition is equivalent to $X(\Sigma)$ being Fano, and P is sometimes called a Fano polytope. The reader should not confuse the polytopes Δ and P: the second is always a lattice polytope, whereas the first may not be. The two polytopes are related by polar duality $\Delta = P^\circ$.

Definition 4.2.1. *If $X \subset \mathbb{P}^M$ is a smooth subvariety of complex dimension N, an embedded toric degeneration $X \rightsquigarrow X(\Sigma)$ is a closed subscheme $\mathcal{X} \subset \mathbb{P}^M \times \mathbb{C}$ such that the map $p : \mathcal{X} \to \mathbb{C}$ obtained by restriction of the projection satisfies the following properties:*

- *$p^{-1}(\mathbb{C}^\times) \cong X \times \mathbb{C}^\times$ as schemes over $\mathbb{C}^\times$;*
- *$p^{-1}(0) \subset \mathbb{P}^M$ is an orbit closure for some linear torus action $(\mathbb{C}^\times)^N \curvearrowright \mathbb{P}^M$;*
- *$p^{-1}(0)$ is a toric variety with fan Σ .*

Proposition 4.2.2. *(Rietsch-Williams [70, Theorem 1.1]) Every Plücker sequence $\mathfrak{s}$ of mutations of type (k, n) has an associated embedded toric degeneration $\mathrm{Gr}_k(n) \rightsquigarrow X(\Sigma_\mathfrak{s})$, where $\Sigma_\mathfrak{s} = \Sigma^f P_\mathfrak{s}$ is the face fan of the Newton polytope $P_\mathfrak{s}$ of the final potential $W_\mathfrak{s}$.*

Proof. For the reader's convenience, we provide details on how to specialize the result of Rietsch-Williams [70, Theorem 1.1] to recover this statement. Each step (Q_i, W_i) of the Plücker sequence $\mathfrak{s}$ corresponds to a reduced plabic graph G_i of type $\pi_{k,n}$ [70, Section 3], which is a combinatorial object encoding the quiver Q_i and the Laurent polynomial W_i simultaneously. Nodes in Q_i correspond to faces in G_i, and each arrow of Q_i is dual to an edge of G_i, with black/white nodes of the plabic graph respectively to the right/left of the arrow. The frozen nodes of Q_i correspond to boundary faces of G_i, and the mutable nodes to interior faces. Mutations at some mutable node with two incoming and outgoing arrows in Q_i correspond to a square move on the plabic graph G_i. The Plücker variables on nodes of Q_i are labeled by the Young diagrams appearing on the faces of G_i, which are induced by trips as in [70, Definition 3.5]. The Laurent polynomial W_i is a generating function counting matchings on the plabic graph G_i [70, Theorem 18.2]; see also Marsh-Scott [54] for a proof. The initial seed (Q_0, W_0) corresponds to a particular plabic graph $G_0 = G^{rec}_{k,n}$, called the rectangle plabic graph in [70, Section 4]. Consider the divisor $D_i \subset \mathrm{Gr}_k(n)$ cut out by the equation $x_{d_i} = 0$, with $d_i \subseteq k \times (n-k)$ one of the n frozen Young diagrams, and call $D = r_1 D_1 + \cdots + r_n D_n$ a general effective divisor with the same support. One can associate to the pair $(D, G_\mathfrak{s})$ a convex polytope $\Delta_{G_\mathfrak{s}}(D)$ known as Okounkov body [70, Section 1.2]. From now on set $r_1 = \ldots = r_n = 1$, and call $D_{FZ} = D_1 + \cdots + D_n$ the corresponding divisor. There exists a scaling factor $r_\mathfrak{s} \in \mathbb{Q}^+$ such that $r_\mathfrak{s}\Delta_{G_\mathfrak{s}}(D_{FZ})$ is a normal lattice polytope [20, Definition 2.2.9]; normality is referred to as integer decomposition property in [70, Definition 17.7], and from [70, Proposition 19.4] one sees that the scaling factor mentioned there is related to ours by $r_\mathfrak{s} = \frac{r_{G_\mathfrak{s}}}{n}$. From [70, Section 17] one gets a degeneration of $\mathrm{Gr}_k(n)$ to the toric variety associated with the polytope $r_\mathfrak{s}\Delta_{G_\mathfrak{s}}(D_{FZ})$, and this is an embedded toric degeneration in the sense of Definition 4.2.1 with fan $\Sigma_\mathfrak{s} = \Sigma^n r_\mathfrak{s}\Delta_{G_\mathfrak{s}}(D_{FZ}) = \Sigma^n \Delta_{G_\mathfrak{s}}(D_{FZ})$, where we used that the normal fan of a polytope doesn't change under scaling. In [70, Theorem 1.1] and [70, Definition 10.14], an interpretation of $\Delta_{G_\mathfrak{s}}(r_1 D_1 + \cdots + r_n D_n)$ is given in terms of the tropicalization of $W_\mathfrak{s}$. Setting $r_1 = \ldots = r_n = 1$, one finds in particular that for $D_{FZ} = D_1 + \cdots + D_n$ in fact

$$\Delta_{G_\mathfrak{s}}(D_{FZ}) = \{v \in \mathbb{R}^{k(n-k)} \;:\; \langle v, u\rangle \geqslant -1 \text{ for every vertex } u \in P_\mathfrak{s}\} \quad ;$$

here $P_\mathfrak{s}$ denotes the Newton polytope of the Laurent polynomial $W_\mathfrak{s}$, i.e. the convex hull of its exponents. This is precisely the definition of polar dual polytope, so denote $\Delta_{G_\mathfrak{s}}(D_{FZ}) = P_\mathfrak{s}^\circ$. Since the normal fan of a polytope equals the face fan of its polar dual and polar duality is an involution, we find that $\Sigma_\mathfrak{s} = \Sigma^n \Delta_{G_\mathfrak{s}}(D_{FZ}) = \Sigma^f P_\mathfrak{s}$ as in the statement.

□

Proposition 4.2.3. *(Harada-Kaveh [41, Theorem B]) Every Plücker sequence $\mathfrak{s}$ of mutations of type (k,n) has an associated Lagrangian torus $L_{\mathfrak{s}} \subset \mathrm{Gr}_k(n)$, and it comes with a canonical basis of $H_1(L_{\mathfrak{s}};\mathbb{Z})$.*

Proof. For the reader's convenience, we provide details on how to specialize the result of Harada-Kaveh [41, Theorem B] to recover this statement. Recall from Proposition 4.2.2 that $\mathfrak{s}$ determines a degeneration of $\mathrm{Gr}_k(n)$ to the toric variety associated with the polytope $r_{\mathfrak{s}}\Delta_{G_{\mathfrak{s}}}(D_{FZ})$, known as Okounkov body; for a detailed description of the value semigroup underlying this Okounkov body and of why it satisfies the assumptions of [41, Theorem B], see [70, Section 17.3]. From [41, Theorem B] one deduces the existence of an open set $U_{\mathfrak{s}} \subset \mathrm{Gr}_k(n)$ and a smooth submersion $\mu_{\mathfrak{s}} : U_{\mathfrak{s}} \to \mathbb{R}^{k(n-k)}$ whose image is the interior of the polytope, and whose fibers are Lagrangian tori. Since $\mu_{\mathfrak{s}}$ is a regular Lagrangian fibration, the standard basis of $\mathbb{R}^{k(n-k)}$ lifts to a basis of $H_1(L_{\mathfrak{s}};\mathbb{Z})$, by dualizing with the symplectic structure a lift to some point of the fiber. □

Definition 4.2.4. *The Lagrangians $L_{\mathfrak{s}} \subset \mathrm{Gr}_k(n)$ of Proposition 4.2.3 are called Plücker tori, and the elements $\gamma_d \in H_1(L_{\mathfrak{s}};\mathbb{Z})$ of the canonical basis are called canonical cycles. We index the canonical cycles by Young diagrams $d \subseteq k \times (n-k)$ such that $d \neq \varnothing$ and d appears in a label x_d of the final quiver $Q_{\mathfrak{s}}$.*

Definition 4.2.5. *For each Plücker torus $L_{\mathfrak{s}} \subset \mathrm{Gr}_k(n)$ and set I, denote ξ_I the rank one local system whose holonomy $\mathrm{hol}_{\xi_I} : H_1(L_{\mathfrak{s}};\mathbb{Z}) \to \mathbb{C}^\times$ around the canonical cycles of Definition 4.2.4 is given by the formula*

$$\mathrm{hol}_{\xi_I}(\gamma_d) = S_d(I) \in \mathbb{C}^\times \quad ;$$

if $S_d(I) = 0$ for some d appearing in a label x_d of the final quiver of $\mathfrak{s}$, then ξ_I is not defined.

If $\mathfrak{s}$ is a Plücker sequence of type (k,n), after setting $x_\varnothing = 1$ the Laurent polynomial $W_{\mathfrak{s}}$ can be thought of as a regular function on the algebraic torus $H_1(L_{\mathfrak{s}};\mathbb{Z}) \otimes \mathbb{C}^\times \cong (\mathbb{C}^\times)^{k(n-k)}$. Setting $x_\varnothing = 1$ corresponds to thinking $\mathcal{A}_{k,n} = \mathcal{O}(\mathcal{U}_{k,n})$ as algebra of regular functions on $\mathcal{U}_{k,n} = \mathrm{Gr}_k^\vee(n) \backslash D_{FZ}^\vee$ rather than on its affine cone.

Definition 4.2.6. *For any Pücker sequence $\mathfrak{s}$ of type (k,n), define $H_1(L_\mathfrak{s};\mathbb{Z})\otimes\mathbb{C}^\times = T_\mathfrak{s}$ to be the cluster chart corresponding to $L_\mathfrak{s}$.*

The canonical cycles $\gamma_d \in H_1(L_\mathfrak{s};\mathbb{Z})$ of Definition 4.2.4 give an isomorphism of schemes $T_\mathfrak{s} \cong (\mathbb{C}^\times)^{k(n-k)}$, where one thinks the latter torus as having coordinates x_d labeled by Young diagrams $d \subseteq k \times (n-k)$ such that $d \neq \varnothing$ and d appears in some label of the quiver $Q_\mathfrak{s}$. Alternatively, one can think $T_\mathfrak{s} \subset \mathrm{Gr}_k^\vee(n)$ as the open subscheme

$$\{[M] \in \mathrm{Gr}_k^\vee(n) \ : \ x_d(M) \neq 0 \ \forall d \text{ label of } Q_\mathfrak{s}\} \quad ;$$

this identification is described by Scott [74, Theorem 4].

Conjecture 4.2.7. *If $\mathfrak{s}$ and $\mathfrak{s}'$ are two Plücker sequences of type (k,n), and ϕ is a Hamiltonian isotopy of $\mathrm{Gr}_k(n)$ such that $\phi(L_\mathfrak{s}) = L_{\mathfrak{s}'}$, then the induced map $\phi_* : H_1(L_\mathfrak{s};\mathbb{Z}) \to H_1(L_{\mathfrak{s}'};\mathbb{Z})$ is such that*

$$W_\mathfrak{s} \sim W_{\mathfrak{s}'} \circ (\phi_* \otimes \mathrm{id}_{\mathbb{C}^\times}) \quad ,$$

where $\sim$ denotes equality up to automorphisms of $T_\mathfrak{s}$.

Under some assumptions on the singularities of the toric varieties $X(\Sigma_\mathfrak{s})$ appearing as limits of the degenerations $\mathrm{Gr}_k(n) \rightsquigarrow X(\Sigma_\mathfrak{s})$, the conjecture above can be verified. We describe below how, and give some sample applications in Section 4.3.

Definition 4.2.8. *If $X(\Sigma)$ is a projective toric variety, a toric resolution consists of a smooth projective toric variety $X(\widetilde{\Sigma})$ with a toric morphism $r : X(\widetilde{\Sigma}) \to X(\Sigma)$ which is a birational equivalence.*

Any toric variety $X(\Sigma)$ has a toric resolution; see for example [20, Chapter 11]. Toric resolutions can be constructed by taking refinements $\widetilde{\Sigma}$ of the fan Σ, which have natural associated morphisms r. The refined fan $\widetilde{\Sigma}$ has in general more rays than Σ, and these correspond to torus invariant divisors in the exceptional locus $r^{-1}(\mathrm{Sing}\, X(\Sigma))$.

Definition 4.2.9. *A toric resolution $r : X(\widetilde{\Sigma}) \to X(\Sigma)$ is small if $\widetilde{\Sigma}$ and Σ have the same rays. Being small is equivalent to* $\mathrm{codim}_\mathbb{C}(r^{-1}(\mathrm{Sing}\, X(\Sigma))) \geqslant 2$*; see for example [20, Proposition 11.1.10].*

Proposition 4.2.10. *If $\mathfrak{s}$ is a Plücker sequence of type (k,n), and the toric variety $X(\Sigma_\mathfrak{s})$ admits a small resolution, then $L_\mathfrak{s} \subset \mathrm{Gr}_k(n)$ is monotone and has Maslov 2 disk potential $W_\mathfrak{s}$ with respect to the basis of canonical cycles for $H_1(L_\mathfrak{s};\mathbb{Z})$.*

Proof. Recall from Proposition 4.2.3 that there is a smooth submersion $\mu_{\mathfrak{s}} : U_{\mathfrak{s}} \to \mathbb{R}^{k(n-k)}$ with Lagrangian torus fibers, defined on some open set $U_{\mathfrak{s}} \subset \mathrm{Gr}_k(n)$. If $P_{\mathfrak{s}}$ is the Newton polytope of the Laurent polynomial $W_{\mathfrak{s}}$, the image of this map is the interior of the polytope described in Proposition 4.2.2:

$$r_{\mathfrak{s}}\Delta_{G_{\mathfrak{s}}}(D_{FZ}) = \{v \in \mathbb{R}^{k(n-k)} \;:\; \langle v, u\rangle \geqslant -r_{\mathfrak{s}} \text{ for every vertex } u \in P_{\mathfrak{s}}\} \quad .$$

Call v a point in the interior, and $L_{\mathfrak{s}}(v) = \mu_{\mathfrak{s}}^{-1}(v)$ the corresponding Lagrangian torus fiber. The assumption that $X(\Sigma_{\mathfrak{s}})$ has a small toric resolution allows to invoke a theorem of Nishinou-Nohara-Ueda [58, Theorem 10.1], and conclude that the Maslov 2 disk potential of $L_{\mathfrak{s}}(v) \subset \mathrm{Gr}_k(n)$ has one monomial for each facet $\langle v, u\rangle = -r_{\mathfrak{s}}$ of $r_{\mathfrak{s}}\Delta_{G_{\mathfrak{s}}}(D_{FZ})$, with exponent $u \in H_1(L_{\mathfrak{s}}(v); \mathbb{Z})$. The symplectic area of a Maslov 2 disk with boundary u is $2\pi(\langle v, u\rangle + r_{\mathfrak{s}})$; see Cho-Oh [17, Theorem 8.1] for a proof. The choice $v = 0$ guarantees that all the areas are equal, and thus $L_{\mathfrak{s}} = L_{\mathfrak{s}}(0)$ is monotone. □

4.3. Analysis of critical points and f-vectors

In this section, we prove that the Plücker tori constructed in Section 4.2 are in general not Hamiltonian isotopic, and can support objects in different summands of the Fukaya category. These results are by no means optimal; they are meant to illustrate new phenomena, and we give some indications on how one can prove analogous statements using the same techniques.

We begin by focusing on Grassmannians of planes $\mathrm{Gr}_2(n)$. In this case, the Plücker coordinates appearing as labels of a quiver $Q_{\mathfrak{s}}$ have a simple combinatorial description.

Definition 4.3.1. *Let $n > 2$, and consider n points on S^1, labeled counter-clockwise from 1 to n. A triangulation Γ of $[n]$ is a collection of subsets $\{i, j\} \subset [n]$ with $i \neq j$, such that connecting i and j with an arc in D^2 for all $\{i, j\} \in \Gamma$ one gets a triangulation of the n-gon with vertices at $[n]$.*

Lemma 4.3.2. *(Fomin-Zelevinsky [27, Proposition 12.5]) A collection of Young diagrams $d \subseteq 2 \times (n-2)$ labels the nodes of $Q_{\mathfrak{s}}$ for some Plücker sequence $\mathfrak{s}$ of type $(2, n)$ if and only if the set $\Gamma = \{d^{|} \subset [n]\}$ is a triangulation of $[n]$.*

Lemma 4.3.3. *(Nohara-Ueda [59, Theorem 1.5] and [60, Theorem 1.1]) If $k = 2$ then*

Conjecture 4.2.7 holds, and the Lagrangian tori $L_{\mathfrak{s}} \subset \mathrm{Gr}_2(n)$ are monotone for all $\mathfrak{s}$ and have disk potential $W_{L_{\mathfrak{s}}} = W_{\mathfrak{s}}$.

Proof. In view of Proposition 4.2.10, it suffices to prove that for any Plücker sequence $\mathfrak{s}$ of type $(2, n)$ the toric variety $X(\Sigma_{\mathfrak{s}})$ has a small toric resolution. From Lemma 4.3.2, the labels of $Q_{\mathfrak{s}}$ define a triangulation $\Gamma_{\mathfrak{s}}$ of $[n]$. Nohara-Ueda [60, Theorem 1.1] describe an open embedding $\iota_{\Gamma_{\mathfrak{s}}} : (\mathbb{C}^\times)^{2(n-2)} \to \mathrm{Gr}_k^\vee(n)$ such that $\iota_{\Gamma_{\mathfrak{s}}}^* W = W_{\Gamma_{\mathfrak{s}}}$, where $W \in \mathcal{A}_{k,n}$ is the Landau-Ginzburg potential defined by Marsh-Rietsch [53] and $W_{\Gamma_{\mathfrak{s}}}$ is a Laurent polynomial associated to the triangulation $\Gamma_{\mathfrak{s}}$. It was shown earlier by Nohara-Ueda [59, Proposition 7.4] that the polar dual of the Newton polytope of $W_{\Gamma_{\mathfrak{s}}}$ is a lattice polytope $\Delta_{\Gamma_{\mathfrak{s}}} = \mathrm{Newt}^\circ(W_{\Gamma_{\mathfrak{s}}})$ (as opposed to just a rational polytope) and that the associated toric variety $X(\Delta_{\Gamma_{\mathfrak{s}}})$ has a small toric resolution [59, Theorem 1.5]. Since polar duality exchanges normal and face fans $X(\Sigma^n \Delta_{\Gamma_{\mathfrak{s}}}) = X(\Sigma^f \,\mathrm{Newt}(W_{\Gamma_{\mathfrak{s}}}))$. The image of the embedding $\iota_{\Gamma_{\mathfrak{s}}}$ is the cluster chart $T_{\mathfrak{s}}$ and $W_{\mathfrak{s}} = W_{|T_{\mathfrak{s}}}$, so $W_{\Gamma_{\mathfrak{s}}}$ and $W_{\mathfrak{s}}$ are Laurent polynomials related by an automorphism of the torus, therefore their Newton polytopes $\mathrm{Newt}(W_{\Gamma_{\mathfrak{s}}})$ and $P_{\mathfrak{s}}$ are equivalent under the action of $GL(2(n-2), \mathbb{Z})$. We conclude that $X(\Sigma^f \,\mathrm{Newt}(W_{\Gamma_{\mathfrak{s}}})) \cong X(\Sigma^f P_{\mathfrak{s}}) = X(\Sigma_{\mathfrak{s}})$ and therefore $X(\Sigma_{\mathfrak{s}})$ has a small toric resolution too. $\square$

As described by Sheridan [77], the Fukaya category of a monotone symplectic manifold like the Grassmannian has a spectral decomposition

$$\mathcal{F}(\mathrm{Gr}_k(n)) = \bigoplus_{\lambda} \mathcal{F}_\lambda(\mathrm{Gr}_k(n)) \quad .$$

The summands are A_∞-categories indexed by the eigenvalues λ of the operator $c_1\star$ of multiplication by the first Chern class acting on the small quantum cohomology. The objects of the λ-summand are monotone Lagrangians with rank one local systems L_ξ as described in Appendix B. The following proposition holds for general Grassmannians.

Proposition 4.3.4. *For any $1 \leqslant k < n$ and any Plücker sequence $\mathfrak{s}$ of type (k, n):*

1. *if $\mathcal{F}_\lambda(\mathrm{Gr}_k(n)) \neq 0$ then $\lambda = n(\zeta_1 + \ldots + \zeta_k)$ for some $\{\zeta_1, \ldots, \zeta_k\} = I \subset \{\, \zeta \in \mathbb{C} : \zeta^n = (-1)^{k+1} \,\}$ with $|I| = k$;*

2. *if $X(\Sigma_{\mathfrak{s}})$ has a small toric resolution, then $(L_{\mathfrak{s}})_{\xi_I}$ is a nonzero object of $\mathcal{F}_\lambda(\mathrm{Gr}_k(n))$*

if and only if $S_d(I) \neq 0$ for all Young diagrams d appearing as labels on the nodes of $Q_{\mathfrak{s}}$, and moreover $\lambda = n(\zeta_1 + \cdots + \zeta_k)$.

Proof. 1. By [12, Proposition 1.3], $\lambda \in \mathbb{C}$ is an eigenvalue of the operator $c_1\star$ of multiplication by the first Chern class acting on the small quantum cohomology if and only if $\lambda = n(\zeta_1+\ldots+\zeta_k)$ for some $\{\zeta_1,\ldots,\zeta_k\} = I \subset \{\, \zeta \in \mathbb{C} : \zeta^n = (-1)^{k+1} \,\}$ with $|I| = k$. By Auroux [8, Proposition 6.8], any monotone Lagrangian L with a rank one local system ξ having Floer cohomology $HF(L_\xi, L_\xi) \neq 0$ must have $m^0(L_\xi)$ which is an eigenvalue of $c_1\star$.

2. By a Auroux [8, Proposition 6.9] and Sheridan [77, Proposition 4.2], a monotone Lagrangian torus L with a fixed basis of $H_1(L;\mathbb{Z})$ and a rank one local system ξ has Floer cohomology $HF(L_\xi, L_\xi) \neq 0$ if and only if the holonomies of ξ along the fixed cycles give coordinates for a critical point $\mathrm{hol}_\xi \in H_1(L;\mathbb{Z}) \otimes \mathbb{C}^\times$ of the Maslov 2 disk potential W_L. By Proposition 4.2.10 and the assumption of small resolution, we can apply this to the monotone torus $L = L_{\mathfrak{s}}$ and the local system $\xi = \xi_I$, and recalling that $H_1(L;\mathbb{Z}) \otimes \mathbb{C}^\times = T_{\mathfrak{s}}$ is the cluster chart of $\mathrm{Gr}_k^\vee(n)$ corresponding to $\mathfrak{s}$, we have that L_{ξ_I} is a nonzero object of $\mathcal{F}_\lambda(\mathrm{Gr}_k(n))$ if and only if $\mathrm{hol}_{\xi_I} \in T_{\mathfrak{s}}$ and it is a critical point of $W_{\mathfrak{s}}$. In fact $W_{\mathfrak{s}} = W_{|T_{\mathfrak{s}}}$, where W is the global Landau-Ginzburg potential on $\mathrm{Gr}_k^\vee(n)$ defined by Marsh-Rietsch [53]. The critical points of W can be explicitly described as

$$[M_{I^\vee}] = \begin{bmatrix} 1 & 1 & 1 & \ldots & 1 \\ \zeta_1 & \zeta_2 & \zeta_3 & \ldots & \zeta_{n-k} \\ \zeta_1^2 & \zeta_2^2 & \zeta_3^2 & \ldots & \zeta_{n-k}^2 \\ \vdots & \vdots & \vdots & & \vdots \\ \zeta_1^{n-1} & \zeta_2^{n-1} & \zeta_3^{n-1} & \ldots & \zeta_{n-k}^{n-1} \end{bmatrix}$$

where $I^\vee = \{\zeta_1,\ldots,\zeta_{n-k}\}$ is a set of $n-k$ distinct roots of $\zeta^n = (-1)^{n-k+1}$; see [53, Proposition 9.3], [67, Theorem 3.4 and Lemma 3.7] and [42, Theorem 1.1 and Corollary 3.12]. Denote $(I^\vee)^c$ the set of roots of $\zeta^n = (-1)^{n-k+1}$ that are not in $I^\vee$, and observe that $I = e^{\pi i}(I^\vee)^c$ is a set of k distinct roots of $\zeta^n = (-1)^{k+1}$. The condition $[M_{I^\vee}] \in T_{\mathfrak{s}}$ is equivalent to $x_d(M_{I^\vee}) \neq 0$ for all Young diagrams d appearing as labels of $Q_{\mathfrak{s}}$, by definition of cluster chart. In fact, calling

$d^T \subseteq (n-k) \times k$ the transpose Young diagram to d, the condition $x_d(M_{I^\vee}) \neq 0$ is equivalent to $S_{d^T}(I^\vee) \neq 0$: the argument in part (1) of [12, Proposition 2.3] applies, once one replaces the rectangular Young diagrams (which label the initial quiver Q_0 of the Plücker sequence $\mathfrak{s}$) with the ones labeling $Q_{\mathfrak{s}}$. To conclude and get the desired statement, observe that $S_{d^T}(I^\vee) = S_d(I)$; see Rietsch [67, Lemma 4.4].

□

Lemma 4.3.5. *If n is odd, the eigenvalues of $c_1\star$ acting on* $\mathrm{QH}(\mathrm{Gr}_2(n))$ *are pairwise distinct.*

Proof. It was explained in part (2) of Proposition 4.3.4 that the eigenvalues of $c_1\star$ acting on $\mathrm{QH}(\mathrm{Gr}_k(n))$ correspond to critical values of the Landau-Ginzburg potential W on $\mathrm{Gr}_k^\vee(n)$ defined by Marsh-Rietsch [53], and that the corresponding critical points can be explicitly described. In particular, there are $\binom{n}{k}$ critical points, and thus at most the same number of critical values. Therefore the statement is equivalent to proving that there are precisely $\binom{n}{2}$ distinct eigenvalues. From part (1) of Proposition 4.3.4, each eigenvalue is of the form $\lambda = n(\zeta_1 + \zeta_2)$, with ζ_1 and ζ_2 distinct roots of $\zeta^n = -1$. Write $\zeta_1 = e^{\frac{\pi i}{n}a}$ and $\zeta_1 = e^{\frac{\pi i}{n}b}$ with $0 < a < b < 2n$ odd integers. The norm of one such eigenvalue is

$$|\lambda| = n\sqrt{2}\left(1 + 2\cos\left(\frac{\pi}{n}(b-a)\right)\right)^{1/2} .$$

The function $\cos(x)$ is decreasing for $0 \leqslant x \leqslant \pi$ and $\cos(2\pi - x) = \cos(x)$; in our case $0 \leqslant \frac{\pi}{n}(b-a) \leqslant \pi$ whenever $0 \leqslant b-a \leqslant n$. Since n is odd by assumption, by varying a and b among all odd integers with $0 < a < b < 2n$ one finds $l = (n-1)/2$ eigenvalues with $0 < |\lambda_1| < \cdots < |\lambda_l|$, corresponding to $b-a$ attaining all the even integer values in the interval $[2, n-1]$. Moreover, fixed any $1 \leqslant t \leqslant l$, the n complex numbers $\lambda_t, (e^{\frac{2\pi}{n}i})\lambda_t, \ldots, (e^{\frac{2\pi}{n}i})^{n-1}\lambda_t$ are eigenvalues of $c_1\star$ too, and they have the same norm as λ_t; see also [12, Proposition 1.12] for more on the symmetries of the spectrum of $c_1\star$. Overall, we found $n(n-1)/2 = \binom{n}{2}$ distinct eigenvalues. □

Lemma 4.3.6. *Let $d \subseteq 2 \times (n-2)$ be a Young diagram, and denote by $d^| = \{s,t\}$ with $1 \leqslant s < t \leqslant n$ its vertical steps. Writing an arbitrary set $I \subset \{\zeta \in \mathbb{C} \ : \ \zeta^n = -1\}$ with*

$|I| = 2$ as $I_{a,b} = \{e^{\frac{\pi}{n}ia}, e^{\frac{\pi}{n}ib}\}$ with $0 < a < b < 2n$ odd integers, then

$$S_d(I_{a,b}) = 0 \qquad \Longleftrightarrow \qquad n \mid \frac{b-a}{2}(t-s) \quad .$$

Proof. Consider the full rank $2 \times n$ matrix

$$[M_{I_{a,b}}] = \begin{bmatrix} 1 & e^{\frac{\pi}{n}ia} & (e^{\frac{\pi}{n}ia})^2 & \dots & (e^{\frac{\pi}{n}ia})^{n-1} \\ 1 & e^{\frac{\pi}{n}ib} & (e^{\frac{\pi}{n}ib})^2 & \dots & (e^{\frac{\pi}{n}ib})^{n-1} \end{bmatrix}$$

One has $S_d(I_{a,b}) = 0$ if and only if $x_d(M_{I_{a,b}}) = 0$, where x_d denotes the Plücker coordinate corresponding to d; see for example [12, Proposition 2.3]. One can compute

$$x_d(M_{I_{a,b}}) = e^{\frac{\pi}{n}ia(s-1)}e^{\frac{\pi}{n}ib(t-1)} - e^{\frac{\pi}{n}ia(t-1)}e^{\frac{\pi}{n}ib(s-1)} \quad ,$$

from which $x_d(M_{I_{a,b}}) = 0$ if and only if $e^{\frac{\pi}{n}i(as+bt-at-bs)} = 1$. The last condition is verified precisely when $2n \mid (b-a)(t-s)$, and since $b-a$ is the difference of two odd integers this can be rewritten as in the statement. □

Theorem 4.3.7. *If $n = 2^t+1$ for some $t \in \mathbb{N}^+$, the derived Fukaya category $\mathbf{D}\mathcal{F}(\mathrm{Gr}_2(2^t+1))$ is split-generated by objects supported on a single Plücker torus.*

Proof. Up to replacing 2 with $n-2$, we can think of the critical points $[M_{I_{a,b}}]$ of the Landau-Ginzburg potential W on $\mathrm{Gr}^\vee(2,n)$ defined by Marsh-Rietsch [53] as being parametrized by sets $I_{a,b} = \{e^{\frac{\pi}{n}ia}, e^{\frac{\pi}{n}ib}\}$ with $0 < a < b < 2n$ odd integers; compare with part (2) of Proposition 4.3.4. We claim that there exists a Plücker sequence $\mathfrak{s}$ of type $(2,n)$ such that the corresponding cluster chart $T_\mathfrak{s} \subset \mathrm{Gr}^\vee(2,n)$ contains all critical points $[M_{I_{a,b}}]$. If this is true, then these will be also critical points of the Laurent polynomial $W_\mathfrak{s} = W_{|T_\mathfrak{s}}$, which is the Maslov 2 disk potential of the monotone Lagrangian torus $L_\mathfrak{s} \subset \mathrm{Gr}_2(n)$ by Proposition 4.2.10 and Lemma 4.3.3. By Sheridan [77, Corollary 2.19], if the generalized eigenspace $\mathrm{QH}_\lambda(X)$ of the operator $c_1\star$ is one-dimensional, any monotone Lagrangian brane L_ξ with $HF(L_\xi, L_\xi) \neq 0$ split-generates $\mathbf{D}\mathcal{F}_\lambda(X)$. Since $n = 2^t+1$ is odd, by Lemma 4.3.5 we can apply this to $X = \mathrm{Gr}_2(n)$, $L = L_\mathfrak{s}$ and any $\xi = \xi_{I_{a,b}}$ for all $0 < a < b < 2n$ odd integers, thus concluding that the objects $(L_\mathfrak{s})_{I_{a,b}}$ split-generate every summand of $\mathbf{D}\mathcal{F}(\mathrm{Gr}_2(2^t+1))$. The construction of the Plücker sequence $\mathfrak{s}$ mentioned in the claim above proceeds as follows. Consider the following incremental construction of a set Γ (an example with $t = 3$ is given in Figure 1.4):

1. start with a segment partitioned in $n-1 = 2^t$ intervals, which are added to Γ as new edges $\{1,2\}$, $\{2,3\}$, ..., $\{2^t, 2^t+1\}$;
2. partition the segment into $(n-1)/2 = 2^{t-1}$ pairs of consecutive intervals, and add a new arc connecting the left end of the left interval to the right end of the right interval in each pair, thus adding new edges $\{1,3\}$, $\{3,5\}$, ...,$\{2^{t-1}, 2^{t+1}\}$ to Γ ;
3. partition the segment in $(n-1)/2^2 = 2^{t-2}$ tuples of 2^2 consecutive intervals, and add a new arc connecting the left end of the leftmost interval to the right end of the rightmost interval in each tuple, thus adding new edges $\{1,5\}$, $\{5,9\}$, ...,$\{2^{t+1}-2^2, 2^{t+1}\}$ to Γ ;
4. proceed as above until the initial segment is partitioned in two tuples of 2^{t-1} consecutive intervals, and add the edge $\{1,n\} = \{1, 2^t+1\}$ to Γ, so that it becomes a triangulation of $[n]$ in the sense of Definition 4.3.1 .

Let (Q_0, W_0) be the initial seed of Definition 4.1.2, and call Γ_0 the triangulation of $[n]$ corresponding to Young diagrams labeling the nodes of Q_0 as in Lemma 4.3.2. The triangulation Γ_0 is connected to Γ constructed above by a sequence of flips, which correspond to mutations of the quiver Q_0 at nodes with to incoming and two outgoing arrows. From Proposition 4.1.4, this gives a Plücker sequence of mutations of type $(2,n)$ in the sense of Definition 4.1.5, which ends at $(Q_{\mathfrak{s}}, W_{\mathfrak{s}})$ and such that the labels of $Q_{\mathfrak{s}}$ correspond to the triangulation $\Gamma_{\mathfrak{s}} = \Gamma$, again by Lemma 4.3.2. It remains to show that $[M_{I_{a,b}}] \in T_{\mathfrak{s}}$ for all odd integers a and b such that $0 < a < b < 2n$. Suppose not, then there exist some a, b and some Young diagram $d \subseteq 2 \times (n-2)$ such that $x_d(M_{I_{a,b}}) = 0$. By Lemma 4.3.6, this implies that $n \mid \frac{b-a}{2}(t-s)$, where $d^| = \{s,t\}$ are the vertical steps of d. By construction, for any $d^| \in \Gamma_{\mathfrak{s}}$, if $d^| = \{s,t\}$ then $t-s$ is a power of 2, and since $n = 2^t+1$ is odd by assumption we must have $n \mid \frac{b-a}{2}$. This is impossible, because $\frac{b-a}{2} < n$. □

Example 4.3.8. $\mathbf{D}\mathcal{F}(\mathrm{Gr}_2(9))$ is generated by a single Plücker torus. Note that instead the Gelfand-Zetlin torus mentioned in Section 3.2 does not support enough nonzero objects to generate.

The arguments above can be generalized to prove that certain collections of Plücker tori split generate $\mathbf{D}\mathcal{F}(\mathrm{Gr}_2(n))$.

Definition 4.3.9. *Let p be a prime number. A triangulation Γ of $[n]$ as in Definition 4.3.1 is called p-avoiding if for all $\{s,t\} \in \Gamma$ one has $p \nmid (t-s)$.*

Theorem 4.3.10. *Let $n > 2$ be odd, and consider its prime factorization $n = p_1^{e_1} \cdots p_l^{e_l}$. Assume that for all $1 \leqslant i \leqslant l$ there exists a triangulation Γ_i of $[n]$ that is p_i-avoiding, then $\mathbf{D}\mathcal{F}(\mathrm{Gr}_2(n))$ is split generated by objects supported on l Plücker tori.*

Proof. Recall that up to replacing 2 with $n-2$, we can think of the critical points $[M_{I_{a,b}}]$ of the Landau-Ginzburg potential W on $\mathrm{Gr}^\vee(2,n)$ defined by Marsh-Rietsch [53] as being parametrized by sets $I_{a,b} = \{e^{\frac{\pi}{n}ia}, e^{\frac{\pi}{n}ib}\}$ with $0 < a < b < 2n$ odd integers; compare with part (2) of Proposition 4.3.4. Denote $\mathcal{C}$ the set of all critical points of W, and for $1 \leqslant i \leqslant l$ define

$$\mathcal{C}_{p_i} = \{[M_{I_{a,b}}] \in \mathcal{C} \ : \ p_i^{e_i} \nmid \frac{b-a}{2}\} \quad .$$

Observe that $\mathcal{C} = \mathcal{C}_{p_1} \cup \cdots \cup \mathcal{C}_{p_l}$. Indeed, if $p_i^{e_i} \mid (b-a)/2$ for all $1 \leqslant i \leqslant l$ then $p_1^{e_1} \cdots p_l^{e_l} = n \mid (b-a)/2$, against the fact that $(b-a)/2 < n$. By assumption, for each $1 \leqslant i \leqslant l$ there exist a triangulation Γ_i of $[n]$ that is p_i-avoiding, and arguing as in Theorem 4.3.7 one finds a Plücker sequence $\mathfrak{s}_i$ of type $(2,n)$ that starts with the initial seed (Q_0, W_0) and ends with $(Q_{\mathfrak{s}_i}, W_{\mathfrak{s}_i})$, and such that the labels of $Q_{\mathfrak{s}_i}$ correspond to the triangulation $\Gamma_{\mathfrak{s}_i} = \Gamma_i$ as in Lemma 4.3.2. Each of the l Plücker tori $L_{\mathfrak{s}_i} \subset \mathrm{Gr}_2(n)$ has an associated cluster chart $T_{\mathfrak{s}_i} \subset \mathrm{Gr}^\vee(2,n)$, and we claim that $\mathcal{C}_{p_i} \subset T_{\mathfrak{s}_i}$. Suppose not, then there exists some $[M_{I_{a,b}}] \in \mathcal{C}_{p_i}$ such that $[M_{I_{a,b}}] \notin T_{\mathfrak{s}_i}$. This means that $p_i^{e_i} \nmid \frac{b-a}{2}$ and there exists some Young diagram $d \subseteq 2 \times (n-2)$ such that $x_d(M_{I_{a,b}}) = 0$, and denoting $d^| = \{s,t\}$ its vertical steps $\{s,t\} \in \Gamma_{\mathfrak{s}_i}$. By Lemma 4.3.6, this implies that $n \mid \frac{b-a}{2}(t-s)$, and so in particular $p_i^{e_i} \mid \frac{b-a}{2}(t-s)$. Since $\Gamma_{\mathfrak{s}_i}$ is p_i-avoiding, this means that $p_i^{e_i} \mid \frac{b-a}{2}$, against the fact that $[M_{I_{a,b}}] \in \mathcal{C}_{p_i}$. As in Theorem 4.3.7, the assumption n odd and Lemma 4.3.5 guarantee, by Sheridan [77, Corollary 2.19], that any nonzero object of the Fukaya category supported on one of the l monotone Plücker tori $L_{\mathfrak{s}_1}, \ldots, L_{\mathfrak{s}_l} \subset \mathrm{Gr}_2(n)$ split-generates the summand $\mathbf{D}\mathcal{F}_\lambda(\mathrm{Gr}_2(n))$ of the derived Fukaya category containing it. The objects supported on $L_{\mathfrak{s}_i}$ are obtained by endowing it with local systems $\xi_{I_{a,b}}$ as in Definition 4.2.5 corresponding to critical points $[M_{I_{a,b}}] \in T_{\mathfrak{s}_i}$; these are such that $HF((L_{\mathfrak{s}_i})_{\xi_{I_{a,b}}}, (L_{\mathfrak{s}_i})_{\xi_{I_{a,b}}}) \neq 0$ because the Maslov 2 disk potential of $L_{\mathfrak{s}_i}$ is $W_{\mathfrak{s}_i} = W_{|T_{\mathfrak{s}_i}}$. □

Example 4.3.11. **D**$\mathcal{F}(\mathrm{Gr}_2(15))$ is generated by two Plücker tori, whose corresponding triangulations are shown in Figure 1.5. To get the two triangulations, one starts by constructing a partial triangulation of the 15-gon with dyadic arcs as in Theorem 4.3.7 (solid arcs in Figure 1.5). The partial triangulation is p-avoiding for every prime $p > 2$ by construction. Since $15 = 3 \cdot 5$, by Theorem 4.3.10 one needs to find completions of the partial triangulation to full triangulations that are 3-avoiding and 5-avoiding respectively. In Figure 1.5, the remaining arcs $\{i, j\}$ with $3 \mid (j-i)$ are coarsely dashed, while the one with $5 \mid (j-i)$ is finely dashed; triangulation (A) is obtained by adding two shaded arcs and is 3-avoiding, while triangulation (B) is obtained by adding two different shaded arcs and is 5-avoiding.

We focus now on how to distinguish exotic tori in general Grassmannians.

Definition 4.3.12. *If $L_{\mathfrak{s}} \subset \mathrm{Gr}_k(n)$ is a Plücker Lagrangian of type (k, n), define its f-vector to be*

$$\mathbf{f}(L_{\mathfrak{s}}) = (f_1, \ldots, f_{k(n-k)}) \in \mathbb{N}^{k(n-k)} \quad ,$$

where f_i is the number of $(i-1)$-dimensional faces in the Newton polytope $P_{\mathfrak{s}}$ of the potential $W_{\mathfrak{s}}$.

Definition 4.3.13. *If $L_{\mathfrak{s}} \subset \mathrm{Gr}_k(n)$ is a Plücker Lagrangian of type (k, n), define its weight $\mathbf{wt}(L_{\mathfrak{s}}) \in \mathbb{N}$ to be the number of sets*

$$I \subset \{\zeta \in \mathbb{C} \; : \; \zeta^n = (-1)^{k+1}\}$$

such that $|I| = k$ and $S_d(I) \neq 0$ for all Young diagrams d appearing as labels of the quiver $Q_{\mathfrak{s}}$.

Lemma 4.3.14. *Assume $\mathfrak{s}, \mathfrak{s}'$ are Plücker sequences of type (k, n) satisfying Conjecture 4.2.7. If $\mathbf{f}(L_{\mathfrak{s}}) \neq \mathbf{f}(L_{\mathfrak{s}'})$ or $\mathbf{wt}(L_{\mathfrak{s}}) \neq \mathbf{wt}(L_{\mathfrak{s}'})$, then the Lagrangian tori $L_{\mathfrak{s}}, L_{\mathfrak{s}'} \subset \mathrm{Gr}_k(n)$ are not Hamiltonian isotopic.*

Proof. Suppose that there exists a Hamiltonian isotopy ϕ such that $\phi(L_{\mathfrak{s}}) = L_{\mathfrak{s}'}$. Then by assumption the induced map $\phi_* : H_1(L_\mathfrak{s};\mathbb{Z}) \to H_1(L_{\mathfrak{s}'};\mathbb{Z})$ is such that

$$W_\mathfrak{s} \sim W_{\mathfrak{s}'} \circ (\phi_* \otimes \mathrm{id}_{\mathbb{C}^\times}) \quad ,$$

where $\sim$ denotes equality up to automorphisms of $T_\mathfrak{s}$. This means that the Newton polytopes $P_\mathfrak{s}$ and $P_{\mathfrak{s}'}$ of the Laurent polynomials $W_\mathfrak{s}$ and $W_{\mathfrak{s}'}$ are related by a transformation of $GL(k(n-k),\mathbb{Z})$, and hence have the same f-vector, because the number of faces of any given dimension of a polytope is a unimodular invariant; this proves that $\mathbf{f}(L_\mathfrak{s}) = \mathbf{f}(L_{\mathfrak{s}'})$. Moreover, the Laurent polynomials $W_\mathfrak{s}$ and $W_{\mathfrak{s}'}$ can be thought of as regular functions on a torus $(\mathbb{C}^\times)^{k(n-k)}$, which agree up to an automorphism. Since the number of critical points of a function is invariant under automorphisms of its domain, it follows from part (2) of Proposition 4.3.4 that $\mathbf{wt}(L_\mathfrak{s}) = \mathbf{wt}(L_{\mathfrak{s}'})$. $\square$

Theorem 4.3.15. *The Grassmannian* $\mathrm{Gr}_3(6)$ *contains at least* 6 *monotone Lagrangian tori that are not displaceable nor equivalent under Hamiltonian isotopy.*

Proof. The table below contains informations about the steps of a Plücker sequence $\mathfrak{s}$ of type $(3,6)$. In each row, the reader can find the Young diagrams $d \subseteq 3\times 3$ appearing as labels of $Q_\mathfrak{s}$ at a given step, identified by their sets of vertical sets $\{i,j,k\} \subset [6]$. Each potential $W_\mathfrak{s}$ has an associated Newton polytope $P_\mathfrak{s}$, whose f-vector is $\mathbf{f}(L_\mathfrak{s})$ as in Definition 4.3.12. Following Definition 4.3.13, the weight $\mathbf{w}(L_\mathfrak{s})$ is computed by counting how many of the $\binom{6}{3}$ sets I of roots of $\zeta^6 = 1$ with $|I| = 3$ have the property that $S_d(I) \neq 0$ for all Young diagrams $d \subseteq 3\times 3$ that appear as labels on the nodes of the quiver $Q_\mathfrak{s}$. Calling $\Sigma_\mathfrak{s} = \Sigma^f P_\mathfrak{s}$ the face fan of the Newton polytope, by Proposition 4.2.10 the Lagrangian torus $L_\mathfrak{s} \subset \mathrm{Gr}_k(n)$ is monotone and has Maslov 2 disk potential $W_\mathfrak{s}$ whenever the toric variety $X(\Sigma_\mathfrak{s})$ has a small toric resolution in the sense of Definition 4.2.9. This condition can be checked algorithmically at each step, since every fan has finitely many simplicial refinements with the same rays, and every smooth refinement is in particular simplicial. For the 34 steps in the table, the code [11] finds small resolutions in 32 cases; the remaining 2 cases are marked gray in the table (we did not actually check all possible simplicial refinements in these cases, so small toric resolutions for them may still exist). From Lemma 4.3.14, we conclude that $\mathrm{Gr}_3(6)$ contains at least 6 monotone Lagrangian tori that are pairwise not Hamiltonian isotopic. Regarding nondisplaceability, it suffices to show that the 32 tori $L_{\mathfrak{s}} \subset \mathrm{Gr}_3(6)$ have Floer cohomology $HF(L_\xi, L_\xi) \neq 0$ for some local system ξ. By Auroux [8, Proposition 6.9] and Sheridan [77, Proposition 4.2], the Floer cohomology of a monotone Lagrangian torus brane L_ξ is nonzero if and only if the holonomy hol_ξ of its local system ξ is a critical point of the disk potential Maslov 2 disk potential $W_{\mathfrak{s}}$. Therefore, it suffices to show that each of the 32 Laurent polynomials $W_{\mathfrak{s}}$ has at least one critical point. Thinking $W_{\mathfrak{s}}$ as restriction $W_{\mathfrak{s}} = W_{|T_{\mathfrak{s}}}$ of the Landau-Ginzburg potential W on $\mathrm{Gr}^\vee(3,6)$ defined by Marsh-Rietsch [53] to the cluster chart $T_{\mathfrak{s}} \subset \mathrm{Gr}^\vee(3,6)$, it suffices to show that each of the charts contains at least one critical point of W. In fact, something stronger is true: there is a critical point of W that is contained in $T_{\mathfrak{s}}$ for all $\mathfrak{s}$. As proved by Rietsch [68] (see also Karp [42]), for any $1 \leqslant k < n$ there is a (unique) critical point of W in the totally positive part $\mathrm{Gr}_k^\vee(n)_{>0} \subset \mathrm{Gr}_k^\vee(n)$, i.e. the locus where all Plücker coordinates are real and positive. Following the notation of part (2) in Proposition 4.3.4, this point is $[M_{I_0}] \in \mathrm{Gr}_k^\vee(n)$ with I_0 the set of k roots of $\zeta^n = (-1)^{k+1}$ closest to 1. Applying this to $(k,n) = (3,6)$, and recalling that $[M_{I_0}] \in T_{\mathfrak{s}}$ if and only if $x_d(M_{I_0})$ for all Young diagrams $d \subseteq 3 \times 3$ appearing as labels on the nodes of $Q_{\mathfrak{s}}$, we conclude that the total positivity of $[M_{I_0}]$ implies that it belongs to every cluster chart $T_{\mathfrak{s}}$, and this proves that all $L_{\mathfrak{s}}$ are nondisplaceable. $\square$

$k=3,\ n=6$			
$L_{\mathfrak{s}}$	Labels of $Q_{\mathfrak{s}}$	$\mathbf{f}(L_{\mathfrak{s}})$	$\mathbf{wt}(L_{\mathfrak{s}})$
1	123, 124, 125, 126, 156, 234, 245, 256, 345, 456	(14, 83, 276, 571, 766, 670, 372, 122, 20)	18
2	123, 124, 125, 126, 145, 156, 234, 245, 345, 456	(14, 83, 276, 571, 766, 670, 372, 122, 20)	18
3	123, 125, 126, 135, 145, 156, 234, 235, 345, 456	(15, 91, 302, 615, 807, 690, 376, 122, 20)	6
4	123, 126, 134, 136, 146, 156, 234, 345, 346, 456	(14, 83, 276, 571, 766, 670, 372, 122, 20)	18
5	123, 126, 156, 234, 235, 236, 245, 256, 345, 456	(15, 91, 302, 615, 807, 690, 376, 122, 20)	6
6	123, 125, 126, 156, 234, 235, 245, 256, 345, 456	(14, 83, 276, 571, 766, 670, 372, 122, 20)	18
7	123, 124, 125, 126, 134, 145, 156, 234, 345, 456	(15, 91, 302, 615, 807, 690, 376, 122, 20)	18
8	123, 125, 126, 134, 135, 145, 156, 234, 345, 456	(16, 98, 322, 645, 832, 701, 378, 122, 20)	6
9	123, 124, 126, 146, 156, 234, 245, 246, 345, 456	(16, 98, 322, 645, 832, 701, 378, 122, 20)	6
10	123, 126, 156, 234, 236, 246, 256, 345, 346, 456	(15, 91, 302, 615, 807, 690, 376, 122, 20)	6
11	123, 124, 126, 146, 156, 234, 246, 345, 346, 456	(15, 91, 302, 615, 807, 690, 376, 122, 20)	6
12	123, 124, 126, 145, 146, 156, 234, 245, 345, 456	(15, 91, 302, 615, 807, 690, 376, 122, 20)	18
13	123, 126, 146, 156, 234, 236, 246, 345, 346, 456	(16, 98, 322, 645, 832, 701, 378, 122, 20)	6
14	123, 126, 156, 234, 236, 256, 345, 346, 356, 456	(14, 83, 276, 571, 766, 670, 372, 122, 20)	18
15	123, 126, 146, 156, 234, 236, 245, 246, 345, 456	(18, 111, 358, 700, 882, 728, 386, 123, 20)	6
16	123, 126, 156, 234, 235, 236, 256, 345, 356, 456	(14, 83, 276, 571, 766, 670, 372, 122, 20)	18
17	123, 124, 126, 134, 145, 146, 156, 234, 345, 456	(14, 83, 276, 571, 766, 670, 372, 122, 20)	18
18	123, 126, 134, 135, 136, 156, 234, 345, 356, 456	(16, 98, 322, 645, 832, 701, 378, 122, 20)	6
19	123, 126, 134, 136, 145, 146, 156, 234, 345, 456	(14, 83, 276, 571, 766, 670, 372, 122, 20)	18
20	123, 126, 135, 136, 145, 156, 234, 235, 345, 456	(15, 93, 317, 661, 882, 760, 413, 132, 21)	6
21	123, 126, 136, 146, 156, 234, 236, 345, 346, 456	(15, 91, 302, 615, 807, 690, 376, 122, 20)	18
22	123, 125, 126, 134, 135, 156, 234, 345, 356, 456	(18, 111, 358, 700, 882, 728, 386, 123, 20)	6
23	123, 126, 136, 156, 234, 235, 236, 345, 356, 456	(14, 83, 276, 571, 766, 670, 372, 122, 20)	18
24	123, 126, 134, 135, 136, 145, 156, 234, 345, 456	(15, 91, 302, 615, 807, 690, 376, 122, 20)	6
25	123, 124, 126, 156, 234, 245, 246, 256, 345, 456	(15, 91, 302, 615, 807, 690, 376, 122, 20)	6
26	123, 126, 134, 136, 156, 234, 345, 346, 356, 456	(15, 91, 302, 615, 807, 690, 376, 122, 20)	18
27	123, 126, 135, 136, 156, 234, 235, 345, 356, 456	(15, 91, 302, 615, 807, 690, 376, 122, 20)	6
28	123, 124, 126, 134, 146, 156, 234, 345, 346, 456	(14, 83, 276, 571, 766, 670, 372, 122, 20)	18
29	123, 126, 156, 234, 236, 245, 246, 256, 345, 456	(16, 98, 322, 645, 832, 701, 378, 122, 20)	18
30	123, 126, 136, 156, 234, 236, 345, 346, 356, 456	(14, 83, 276, 571, 766, 670, 372, 122, 20)	18
31	123, 125, 126, 145, 156, 234, 235, 245, 345, 456	(14, 83, 276, 571, 766, 670, 372, 122, 20)	18
32	123, 125, 126, 135, 156, 234, 235, 345, 356, 456	(16, 98, 322, 645, 832, 701, 378, 122, 20)	6
33	123, 125, 126, 156, 234, 235, 256, 345, 356, 456	(15, 91, 302, 615, 807, 690, 376, 122, 20)	18
34	123, 124, 126, 156, 234, 246, 256, 345, 346, 456	(15, 93, 317, 661, 882, 760, 413, 132, 21)	6

Chapter 5

RANDOM WALK ON THE CLUSTER GRAPH

This chapter contains the source code of ClusterExplorer. This is a random walk on a graph, whose nodes are seeds of the cluster algebra $\mathcal{A}_{k,n}$ whose cluster variables are Plücker coordinates, and whose edges are cluster mutations in the sense of Fomin-Zelevinsky [26]. The walk starts from a canonical initial seed and chooses mutation instructions uniformly at random at each step.

ClusterExplorer can be run in BraneCounting mode or NewtonPolytope mode. In BraneCounting mode, the walk computes critical points and critical values of the restriction of $W \in \mathcal{A}_{k,n}$ to the cluster chart corresponding to each step. In NewtonPolytope mode, the walk computes the restriction of W as Laurent polynomial in the cluster variables, its Newton polytope, and several discrete invariants of this polytope and its face fan.

5.1. Main modules

Listing 5.1: BraneCounting.py

```
import copy
import itertools
import math

import sage.all
import sage.rings

import critpoints
import plucker
import schurpol
import spectrum
import walk
import youngd


# Take in input k and n

print('Input k: ')
k = input()
```

```
print('Input n: ')
n = input()

# Ask if user wants pictures of critical values of W and subsets
# of critical values corresponding to different cluster charts

print('Pictures? ')
show_spectrum = input()

# Compute N = {n choose n-k}, total number of critical points of mirror
# Landau-Ginzburg superpotential on Gr(n-k, n)

N = math.factorial(n) / ( math.factorial(k)*math.factorial(n-k) )
print('Total number of critical points: {}'.format(N))

# Construct the homogeneous coordinate ring of the ambient
# projective space for the Plucker embedding, and inject its generators
# in the variables namespace

proj_ring = sage.rings.all.PolynomialRing(sage.all.QQ, 'x', N)
proj_ring.inject_variables(verbose=False)

# Define the Plucker coordinates corresponding to the generators
# of the homogeneous coordinate ring of the ambient projective space

p = plucker.variables(n-k, n, proj_ring)

# Construct the Plucker relations describing the homogeneous
# coordinate ring of Gr(n-k,n) in the Plucker embedding

relations = plucker.rel_list(n-k, n, p)

# Run a random walk that constructs the list of plabic cluster charts
# of the Grassmannian Gr(n-k,n)

cluster_list = walk.random_walk(n-k, n, p, relations)

# Initialize roots of unity

roots = critpoints.basic_roots(n-k, n, critpoints.cyclotomic(n-k, n))

# Construct the list e of eigenvalues of multiplication by c_1 in
# the quantum cohomology QH(Gr(k,n)), or equivalently of critical
# values of Marsh-Rietsch Landau-Ginzburg superpotential W

e = []
for S in itertools.combinations(range(1,n+1), n-k):
   sum_S = 0
   for t in S:
      sum_S = sum_S + roots[t-1]
   e.append(complex(n*sum_S))

lagrangian_weights = []
i = 0
for C in cluster_list:

   # Initialize the list c_values of critical values of critical points
   # of W contained in the cluster chart corresponding to the cluster C

   c_values = []

   crit_counter = 0
   for S in itertools.combinations(range(1,n+1), n-k):
```

```
      roots_S = []
      sum_S = 0
      for t in S:
         roots_S.append(roots[t-1])
         sum_S = sum_S + roots[t-1]
      is_in_chart = True
      for d in C:
         d = youngd.vstep_to_part(n-k, n, d)
         if (schurpol.schur_sage(n-k, n, [d])[tuple(d)])(roots_S) == 0:
            is_in_chart = False
            break
      if is_in_chart == True:
         crit_counter = crit_counter + 1
         c_values.append(complex(n*sum_S))
   print('Cluster chart #{} = {}'.format(i, cluster_list[i]))
   print('The chart contains {} critical points'.format(crit_counter))
   if crit_counter not in lagrangian_weights:
      lagrangian_weights.append(crit_counter)
   if show_spectrum == 1:
      spectrum.spectrum_combined_picture(c_values, e, "BranesGr({},{})
    Cluster{}".format(k,n,i), k, n)
   i = i + 1

print('There are {} Lagrangian weights: {}'.format(len(lagrangian_weights
    ), lagrangian_weights))
```

Listing 5.2: NewtonPolytopes.py

```
import copy
import itertools
import math
import random

import sage.all
import sage.graphs.all
import sage.graphs.digraph
import sage.combinat.sf.classical
import sage.geometry.lattice_polytope
import sage.geometry.fan
import sage.interfaces.latte
import sage.rings
import sage.structure.factory

import newton
import plucker
import potentials
import walk

# Take in input k and n

print('Input k: ')
k = input()
print('Input n: ')
n = input()
print('Type 0 for exhaustive mode or 1 for random mode: ')
newton_mode = input()
if newton_mode == 1:
   print('Type size of the sample as % of the total: ')
   newton_percentage = input()
print('Compute f-vectors?')
show_fvector = input()
print('Check reflexivity?')
show_reflexive = input()
print('Check terminality?')
```

```
show_terminal = input()
print('Check existence of small resolution?')
show_small = input()
print('Compute volume?')
show_volume = input()

# Compute N = {n choose n-k}, total number of critical points of mirror
# Landau-Ginzburg superpotential on Gr(n-k, n)

N = math.factorial(n) / ( math.factorial(k)*math.factorial(n-k) )
print('Total number of critical points: {}'.format(N))

# Construct the homogeneous coordinate ring of the ambient
# projective space for the Plucker embedding, and inject its generators
# in the variables namespace

proj_ring = sage.rings.all.PolynomialRing(sage.all.QQ, 'x', N)
proj_ring.inject_variables(verbose=False)

# Define the Plucker coordinates corresponding to the generators
# of the homogeneous coordinate ring of the ambient projective space

p = plucker.variables(n-k, n, proj_ring)

# Construct the Plucker relations describing the homogeneous coordinate
# ring of Gr(n-k,n) in the Plucker embedding

relations = plucker.rel_list(n-k, n, p)

# Compute the local Landau-Ginzburg potentials of the mirror to Gr(k,n)

print('About to start random walk')
W = walk.random_walk(n-k, n, p, relations, loc_potentials=True)
print('Random walk is over')

# Compute Newton polytopes and visualize the desired combinatorial
# informations for all clusters or MAX_NEWTON random clusters
# depending on whether user specified exhaustive or random mode.

if newton_mode == 0:
   for C in W.keys():
      print('Cluster: {}'.format(C))
      P = newton.newton_polytope(n-k, n, potentials.force_laurent(W[tuple
    (C)], sage.all.LaurentPolynomialRing(sage.all.QQ, 'x', N)), C)
      if show_fvector == 1:
         print('f-vector = {}'.format(P.f_vector()))
      if show_reflexive == 1:
         print('reflexive = {}'.format(P.is_reflexive()))
      if show_terminal == 1:
         print('terminal = {}'.format(newton.is_terminal(P)))
      if show_small == 1:
         print('small resolution: {}'.format(newton.is_small(P)))
      if show_volume == 1:
         print('volume: {}'.format(P.volume()))
else:
   sample_size = int( math.ceil( float(newton_percentage)/float(100) *
    len(W) ) )
   for C in random.sample(list(W.keys()), sample_size):
      print('Cluster: {}'.format(C))
      P = newton.newton_polytope(n-k, n, potentials.force_laurent(W[tuple
    (C)], sage.all.LaurentPolynomialRing(sage.all.QQ, 'x', N)), C)
      if show_fvector == 1:
         print('f-vector = {}'.format(P.f_vector()))
```

```
      if show_reflexive == 1:
         print('reflexive = {}'.format(P.is_reflexive()))
      if show_terminal == 1:
         print('terminal = {}'.format(newton.is_terminal(P)))
      if show_small == 1:
         print('small resolution: {}'.format(newton.is_small(P)))
      if show_volume == 1:
         print('volume: {}'.format(P.volume()))
```

5.2. Auxiliary modules

Listing 5.3: critpoints.py

```
import sage.rings.number_field.number_field

# Given k and n, return a SageMath cyclotomic field containing all
# coordinates of critical points of the LG superpotential mirror to
# Gr(k,n), following Karp. These are polynomials in the roots of
# x^n = (-1)^{k+1}, so for k odd we work with the cyclotomic field
# generated by a primitive n-th root of unity whereas when k even we
# work with one generated by a primitive (2n)-th root of unity. Doing
# calculations in this ambient field is faster than letting SageMath
# guess tower of extensions on the fly.

def cyclotomic(k, n):

   if k % 2 == 1:
      KK = sage.rings.number_field.number_field.CyclotomicField(n)
   else:
      KK = sage.rings.number_field.number_field.CyclotomicField(2*n)

   return KK

# Given k, n and the smallest cyclotomic field KK containing the roots
# of x^n = (-1)^{k+1}, return a list containing the roots as SageMath
# symbolic objects.

def basic_roots(k, n, KK):

   l = []

   if (k % 2) == 1:
      r = (-1)*(k-1)/2
      while r <= (2*n-k-1)/2:
         l.append(KK.gen()**r)
         r = r + 1
   else:
      r_double = (-1)*(k-1)
      while r_double <= 2*n-k-1:
         l.append(KK.gen()**r_double)
         r_double = r_double + 2

   return l
```

Listing 5.4: newton.py

```
import itertools
import math

import sage.all

# Given k, n and a Laurent polynomial f in the Plucker variables
# of a plabic cluster C of type (k,n), return the Newton polytope of f.
```

```
def newton_polytope(k, n, f, C):

   N = math.factorial(n) / ( math.factorial(k)*math.factorial(n-k) )
   # Compute exponent vectors of Laurent polynomial f, and then
   # remove for each the entries not corresponding to Plucker
   # coordinates not labelled by Young diagrams in C and the one
   # corresponding to the empty diagram

   exponents = f.exponents()
   mask = [0,]*N
   i = 0
   for S in itertools.combinations(range(1,n+1), k):
      if tuple(sorted(tuple(S))) in C:
         mask[i] = 1
      i = i + 1
   mask[N-1] = 0
   for i in range(len(exponents)):
      exponents[i] = list(itertools.compress(exponents[i], mask))

   P = sage.all.Polyhedron(exponents)

   return P

# Given a Newton polytope P, test if it's a terminal lattice polytope
# or not, i.e. if the vertices are the only lattice points besides the
# origin.

def is_terminal(P):

   if P.integral_points_count() == P.n_vertices()+1:
      return True
   else:
      return False

# Given a Newton polytope P, test if the naive simplicial refinement
# on smae rays of the face fan is automatically smooth.

def is_small(P):

   fan_P = sage.all.FaceFan(P)
   fan_P = fan_P.make_simplicial()
   if fan_P.is_smooth():
      return True
   else:
      return False



# Given a list of ray generators, return True if the corresponding cone
# has a small simplicial resolution and False otherwise

def small_res_cone(rays_list):

   main_cone = sage.all.Cone(rays_list)
   d = len(rays_list)
   main_cone_dim = main_cone.dim()

   # Construct a list of all possible sets of rays of simplicial cones
   # contained in main_cone with no new rays

   T_list = []
   for T in itertools.combinations(range(d), main_cone_dim):
```

```
        T_list.append(T)

    # For each possible collection of sets above, verify if it gives
    # rise to a small resolution of main_cone

    for triang_size in range(1,len(T_list)+1):

        for triang in itertools.combinations(T_list, triang_size):
            rays_used = [0,]*d
            cones_triang = []
            discard_triang = False
            for T in triang:
                rays_T = []
                for i in range(len(rays_list)):
                    if i in T:
                        rays_T.append(rays_list[i])
                        rays_used[i] = 1
                cone_T = Cone(rays_T)
                if cone_T.is_smooth():
                    cones_triang.append(Cone(rays_T))
                else:
                    discard_triang = True
                    break
            if discard_triang == False:

                # Check covering condition
                covering_check = True
                for flag in rays_used:
                    if flag == 0:
                        covering_check = False
                        break

                if covering_check:

                    # Check intersection condition
                    intersection_check = True
                    try:
                        F = sage.all.Fan(cones_triang)
                    except ValueError:
                        intersection_check = False

                # Check if the resulting simplicial refinement of main_cone
                # is actually smooth
                if covering_check and intersection_check:
                    return True

    return False
```

Listing 5.5: plucker.py

```
import copy
import itertools
import sage.rings
import sage.all

# Given k, n and the homogeneous coordinate ring of the ambient
# projective space, return a dictionary of Plucker coordinates for
# the Grassmannian Gr(k,n): the keys are increasing sequences of
# length k in {1, ..., n}, interpreted as vertical steps of a Young
# diagram in the k x (n-k) grid; ordering them by lex, the i-th has
# value a SageMath symbolic variable named 'xi'

def variables(k, n, proj_ring):
```

```
    p = {}

    i = 0
    gen_list = proj_ring.gens()
    for S in itertools.combinations(range(1,n+1), k):
        p[tuple(sorted(tuple(S)))] = gen_list[i]
        i = i + 1

    return p

# Return +/- 1 according to the sign of permutation that sorts the input
# list in increasing order, without modifying it

def signsort(l):

    inversions = 0
    for i in range(len(l)):
        j = i + 1
        while (i < j) and (j < len(l)):
            if l[i] > l[j]:
                inversions = inversions + 1
            j = j + 1

    if (inversions % 2) == 0:
        return 1
    else:
        return -1


# Give k, n and the list of Plucker variables correspoding to Young
# diagrams in the k x (n-k) grid, generate a list whose elements are
# SageMath symbolic expressions encoding the Plucker relations for
# the Grassmannian Gr(k,n) according to Fulton.
#
# [TODO] Make this faster. This is currently O(2^k * n^{2k}), whereas the
# number of Plucker relations is O(1/(k!)^2 * n^{2k}).

def rel_list(k, n, p):

    relations = []

    for d1 in itertools.combinations(range(1,n+1), k):
        for d2 in itertools.combinations(range(1,n+1), k):
            for u in range(1,k+1):
            # Recall that itertools.combination returns tuples
            # ordered in increasing order
                plucker_lhs = p[d1]*p[d2]
                plucker_rhs = 0
                for l in itertools.combinations(range(1,k+1), u):
                    monomial = 0
                    l = sorted(list(l))
                    temp1 = []
                    for i in l:
                        temp1.append(d1[i-1])
                    temp2 = list(d2[k-u:])
                    d1_swapped = list(copy.copy(d1))
                    d2_swapped = list(copy.copy(d2))
                    for i in l:
                        d1_swapped[i-1] = temp2.pop(0)
                    for i in range(k-u,k):
                        d2_swapped[i] = temp1.pop(0)
                    sign1 = 0
                    if len(d1_swapped) == len(set(d1_swapped)):
```

```
                sign1 = signsort(d1_swapped)
            sign2 = 0
            if len(d2_swapped) == len(set(d2_swapped)):
                sign2 = signsort(d2_swapped)
            if sign1*sign2 != 0:
                plucker_rhs = plucker_rhs + sign1*sign2*p[tuple(sorted(
    d1_swapped))]*p[tuple(sorted(d2_swapped))]
        if plucker_lhs != plucker_rhs:
            relations.append(plucker_lhs - plucker_rhs)

    return relations
```

Listing 5.6: potentials.py

```
import sage.all
from sage.symbolic.expression_conversions import laurent_polynomial

import youngd


# Make sure that SageMath understands a rational function f with monomial
# denominator as a Laurent polynomial in the ring R_laurent, and not just
# as element of the function field

def force_laurent(f, R_laurent):

    num = f.numerator()
    den = f.denominator()

    den_inverse_laurent = 1
    for t in den.variables():
        t = sage.all.var(t)
        den_inverse_laurent = den_inverse_laurent * laurent_polynomial(1/t,
    ring=R_laurent)

    return num * den_inverse_laurent


# Given k, n and the Plucker variables p, return the initial Laurent
# polynomial associated to the rectangular plabic cluster of Gr(k,n),
# according to Marsh-Rietsch

def rectangular_potential(k, n, p):

    term1 = p[tuple(youngd.vstep_of_rect(1, 1, k, n))] * p[tuple(youngd.
    vstep_of_rect(0, 0, k, n))]**-1

    term2 = 0
    for i in range(2,k+1):
        for j in range(1,n-k+1):
            term2 = term2 + p[tuple(youngd.vstep_of_rect(i, j, k, n))] * p[
    tuple(youngd.vstep_of_rect(i-2, j-1, k, n))] * p[tuple(youngd.
    vstep_of_rect(i-1, j-1, k, n))]**-1 * p[tuple(youngd.vstep_of_rect(i
    -1, j, k, n))] **-1

    term3 = p[tuple(youngd.vstep_of_rect(k-1, n-k-1, k, n))] * p[tuple(
    youngd.vstep_of_rect(k, n-k, k, n))]**-1

    term4 = 0
    for i in range(1,k+1):
        for j in range(2,n-k+1):
            term4 = term4 + p[tuple(youngd.vstep_of_rect(i, j, k, n))] * p[
    tuple(youngd.vstep_of_rect(i-1, j-2, k, n))] * p[tuple(youngd.
    vstep_of_rect(i-1, j-1, k, n))]**-1 * p[tuple(youngd.vstep_of_rect(i,
```

```
    j-1, k, n))]**-1

  W = term1 + term2 + term3 + term4

  return W
```

Listing 5.7: quivers.py

```
import sage.all
import sage.graphs.digraph

import youngd

# Given k and n, return the initial quiver associated to rectangular
# plabic cluster, following Rietsch-Williams.

def rectangular_quiver(k, n):

   # Store the indices (i,j) of a size k(n-k) square grid as keys in a
   # dictionary pos, where values are their positions in the total order
   # that arranges the columns to be decreasing chains when read from top
   # to bottom, and decreasing along rows when read from left to right.

   pos = {}
   counter = 0
   for j in reversed(range(1,n-k+1)):
      for i in reversed(range(1,k+1)):
         pos[(i,j)] = counter
         counter = counter + 1

   # Construct the size k(n-k)+1 exchange matrix B of the
   # rectangular quiver

   B = []
   for j in reversed(range(1,n-k+1)):
      for i in reversed(range(1,k+1)):
         row = [0]*(k*(n-k)+1)
         if 1 < i < k and 1 < j < n-k :
            row[pos[(i-1,j-1)]] = 1
            row[pos[(i,j+1)]] = 1
            row[pos[(i+1,j)]] = 1
            row[pos[(i,j-1)]] = -1
            row[pos[(i-1,j)]] = -1
            row[pos[(i+1,j+1)]] = -1
         elif 1 < i < k and j == n-k :
            row[pos[(i-1,j-1)]] = 1
            row[pos[(i,j-1)]] = -1
         elif i == k and 1 < j < n-k :
            row[pos[(i-1,j-1)]] = 1
            row[pos[(i-1,j)]] = -1
         elif 1 < i < k and j == 1 :
            row[pos[(i,j+1)]] = 1
            row[pos[(i+1,j)]] = 1
            row[pos[(i-1,j)]] = -1
            row[pos[(i+1,j+1)]] = -1
         elif i == 1 and 1 < j < n-k :
            row[pos[(i,j+1)]] = 1
            row[pos[(i+1,j)]] = 1
            row[pos[(i,j-1)]] = -1
            row[pos[(i+1,j+1)]] = -1
         elif i == 1 and j == n-k :
            row[pos[(i,j-1)]] = -1
         elif i == k and j == n-k :
            row[pos[(i-1,j-1)]] = 1
```

```
            elif i == k and j == 1:
               row[pos[(i-1,j)]] = -1
            elif i == 1 and j == 1:
               row[pos[(i+1,j)]] = 1
               row[pos[(i,j+1)]] = 1
               row[pos[(i+1,j+1)]] = -1
               row[k*(n-k)] = -1
            B.append(row)
      row = [0]*(k*(n-k)+1)
      row[pos[(1,1)]] = 1
      B.append(row)

      # Construct a directed graph from B

      for i in range(len(B)):
         for j in range(len(B[i])):
            if B[i][j] < 0:
               B[i][j] = 0
      Q = sage.graphs.digraph.DiGraph(sage.all.matrix(B), multiedges=True)

      return Q

# Given k and n, return the list d_label of labels of vertices
# corresponding to rectangular diagrams in the rectangular quiver of
# type (k,n).

def rectangular_labels(k, n):

   d_label = []

   for i in range(n-k):
      for j in range(k):
         d_label.append(tuple(youngd.vstep_of_rect(k-j, n-k-i, k, n)))

   d_label.append(tuple(youngd.vstep_of_rect(0, 0, k, n)))

   return d_label

# Given a quiver Q with list of frozen nodes f, mutate Q
# along the node v. We assume v has two incoming and two outgoing
# edges and is not frozen, so that it corresponds to a 3-term
# Plucker relation according to Rietsch-Williams.

def mutate(Q, f, v):

   v_in = Q.neighbors_in(v)
   v_out = Q.neighbors_out(v)

   # Add edges of type a -> v -> b with a in v_in, b in v_out
   # and at least one among v_in and v_out not frozen, and
   # make sure to erase newly created oriented 2-loops

   for a in v_in:
      for b in v_out:
         if (a in f) and (b in f):
            continue
         else:
            if Q.has_edge(b, a):
               Q.delete_edge(b, a)
            else:
               Q.add_edge(a, b)

   # Flip orientation of edges touching v
```

```
    Q.add_edge(v, v_in[0])
    Q.delete_edge(v_in[0], v)
    Q.add_edge(v, v_in[1])
    Q.delete_edge(v_in[1], v)

    Q.add_edge(v_out[0], v)
    Q.delete_edge(v, v_out[0])
    Q.add_edge(v_out[1], v)
    Q.delete_edge(v, v_out[1])

    return Q
```

Listing 5.8: schurpol.py

```
import sage.combinat.sf.sf

# Given a list of Young diagrams in k x (n-k) grid, return a dictionary
# where they are keys with value the corresponding Schur polynomial in
# k variables, as SageMath symmetric functions.

def schur_sage(k, n, diagrams):

    d = {}

    # initialize k variables of Schur polynomials

    z = []
    for i in range(1,k+1):
        z.append('z{}'.format(i))

    s = sage.combinat.sf.sf.SymmetricFunctions(sage.all.QQ).schur()

    for y in diagrams:
        d[tuple(y)] = s(y).expand(k, alphabet=z)

    return d
```

Listing 5.9: spectrum.py

```
import matplotlib.pyplot as plt
import sympy.functions.elementary.complexes as cpx

# Given two lists branes and e of complex numbers and a string name,
# save image of the corresponding points on complex plane in
# "[name]SpectrumGr(k,n).png", where e are red dots and branes are
# blue crosses

def spectrum_combined_picture(branes, e, name, k, n):

    e_real_parts = []
    e_imaginary_parts = []
    branes_real_parts = []
    branes_imaginary_parts = []

    for z in e:
        z = complex(z)
        e_real_parts.append(cpx.re(z))
        e_imaginary_parts.append(cpx.im(z))
    for z in branes:
        z = complex(z)
        branes_real_parts.append(cpx.re(z))
        branes_imaginary_parts.append(cpx.im(z))
```

```
    plt.clf()
    plt.xlim(-3*n, 3*n)
    plt.ylim(-3*n, 3*n)
    plt.gca().set_aspect('equal', adjustable='box')
    plt.plot(e_real_parts, e_imaginary_parts, 'ro', markersize=2)
    plt.plot(branes_real_parts, branes_imaginary_parts, 'bx', markersize
     =5)

    plt.savefig('{}.png'.format(name))
```

Listing 5.10: walk.py

```
import copy
import random

import potentials
import quivers
import youngd

# Given k, n and the lists of Plucker variables and relations, run
# a random walk starting from the rectangular plabic cluster of
# Gr(k,n) and return the list of visited clusters. The walk stops
# when all edges of the mutation graph are visited, or when the number
# of steps reaches the constant MAX_STEP.
# If the optional switch loc_potential is True, return instead a
# dictionary W, whose keys are the visited clusters and whose values
# are the corresponding local Landau-Ginzburg potentials.

def random_walk(k, n, p, relations, loc_potentials=False):

    MAX_STEP = 10000

    # Create the initial rectangular plabic cluster of type (k,n),
    # made up of all rectangular Young diagrams in the k x (n-k) grid

    C = quivers.rectangular_labels(k, n)
    C.sort()

    # Initialize the list of visited clusters cluster_list

    cluster_list = []
    cluster_list.append(C)

    # Initialize Q to the quiver of the rectangular plabic chart

    Q = quivers.rectangular_quiver(k, n)

    # Construct a list frozen containing indices of nodes
    # in quiver Q labelled by boundary rectangular Young diagrams,
    # corresponding to frozen variables in the cluster algebra
    # generated by the quiver

    frozen = range(1, k)
    for i in range(n-k+1):
       frozen.append(k*i)

    # Initialize a list d_label of size k(n-k)+1, whose value at entry i
    # is the Young diagram labelling that vertex in the current cluster

    d_label = quivers.rectangular_labels(k, n)

    # Initialize a dictionary mutation_statistics, whose keys are indices
    # of visited clusters in cluster_list, and whose values are
    # dictionaries of size k(n-k)+1. The keys of such dictionaries are
```

```
# Young diagrams, and the values are -1 if the corresponding node in
# the quiver of the cluster is frozen or corresponds to a forbidden
# mutation (i.e. not a 3-term Plucker relation), and otherwise a
# non-negative integer counting how many times that node has been
# mutated. The reason why we index mutation statistics by Young
# diagram labels instead of indices of nodes is that a sequence
# of mutations can form a loop from a given cluster to itself,
# but the corresponding labellings of the nodes can be permuted
# along the loop.

mutation_statistics = {}
h = cluster_list.index(C)
mutation_statistics[h] = {}
for d in d_label:
   if youngd.is_frozen(k, n, youngd.vstep_to_part(k, n, list(d))) ==
 True:
      mutation_statistics[h][d] = -1
      continue
   in_deg = Q.in_degree(d_label.index(d))
   out_deg = Q.out_degree(d_label.index(d))
   if in_deg != 2 or out_deg != 2:
      mutation_statistics[h][d] = -1
      continue
   mutation_statistics[h][d] = 0

# Initialize a list of mutable nodes in the current quiver

current_mutable = []
for d in d_label:
   if mutation_statistics[h][d] >= 0:
      current_mutable.append(d_label.index(d))

# If switch loc_potentials is active, initialize a dictionary W
# whose keys are plabic clusters and values are corresponding local
# Landau-Ginzburg potentials

if loc_potentials == True:
   W = {}
   W[tuple(C)] = potentials.rectangular_potential(k, n, p)

# Main iteration of random walk

step = 0

while step < MAX_STEP:

   h = cluster_list.index(C)

   # Choose uniformly at random one of the mutable nodes
   # v of the quiver Q

   v = random.sample(current_mutable, 1)[0]

   # Compute instructions for mutation of Q along v

   v_in = Q.neighbors_in(v)
   v_out = Q.neighbors_out(v)
   vin1 = d_label[v_in[0]]
   vin2 = d_label[v_in[1]]
   vout1 = d_label[v_out[0]]
   vout2 = d_label[v_out[1]]

   # Apply mutation and update cluster list, quiver,
```

```
   # mutation_statistics and label list consistently; caveat:
   # make sure that diagrams in mutated cluster are again
   # sorted according to lex

   d_old = d_label[v]
   plucker_rhs = p[vin1]*p[vin2] + p[vout1]*p[vout2]
   for r in relations:
      if (r - plucker_rhs).is_monomial():
         p_new = (r - plucker_rhs) * p[d_old]**-1
         break
      if (plucker_rhs - r).is_monomial():
         p_new = (plucker_rhs - r) * p[d_old]**-1
         break
   for key, value in p.items():
      if value == p_new:
         d_new = key
         break

   D = list(C)
   D.remove(d_old)
   D.append(d_new)
   D.sort()

   mutation_statistics[h][d_old] = mutation_statistics[h][d_old] + 1

   # If switch loc_potentials is active, update the local potential

   if loc_potentials == True:
      W[tuple(D)] = W[tuple(C)].subs( {p[d_old] : plucker_rhs * p_new
**-1} )

   Q = quivers.mutate(Q, frozen, v)
   d_label[v] = d_new

   # Add D to cluster_list of visited clusters if not already seen,
   # and create the corrisponding entry of mutation_statistic;
   # if already seen simply update mutation_statistic

      if D in cluster_list:
         h = cluster_list.index(D)
      mutation_statistics[h][d_new] = mutation_statistics[h][d_new] +
1
   else:
      cluster_list.append(D)
      h = cluster_list.index(D)
      mutation_statistics[h] = {}
      for d in d_label:
         if youngd.is_frozen(k, n, youngd.vstep_to_part(k, n, list(d))
) == True:
            mutation_statistics[h][d] = -1
            continue
         in_deg = Q.in_degree(d_label.index(d))
         out_deg = Q.out_degree(d_label.index(d))
         if in_deg != 2 or out_deg != 2:
            mutation_statistics[h][d] = -1
            continue
         mutation_statistics[h][d] = 0
      mutation_statistics[h][d_new] = mutation_statistics[h][d_new] +
1

   # Update previously current cluster to newly visited cluster
   # and increase counter of steps
```

```
        C = copy.copy(D)
        step = step + 1

        # Update the list of mutable nodes

        h = cluster_list.index(D)
        current_mutable = []
        for d in d_label:
            if mutation_statistics[h][d] >= 0:
                current_mutable.append(d_label.index(d))

        # Store image of most recent quiver

        #Q_plot = Q.plot()
        #Q_plot.save('Quiver{}.png'.format(step))

    print('Found a total of {} clusters'.format(len(cluster_list)))
    print('[Mutation statistics]')
    for i in range(len(mutation_statistics)):
        print('Cluster {}: {}'.format(i, mutation_statistics[i].values()))

    if loc_potentials == False:
        return cluster_list
    else:
        return W
```

Listing 5.11: youngd.py

```
# Given k and n, generate all Young diagrams in k x (n-k) grid centered
# at top left corner, encoded in a list of k-tuples (d_1, ..., d_k)
# where d_i is the number of boxes in row i

def list_all(k, n):

    l = []
    diagrams = []

    if (k == 1):
        for a in range(n):
            l.append([a])
        return l

    for a in range(n-k+1):
        l = list_all(k-1, a+k-1)
        for i in range(len(l)):
            l[i] = [a] + l[i]
        diagrams = diagrams + l

    return diagrams


# Given a Young diagram in a k x (n-k) grid in terms of the list of its
# k vertical steps, return its partition form (d_1, ..., d_k)

def vstep_to_part(k, n, ver_steps):

    d = []

    d.append(n-k-ver_steps[0]+1)
    for i in range(1, k):
        d.append(d[i-1] - (ver_steps[i]-ver_steps[i-1]) + 1)

    return d
```

```python
# Given a in [0, k] and b in [0, n-k], return the vertical steps of the
# a x b rectangular Young diagram in the k x (n-k) grid

def vstep_of_rect(a, b, k, n):

   v_steps = []

   if a == 0 or b == 0:
      for i in range(n-k+1, n+1):
         v_steps.append(i)
      return v_steps

   for i in range(n-k-b+1, n-k-b+a+1):
      v_steps.append(i)
   for i in range(n-k+a+1, n+1):
      v_steps.append(i)

   return v_steps


# Given a Young diagram d in the k x (n-k) grid represented as partition,
# determine if it's a boundary rectangular diagram or not

def is_frozen(k, n, d):

   # Check if d is the empty diagram

   if d[0] == 0:
      return True

   # Check if d is a rectangle

   for i in range(len(d)):
      if d[i] != d[0] and d[i] > 0:
         return False

   # Check if d is a full width rectangle

   if d[0] == n-k:
      return True

   # Check if d is a full height rectangle

   if d[k-1] > 0:
      return True


   return False
```

Chapter A

LAGRANGIAN FLOER THEORY

This appendix is a brief introduction to a generalization of the Cauchy-Riemann equation from complex analysis: the Floer equation. This is a partial differential equation for a smooth function $u : S \to M$, where S is a Riemann surface with complex structure j and M is a compact manifold with symplectic structure ω and almost-complex structure J such that $g_J = \omega(\cdot, J\cdot)$ is a Riemannian metric. After some brief reference to Hamiltonian Floer theory, which is the case $\partial S = \varnothing$, we focus on Lagrangian Floer theory, where the boundary $\partial S \neq \varnothing$ is mapped to a Lagrangian in M. To simplify the exposition, we do not discuss automorphisms of the domain S.

A.1. From cylinders to strips

Assume that $\pi_1(M) = 0$ and $\omega_{|\pi_2(M)} \subset \mathbb{R}$ is a discrete subgroup; this simplifies the following heuristic derivation of the Floer equation for cylinders, but is not necessary to write the equation itself or to study its properties.

Fix a smooth function $H : M \times \mathbb{R}/\mathbb{Z} \to \mathbb{R}$, and denote $H_t = H(\cdot, t) : M \to \mathbb{R}$; this is called a time-dependent Hamiltonian. The non-degeneracy of ω allows to turn H_t into a vector field X_{H_t} on M, characterized by the equation $\omega(X_{H_t}, \cdot) = dH_t$. Consider the set

$$\mathcal{P}(H) = \{\ x : \mathbb{R}/\mathbb{Z} \to M\ :\ \dot{x}(t) = X_{H_t}(x(t))\ \}$$

of one-periodic Hamiltonian orbits. These orbits correspond to the fixed points of the symplectomorphism $\Psi_1^H : M \to M$, where $\Psi_t^H : M \to M$ is defined by $\dot{\Psi}_t^H = X_{H_t} \circ \Psi_t^H$ and $\Psi_0^H = \mathrm{id}_M$. Call $x \in \mathcal{P}(H)$ nondegenerate if $\det(\mathrm{id}_{T_{x(0)}M} - d_{x(0)}\Psi_1^H) \neq 0$. For autonomous Hamiltonians, i.e. when H_t is constant in t, critical points give constant Hamiltonian orbits and non-degeneracy implies the Morse condition.

Consider the loop space $\mathcal{L}M = C^\infty(\mathbb{R}/\mathbb{Z}, M)$, and think of it as an infinite-dimensional manifold. Define a function $\mathcal{A}_H : \mathcal{L}M \to \mathbb{R}/\mathbb{Z}$, called H-perturbed symplectic action, as follows. Since $\pi_1(M) = 0$, one can choose a cap for x, i.e. a smooth map $v : D^2 \to M$ that restricts to x over the boundary; the corresponding action is

$$\mathcal{A}_H(x) = -\int_{D^2} v^*\omega - \int_0^1 H_t(x(t))dt \quad .$$

This quantity is well-defined if and only if any other cap v' has the same symplectic area as v modulo $\mathbb{Z}$. Gluing the two caps to a smooth map $v\#v' : S^2 \to M$, its symplectic area is zero modulo $\mathbb{Z}$ up to rescaling of ω, thanks to the assumption that $\omega_{|\pi_2(M)} \subset \mathbb{R}$ is a discrete subgroup.

If $x \in \mathcal{L}M$, a tangent vector $\xi \in T_x\mathcal{L}M$ is a function $\xi : \mathbb{R}/\mathbb{Z} \to TM$ such that $\xi(t) \in T_{x(t)}M$ for all t. The differential of the action is

$$(d_x\mathcal{A}_H)\xi = \int_0^1 \omega(\dot{x}(t) - X_{H_t}(x(t)), \xi(t))dt \quad ,$$

and x is a critical point if and only if $x \in \mathcal{P}(H)$. An almost-complex structure J compatible with ω defines a Riemannian metric on $T\mathcal{L}M$ via

$$\langle \xi_1, \xi_2 \rangle_J = \int_0^1 g_J(\xi_1(t), \xi_2(t))dt \quad ,$$

and the corresponding gradient vector field of the action is

$$(\nabla\mathcal{A}_H)_x(t) = J_{x(t)}\dot{x}(t) - (\nabla H_t)(x(t)) \quad .$$

A flow line of $-\nabla\mathcal{A}_H$ is the data of a smooth function $\mathbb{R} \to \mathcal{L}M$ satisfying an ordinary differential equation. One can also think of it as a function of two variables $u : \mathbb{R}\times\mathbb{R}/\mathbb{Z} \to M$ satisfying the partial differential equation

$$\partial_s u(s,t) = -(\nabla\mathcal{A}_H)_{u(s,t)}(t) = -J_{u(s,t)}\partial_t u(s,t) + (\nabla H_t)(u(s,t)) \quad .$$

Using the fact that $JX_{H_t} = \nabla H_t$, one can write this equation as

$$J\partial_s u = \partial_t u - X_{H_t} \quad ;$$

this is the Floer equation. One can think of it as an inhomogeneous perturbation of the Cauchy-Riemann equations: the special case $H \equiv 0$ recovers the condition that the cylinder $u : \mathbb{R} \times \mathbb{R}/\mathbb{Z} \to M$ is J-holomorphic. Solutions of the Floer equation have an associated energy

$$E(u) = \frac{1}{2}\int_0^1 \int_{-\infty}^{\infty} \left(|\partial_s u|_J^2 + |\partial_t u - X_H|_J^2\right) dsdt = \int_{\mathbb{R}\times\mathbb{R}/\mathbb{Z}} \omega(\partial_s u, \partial_t u - X_H) \quad ,$$

that matches the symplectic area for $H \equiv 0$. A solution has $E(u) < \infty$ if and only if it connects two Hamiltonian orbits, in the sense that $u(s, \cdot) \to x^{\pm} \in \mathcal{P}(H)$ as $s \to \pm\infty$; in this case

$$E(u) = \int_{\mathbb{R}\times\mathbb{R}/\mathbb{Z}} u^*\omega + \int_0^1 (H_t(x^+(t)) - H_t(x^-(t)))dt \quad .$$

Let now $L \subset M$ be an orientable Lagrangian submanifold, and $H : M \times [0, 1] \to \mathbb{R}$ such that the intersection $\Psi_1^H(L) \cap L$ is transverse. Consider the set

$$\mathcal{P}_L(H) = \{\ x : [0, 1] \to M\ :\ \dot{x}(t) = X_{H_t}(x(t)) \text{ and } x(0), x(1) \in L\ \}$$

of length-one Hamiltonian chords with boundary on L; since $x(1) = \Psi_1^H(x(0))$ each chord can be interpreted as an intersection point in $\Psi_1^H(L) \cap L$.

It is possible to adapt the heuristic derivation of the Floer equation to the Lagrangian setting, replacing the loop space of M with the path space of L. Instead of doing that, let's simply replace the cylinder $\mathbb{R} \times \mathbb{R}/\mathbb{Z}$ with the strip $\mathbb{R} \times [0, 1]$, and look at those $u : \mathbb{R} \times [0, 1] \to M$ such that

$$J\partial_s u = \partial_t u - X_H \quad \text{and} \quad u(\cdot, 0), u(\cdot, 1) \in L \quad .$$

Again, a solution has energy $E(u) < \infty$ if and only if it connects two Hamiltonian chords, in the sense that $u(s, \cdot) \to x^{\pm} \in \mathcal{P}_L(H)$ as $s \to \pm\infty$. Finally, observe that the Floer equation is equivalent to saying that $(du - X_H) \circ j = J(du - X_H)$, where j is the complex structure of the strip; this formulation more readily generalizes from strips to other domains.

A.2. From strips to disks

By the Riemann mapping theorem, the interior of a strip is biholomorphic to the open unit disk. Any such biholomorphism extends to an homeomorphism of the strip with the closed unit disk minus two boundary points p and q; the location of the points is however arbitrary. Once a biholomorphism is fixed, the direction of the strip (from $-\infty$ to $+\infty$) naturally distinguishes the two points as incoming and outgoing. From now on, consider p ingoing and q outgoing.

In this section, we describe a version of the Floer equation for disks with $d \geqslant 1$ incoming points $p_1, \ldots, p_d$ and one outgoing point q. Denote $\widehat{D}$ the closed unit disk, $\Sigma \subset \partial\widehat{D}$ the set of $d+1$ boundary points, and $D = \widehat{D}\backslash\Sigma$. For each arc $C \subset \partial D$, choose a Lagrangian submanifold $L_C \subset M$. We are interested in smooth maps $u : D \to M$ such that $u(C) \subset L_C$ for all C.

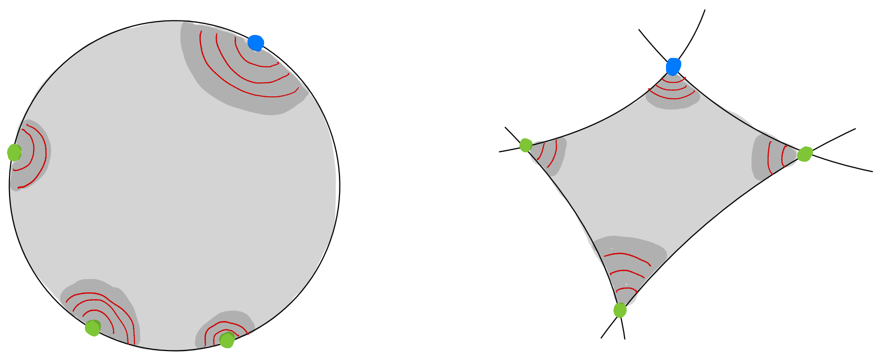

Figure A.1: Examples of strip-like ends.

For each boundary point $\zeta \in \Sigma$, pick a proper holomorphic embedding $\epsilon_\zeta : \mathbb{R}^\pm \times [0,1] \to D$ such that $\epsilon_\zeta^{-1}(\partial D) = \mathbb{R}^\pm \times \{0,1\}$ and $\epsilon_\zeta(s,\cdot) \to \zeta$ as $s \to \pm\infty$; the sign $\pm$ is $-$ if ζ is incoming and $+$ if it is outgoing. The functions $(\epsilon_\zeta)_{\zeta\in\Sigma}$ are called strip-like ends, and are assumed to have disjoint images from now on.

Recall from the cylinder and strip cases that, in order to write the Floer equation, one needs the data (H, J) of a Hamiltonian and an almost-complex structure. In those examples, both were chosen to be invariant under s-translations but allowed to be t-dependent. Since the new domain D has no translational symmetry, in this context one makes a different choice:

- $H \in \Omega^1(D, C^\infty(M, \mathbb{R}))$ is a one-form on D with values in Hamiltonians, such that $H(\xi)_{|L_C} = 0$ for all $C \subset \partial D$ and $\xi \in TC$;
- $J \in C^\infty(D, \mathcal{J}(M, \omega))$ is a family of almost-complex structures compatible with ω, parametrized by the points of D .

We still require that, in each strip-like end ϵ_ζ of D, the choices above have translational symmetry, recovering the typical properties of Floer data for strips:

- $\epsilon_\zeta^* H = (H_\zeta)_t dt$ for some time-dependent Hamiltonian $H_\zeta : M \times [0,1] \to \mathbb{R}$;
- $J(\epsilon_\zeta(s,t)) = (J_\zeta)_t$ for some time-dependent almost-complex structure J_ζ compatible with ω .

Finally, assume that the Hamiltonians H_ζ make the intersections $\Psi_1^{H_\zeta}(L_{\zeta,0}) \cap L_{\zeta,1}$ transverse for all $\zeta \in \Sigma$. Here $L_{\zeta,\bullet}$ denotes the Lagrangian L_C for $C \subset \partial D$ corresponding to $\mathbb{R}^\pm \times \{\bullet\}$ under the map ϵ_ζ. This last property allows to interpret the image of $u : D \to M$ as a $(d+1)$-gon whose vertices connect intersection points between the Lagrangians $L_C \subset M$, after Hamiltonian perturbation. The Floer equation for D is then

$$(du - X_H) \circ j = J(du - X_H) \quad \text{and} \quad u(C) \subset L_C \; \forall C \subset \partial D \quad .$$

As in the case of cylinders and strips, each solution has an energy

$$E(u) = \frac{1}{2} \int_0^1 |du - X_H|_J^2$$

and this quantity is finite if and only if there exist Hamiltonian chords x_ζ from $L_{\zeta,0}$ to $L_{\zeta,1}$ such that $u(\epsilon_\zeta(s,\cdot)) \to x_\zeta$ as $s \to \pm\infty$, where the sign $\pm$ is $-$ for incoming points and $+$ for the outgoing point.

A.3. Energy, breaking and bubbling

Denote $\mathcal{M}_{(H,J)}(x_1, \ldots, x_d, y)$ the set of solutions to the Floer equation with data (H, J) and asymptotic to fixed Hamiltonian chords. If one endows it with the C^∞ topology, this is typically not compact. However, when $H \equiv 0$ any J-holomorphic map is a minimal surface in M with respect to the Riemannian metric g_J, and it has been known since the work of Sacks-Uhlenbeck [71] that bounds on the energy lead to a candidate compactification. In Lagrangian Floer theory, the symplectic area and the energy for arbitrary Floer data (H, J) are related as follows.

Lemma A.3.1. *(Seidel [75, Section (8g)], Biran-Cornea [10, Lemma 3.3.3]) For all* (H, J) *and* $x_1, \ldots, x_d, y$ *there exists a constant* $C > 0$ *such that*

$$E(u) \leqslant \int_D u^*\omega + C \quad \forall u \in \mathcal{M}_{(H,J)}(x_1, \ldots, x_d, y) \quad .$$

Since ω is closed, the symplectic area of u depends only on its homotopy class $[u] \in \pi_2(M, L)$, where $L = \bigcup_C L_C$. Defining for each $\beta \in \pi_2(M, L)$

$$\mathcal{M}_{(H,J)}(x_1, \ldots, x_d, y; \beta) = \{ \, u \in \mathcal{M}_{(H,J)}(x_1, \ldots, x_d, y) \ : \ [u] = \beta \, \} \quad ,$$

solutions in this set have bounded energy by Lemma A.3.1. This allows to construct the so-called Gromov compactification $\overline{\mathcal{M}}_{(H,J)}(x_1, \ldots, x_d, y; \beta)$, that we informally describe below.

Consider a sequence $u_\nu \in \mathcal{M}_{(H,J)}(x_1, \ldots, x_d, y; \beta)$. In the Gromov compactification, this sequence will have a subsequence that converges in a suitable sense to a tree of solutions to the Floer equation; the limit configurations can be obtained as follows. Consider an arbitrary collection of non-intersecting interior arcs $\gamma_1, \ldots, \gamma_c \subset D$, each connecting a pair of non-consecutive $C \subset \partial D$. Removing these arcs, each component of $D \backslash (\gamma_1 \cup \cdots \cup \gamma_c)$ is again homeomorphic to a pointed-boundary disk. Construct a tree with one interior node for each of these components, and one leaf for each of the boundary points of the original unit disk. The tree has c interior edges, each dual to one of the interior arcs $\gamma_1, \ldots \gamma_c$; it also has $d + 1$ natural boundary edges connecting it to the leaves. Since D has only one outgoing boundary point, orienting the corresponding edge towards it induces an orientation on the rest of the tree. Since the tree is embedded in D by construction, the incoming leaves inherit an order from the orientation of ∂D: fix it to be clock-wise and starting after the outgoing leaf.

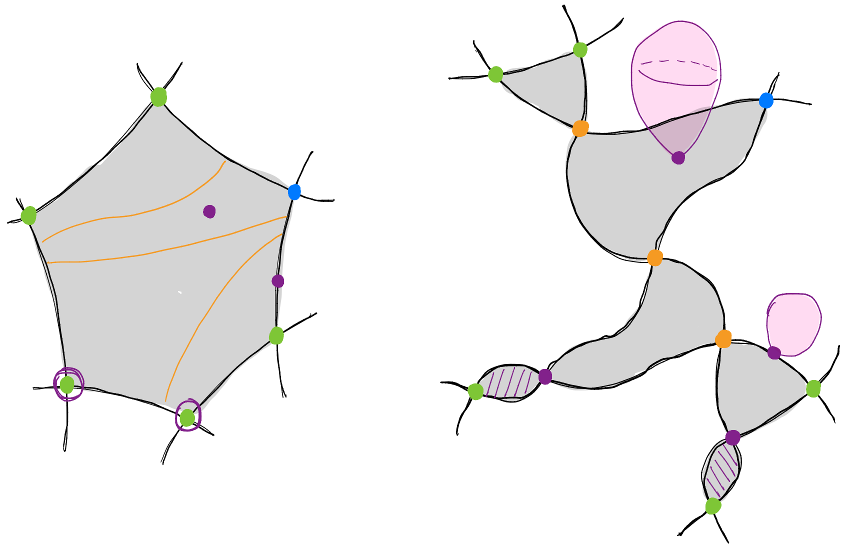

Figure A.2: An example of Gromov convergence.

The data of the arcs and the tree are equivalent, and there are at least two more ways to encode it, that we mention for their relevance in the A_∞ relations of Appendix B. One is a way to parenthesize the word $x_1 \cdots x_d$ with c pairs of parentheses. The other is as a codimension c face of the associahedron K_d, which is a convex polytope of dimension $d-2$ with a rich combinatorics.

Going back to compactness, one can think that, up to subsequences, the sequence u_ν degenerates along some collection of arcs $\gamma_1, \ldots, \gamma_c \subset D$, and that the corresponding tree parametrizes a collection of solutions to the Floer equation that connect together along new Hamiltonian chords as prescribed by the tree. If $\sup_\nu |du_\nu|_{L^\infty(D)} < \infty$ this completes the description of the limit. However, knowing that $\sup_\nu E(u_\nu) < \infty$ does not imply that $\sup_\nu |du_\nu|_{L^\infty(D)} < \infty$, and one has in fact more possible limits in that case. Suppose that $\sup_\nu |du_\nu|_{L^\infty(D)} = \infty$, and choose for each ν a point $z_\nu \in D$ such that $|d_{z_\nu} u_\nu| = |du_\nu|_{L^\infty(D)}$. Up to subsequences, this sequence of points converges in the closed unit disk, i.e. $z_\nu \to z_\infty \in \widehat{D}$ as $\nu \to \infty$. There are three cases:

- if $z_\infty \in \mathrm{int}(D)$, then u_ν degenerates along a small circle around z_∞ which is disjoint from $\gamma_1, \ldots, \gamma_c \subset D$, and the limit acquires a J-holomorphic sphere bubble ;
- if $z_\infty \in C \subset \partial D$, then u_ν degenerates along a small arc around z_∞ with endpoints on C, which is disjoint from $\gamma_1, \ldots, \gamma_c \subset D$, and the limit acquires a J-holomorphic disk bubble with boundary on L_C ;

- if $z_\infty = \zeta \in \widehat{D}\backslash D$, then u_ν degenerates along a small arc around z_∞ with endpoints on $C_{\zeta,0}$ and $C_{\zeta,1}$ which is disjoint from $\gamma_1, \ldots, \gamma_c \subset D$, and the limit acquires a strip component, connected to the rest along a new Hamiltonian chord .

The points $z_\nu \in D$ where $|du_\nu|_{L^\infty(D)}$ is achieved are not in general unique, and varying this choice can lead to different limits $z_\nu \to z_\infty$ as $\nu \to \infty$. This means that the typical limit in the Gromov compactification $\overline{\mathcal{M}}_{(H,J)}(x_1, \ldots, x_d, y; \beta)$ will have bubbles and break off strips at multiple points of $\widehat{D}$. The energies of all limit components sum up to a bounded quantity, and hence there are finitely many thanks to the following result.

Proposition A.3.2. *(McDuff-Salamon [55, Proposition 4.1.4]) For all J and $L \subset M$, there exists a constant $\hbar > 0$ such that $E(u) \geqslant \hbar$ for all J-holomorphic $u : S^2 \to M$ and J-holomorphic $u : D^2 \to M$ such that $u(\partial D^2) \subset L$.*

A.4. Virtual dimension and Maslov index

The Gromov compactification $\overline{\mathcal{M}}_{(H,J)}(x_1, \ldots, x_d, y; \beta)$ shares some properties with manifolds, due to the fact that (limits of) solutions to the Floer equation near a given $u \in \overline{\mathcal{M}}_{(H,J)}(x_1, \ldots, x_d, y; \beta)$ can be presented as zero set of a section of a Banach bundle, whose differential is a Fredholm operator D_u of Banach spaces.

We do not describe the Banach setup here; see Seidel [75, Sections (8h), (8i)]. Simply recall that Fredholm operators have finite-dimensional kernel and cokernel, and therefore a well defined index

$$\operatorname{ind}(D_u) = \dim(\ker(D_u)) - \dim(\operatorname{coker}(D_u)) \in \mathbb{Z} \quad .$$

When D_u is surjective, then $\ker(D_u)$ can be thought of as an analogue of the tangent space at $u \in \overline{\mathcal{M}}_{(H,J)}(x_1, \ldots, x_d, y; \beta)$, and the index $\operatorname{ind}(D_u)$ computes its dimension. The index of D_u is a topological quantity, depending only on $[u] = \beta$. Instead, the surjectivity of D_u can vary with u in general, and it is best to think of $\overline{\mathcal{M}}_{(H,J)}(x_1, \ldots, x_d, y; \beta)$ as having an analogue of the tangent bundle $\ker(D_u) - \operatorname{coker}(D_u)$ which is a virtual bundle in the sense of K-theory, and of $\operatorname{ind}(D_u) = \operatorname{ind}(\beta)$ as computing a virtual dimension.

Sometimes one can show that a generic choice of Floer data (H, J) makes D_u surjective for all u; in such cases one says that transversality is achieved, and the Gromov compactification is regularized. This implies that $\overline{\mathcal{M}}_{(H,J)}(x_1,\ldots,x_d,y;\beta)$ is: empty when $\mathrm{ind}(\beta)<0$, a finite collection of points when $\mathrm{ind}(\beta)=0$, a finite collection of arcs and circles when $\mathrm{ind}(\beta)=1$. It is harder to say what the result of regularization is when $\mathrm{ind}(\beta)>1$, but the $\mathrm{ind}(\beta)=0,1$ cases suffice for the construction of the Fukaya category in Appendix B.

Going back to the general discussion of the (unregularized) Gromov compactification, for each $\beta\in\pi_2(M,L)$ the virtual dimension of $\overline{\mathcal{M}}_{(H,J)}(x_1,\ldots,x_d,y;\beta)$ can be computed more explicitly as

$$\mathrm{ind}(\beta)=d-2+\mu(\beta) \quad ,$$

where $\mu(\beta)\in\mathbb{Z}$ is an integer called Maslov index and defined as follows. Since D is contractible, for any $u\in\overline{\mathcal{M}}_{(H,J)}(x_1,\ldots,x_d,y;\beta)$ the symplectic vector bundle u^*TM admits a trivialization, under which $(u_{|C})^*TL_C$ gives a path λ_C in the Grassmannian $\mathrm{LGr}(n)$ of Lagrangian subspaces of the standard symplectic vector space $\mathbb{R}^{2n}$. By going around $\partial\widehat{D}$ counter-clockwise, to each $\zeta\in\widehat{D}\backslash D$ corresponds a transverse intersection $\Psi_1^{H_\zeta}(L_{\zeta,0})\cap L_{\zeta,1}$, and one can join the Lagrangian tangent spaces at $u(\zeta)$ by the conventional path $(e^{-i\pi/2t}\mathbb{R})^n$ with $t\in[0,1]$. This path is a natural choice, since for $n=1$ it is the shortest counter-clockwise path connecting the transverse Lagrangians $\mathbb{R}$ and $i\mathbb{R}$ in $\mathbb{R}^2=\mathbb{C}$. Concatenating the paths λ_C for every $C\subset\partial D$ and the conventional paths, one gets a closed loop with homotopy class $[u_{|\partial\widehat{D}}]\in\pi_1(\mathrm{LGr}(n))=\mathbb{Z}$, and this is the Maslov index.

As $u\in\overline{\mathcal{M}}_{(H,J)}(x_1,\ldots,x_d,y;\beta)$ varies, it can degenerate as described in Section A.3. In terms of its homotopy class, this corresponds to a decomposition of β in classes of disks and spheres. The Maslov index is additive, and gives a multiple of the Chern class on sphere components:

$$\mu(\beta)=\sum\mu(\beta_{\mathrm{disk}})+\sum 2c_1(\beta_{\mathrm{sphere}}) \quad .$$

Since $\mu(\beta)$ is fixed throughout the degeneration, this formula can be profitably used to classify the possible limit configurations in the Gromov compactification.

A.5. Obstruction and monotonicity

Define the Novikov field to be

$$\Lambda = \left\{ \sum_{i \in \mathbb{N}} a_i T^{\alpha_i} \;:\; a_i \in \mathbb{C} \,, \alpha_i \in \mathbb{R} \,,\ \forall R \in \mathbb{R}\ \#\{i \in \mathbb{N} : a_i \neq 0 \text{ and } \alpha_i < R\} < \infty \right\} \quad ,$$

The homological invariants arising in Floer theory are typically defined over the Novikov field (or even the Novikov ring, that we do not describe). Most important to us is the Floer module $\mathrm{CF}(L_0, L_1)$ of two Lagrangians $L_0, L_1 \subset M$ with Floer data (H, J) over a disk with one input and one output. This is a vector space over Λ with basis the Hamiltonian chords x from L_0 to L_1, and it comes with a linear map defined on chords by

$$m^1(x) = \sum_y \left(\sum_\beta \#\overline{\mathcal{M}}_{(H,J)}(x, y; \beta) T^{\omega(\beta)} \right) y.$$

Crucially, it can happen that $(m^1)^2 \neq 0$; this phenomenon is called obstruction, and has the following topological explanation. Applying m^1 once more to $m^1(x)$ one gets

$$m^1(m^1(x)) = \sum_z \left(\sum_{\beta, \beta'} \left(\sum_y \#\overline{\mathcal{M}}_{(H,J)}(x, y; \beta) \#\overline{\mathcal{M}}_{(H,J)}(y, z; \beta') \right) T^{\omega(\beta) + \omega(\beta')} \right) z \quad .$$

Following a classical argument from Morse theory, one can try to prove that $(m^1)^2 = 0$ by proving that for all β, β' with $\mathrm{ind}(\beta) = \mathrm{ind}(\beta') = 0$ (i.e. $\mu(\beta) = \mu(\beta') = 1$) the following identity holds:

$$\sum_y \#\overline{\mathcal{M}}_{(H,J)}(x, y; \beta) \#\overline{\mathcal{M}}_{(H,J)}(y, z; \beta') = 0 \quad .$$

The class $B = \beta + \beta'$ has $\mu(B) = \mu(\beta) + \mu(\beta') = 2$, and hence the Gromov compactification $\overline{\mathcal{M}}_{(H,J)}(x, z; B)$ has virtual dimension $\mathrm{ind}(B) = 1$. If the data (H, J) achieves transversality, the equation above can be proven by arguing that the boundary of this one-manifold is

$$\partial \overline{\mathcal{M}}_{(H,J)}(x, z; B) = \overline{\mathcal{M}}_{(H,J)}(x, y; \beta) \times \overline{\mathcal{M}}_{(H,J)}(y, z; \beta') \quad .$$

This strategy works when one can rule out disk and sphere bubbling, but generally fails due to the fact that the limit of a sequence $u_\nu \in \mathcal{M}_{(H,J)}(x,z;B)$ that converges to a point in

$$\partial\overline{\mathcal{M}}_{(H,J)}(x,z;B) = \overline{\mathcal{M}}_{(H,J)}(x,z;B)\backslash\mathcal{M}_{(H,J)}(x,z;B)$$

can be more complicated than the concatenation of two strips.

Fukaya-Oh-Ohta-Ono [28] developed a general theory that describes when the map m^1 can be deformed to one that squares to zero. We describe below a simplified setting, that relies on imposing extra assumptions; this suffices for the purposes of this thesis.

A symplectic manifold (M,ω) is monotone if $[\omega] = c_1$ in $H^2(M;\mathbb{R})$; in this case a Lagrangian $L \subset M$ is monotone if $\mu = 2\omega$ on the image of the Hurewicz morphism $\pi_2(M,L) \to H_2(M,L)$. More generally, one has the following relation between symplectic area and Maslov index for solutions to the Floer equation.

Lemma A.5.1. *(Biran-Cornea [10, Lemma 3.3.4]) Assume $L_C \subset M$ is monotone for all $C \subset \partial D$. Then for all $u, u' \in \bigcup_\beta \overline{\mathcal{M}}_{(H,J)}(x_1,\ldots,x_d,y;\beta)$ one has*

$$\int_D u^*\omega - \int_D (u')^*\omega = \frac{1}{2}(\mu(u) - \mu(u')) \quad .$$

Monotonicity has two pleasant consequences. One is that the counts of solutions to the Floer equations tend to have finitely many T-terms in the Novikov ring $\Lambda_{\geqslant 0}$. More precisely, fixed $k \in \mathbb{Z}$ the set

$$\{\ \beta \in \pi_2(M,L)\ :\ \overline{\mathcal{M}}_{(H,J)}(x_1,\ldots,x_d,y;\beta) \neq \varnothing \text{ and } \operatorname{ind}(\beta) = k\ \}$$

is finite, because any sequence in the set has finite range. Indeed, given a sequence of classes $\beta_\nu \in \pi_2(M,L)$ such that $\operatorname{ind}(\beta_\nu) = k$ and a sequence of solutions to the Floer equation $u_\nu \in \overline{\mathcal{M}}_{(H,J)}(x_1,\ldots,x_d,y;\beta_\nu)$, from the index assumption the Maslov index $\mu(\beta_\nu) = 2 - d + k$ is fixed. By Lemma A.5.1 all solutions u_ν have the same symplectic area, and by Lemma A.3.1 they also have bounded energy. This means that a subsequence of u_ν converges to some $u_\infty \in \overline{\mathcal{M}}_{(H,J)}(x_1,\ldots,x_d,y;\beta_\infty)$. The limit class β_∞ is a finite sum of sphere and disk classes, and each β_ν must be a finite sum of such classes with total area $\omega(\beta_\infty)$. This implies that the sequence β_ν has finite range.

The second consequence of monotonicity is that one can be more precise about the particular nature of the obstruction phenomenon for $\mathrm{CF}(L_0, L_1)$.

Theorem A.5.2. *(Oh [61]) If $L_0, L_1 \subset M$ are monotone and oriented, then the equation*

$$m^1(m^1(x)) = (m^0(L_0) - m^0(L_1))x$$

holds in the Floer module $\mathrm{CF}(L_0, L_1)$.

If $L \subset M$ is an oriented monotone Lagrangian, the quantity $m^0(L) \in \mathbb{Z}$ is called curvature and is defined as follows. Denote $\mathcal{M}_J(L)$ the set of J-holomorphic maps $u : \widehat{D} \to M$ such that $u(\partial\widehat{D}) \subset L$ and $\mu(u) = 2$. By monotonicity, fixing the Maslov index also fixes the area of the disks in $\mathcal{M}_J(L)$, and hence their energy (there is no Hamiltonian perturbation here). Constructing the Gromov compactification $\overline{\mathcal{M}}_J(L)$ as in Section A.3, one notices that strip-breaking is impossible due to the absence of Hamiltonian perturbations, and the other degenerations are excluded by monotonicity. This implies that $\overline{\mathcal{M}}_J(L) = \mathcal{M}_J(L)$, and one can show that a generic J achieves regularity and makes $\mathcal{M}_J(L)$ a compact manifold of dimension $n = \dim(L)$. The number $m^0(L) = \deg(\mathrm{ev})$ is the degree of the evaluation map $\mathrm{ev} : \mathcal{M}_J(L) \to L$ that sends u to $u(1)$.

When $m^0(L_0) = m^0(L_1)$ one has $(m^1)^2 = 0$ in $\mathrm{CF}(L_0, L_1)$, and the cohomology is called Floer cohomology $\mathrm{HF}(L_0, L_1)$. More generally, one can endow a monotone Lagrangian $L \subset M$ with a rank one Λ-linear local system ξ and define a generalized curvature $m^0(L_\xi) \in \Lambda$ as follows. Denote $\mathrm{hol}_\xi : \pi_1(L) \to \Lambda^\times$ the holonomy of the local system, and $\mathcal{M}_J(L;\beta) \subset \mathcal{M}_J(L)$ the set of disks u with $[u] = \beta \in \pi_2(M, L)$. Weighting by the holonomy along the boundary of each disk one gets

$$m^0(L_\xi) = \sum_\beta \deg(\mathrm{ev}_{|\mathcal{M}_J(L;\beta)}) \,\mathrm{hol}_\xi(\partial\beta) \in \Lambda \quad ;$$

note that this sum is finite by monotonicity. If ξ_0, ξ_1 are local systems on L_0, L_1 such that $m^0((L_0)_{\xi_0}) = m^0((L_1)_{\xi_1})$, then again $(m^1)^2 = 0$ and one gets a twisted Floer cohomolgy $\mathrm{HF}((L_0)_{\xi_0}, (L_1)_{\xi_1})$.

When $L \cong T^N$ is a torus, the fact that $\Lambda^\times$ is abelian group allows us to think

$$\mathrm{hol}_\xi \in \mathrm{Hom}(H_1(T^N;\mathbb{Z}), \Lambda^\times) \cong H^1(T^N;\Lambda^\times) \cong (\Lambda^\times)^N \quad .$$

The first isomorphism is natural, while the second depends on the choice of a basis $\gamma_1, \dots, \gamma_N$ of 1-cycles. For explicit calculations, it is convenient to specify such a basis and call $x_1, \dots, x_N$ the relative coordinates, so that $\mathrm{hol}_\xi \mapsto m^0(L_\xi)$ gives an algebraic function

$$W_{T^N} \in \mathcal{O}((\Lambda^\times)^N) = \Lambda[x_1^{\pm 1}, \dots, x_N^{\pm 1}]$$

called disk potential of the torus T^N. Disk potentials in different bases are related by an integral linear change of variable, and the $GL(N, \mathbb{Z})$-orbit of W_{T^N} is an Hamiltonian isotopy invariant of T^N.

Chapter B

FUKAYA AND SINGULARITY CATEGORIES

This appendix gives a brief description of the formal properties of general A_∞ categories, and then focuses on one particular version of the Fukaya category in the monotone setting. Under Homological Mirror Symmetry, the Fukaya category is expected to match the category of singularities of a Landau-Ginzburg model, that we describe in the affine case in terms of matrix factorizations. To simplify the exposition, we assume the existence of strict units and do not discuss idempotent completions.

B.1. A_∞ categories

Let Λ be the Novikov field defined in Appendix A.5. A $\mathbb{Z}/2\mathbb{Z}$-graded A_∞ category $\mathcal{C}$ over Λ has a set of objects $\operatorname{Ob}\mathcal{C}$, and sets of morphisms $\mathcal{C}(X_0, X_1)$ which are $\mathbb{Z}/2\mathbb{Z}$-graded vector spaces over Λ. For every integer $d \geqslant 1$ there are compositions of order d, which are linear maps respecting the $\mathbb{Z}/2\mathbb{Z}$-grading

$$m^d : \mathcal{C}(X_{d-1}, X_d) \otimes \cdots \otimes \mathcal{C}(X_0, X_1) \to \mathcal{C}(X_0, X_d)[d] \quad .$$

These maps encode the fact that m^2 is only weakly associative, and they are required to satisfy the relations

$$\forall n \geqslant 1 \ : \ \sum_{r+s+t=n} (-1)^{rs+t} m^{r+1+t}(\mathrm{id}^{\otimes r} \otimes m^s \otimes \mathrm{id}^{\otimes t}) = 0 \quad ,$$

where the sum is over $r, t \geqslant 0$ and $s \geqslant 1$. Taking $X_0 = \cdots = X_d = X$ the relations say that $\mathcal{C}(X, X)$ is an A_∞ algebra over Λ. When $m^d = 0$ for all compositions with $d \geqslant 0$, then $\mathcal{C}$ is a differential graded category.

We make the simplifying assumption that $\mathcal{C}$ has strict units. This means that for each $X \in \operatorname{Ob}\mathcal{C}$ there exists $1_X \in \mathcal{C}(X, X)$ such that:

- $m^1(1_X) = 0$;
- $m^2(1_{X_1}, a) = (-1)^{|a|} m^2(a, 1_{X_0}) = a$ for all homogeneous $a \in \mathcal{C}(X_0, X_1)$;
- $m^d(a_1, \ldots, a_d) = 0$ whenever $d \geqslant 3$ and $a_i = 1_{X_i}$ for some $1 \leqslant i \leqslant d$.

Lemma B.1.1. *For each $X \in \mathrm{Ob}\,\mathcal{C}$, the equation $(m^1)^2 = 0$ holds in $\mathcal{C}(X, X)$. The cohomology $\mathrm{H}(X, X)$ inherits a structure of associative algebra over Λ with unit $[1_X]$.*

Proof. The A_∞ relation with $n = 1$ says precisely that $(m^1)^2 = 0$. The associative algebra structure on $\mathrm{H}(X, X)$ is given on homogeneous elements by

$$[a_2][a_1] = (-1)^{|a_1|}[m^2(a_2, a_1)] \quad .$$

Observe that this makes sense because the A_∞ relation with $n = 2$ says

$$-m^2(\mathrm{id} \otimes m^1) + m^1(m^2) - m^2(m^1 \otimes \mathrm{id}) = 0 \quad ,$$

so that evaluating on $a_2 \otimes a_1$ one has

$$m^1(m^2(a_2, a_1)) = m^2(a_2 \otimes m^1(a_1)) + m^2(m^1(a_2) \otimes a_1) \quad .$$

This implies that $m^1(m^2(a_2, a_1)) = 0$ whenever $m^1(a_2) = m^1(a_1) = 0$. Associativity consists in checking that

$$(-1)^{|a_1| + |m^2(a_2, a_1)|}[m^2(a_3, m^2(a_2, a_1))] = (-1)^{|a_2| + |a_1|}[m^2(m^2(a_3, a_2), a_1)] \quad .$$

This can be done by considering the A_∞ relation with $n = 3$:

$$m^3(\mathrm{id}^{\otimes 2} \otimes m^1) + m^2(\mathrm{id} \otimes m^2) + m^3(\mathrm{id} \otimes m^1 \otimes \mathrm{id}) + m^1(m^3) - m^2(m^2 \otimes \mathrm{id}) + m^3(m^1 \otimes \mathrm{id}^{\otimes 2}) = 0 \quad .$$

Evaluating on $a_3 \otimes a_2 \otimes a_1$ and observing that order 3 multiplications are killed whenever $m^1(a_1) = m^1(a_2) = m^1(a_3) = 0$ one gets

$$-m^2(a_3 \otimes m^2(a_2, a_1)) + m^2(m^2(a_3, a_2) \otimes a_1) = m^1(m^3(a_3, a_2, a_1)) \quad ,$$

thus proving the desired relation in cohomology. $\square$

Sometimes it is useful to consider the cohomological category $\mathrm{H}(\mathcal{C})$, whose objects are the same as $\mathcal{C}$, but whose morphisms spaces are given by cohomology groups $\mathrm{H}(X_0, X_1)$. Unlike $\mathcal{C}$, this is an ordinary category.

Any A_∞ category $\mathcal{C}$ can be thought of as a refinement of an algebra $\mathrm{HH}^\bullet(\mathcal{C})$ defined as follows. The Hochschild complex of $\mathcal{C}$ is the $\mathbb{Z}$-graded complex given in degree $d \geqslant 0$ by

$$CC^d(\mathcal{C}) = \prod_{X_0,\ldots,X_d} \mathrm{Hom}_\Lambda^{\mathbb{Z}/2\mathbb{Z}}(\mathcal{C}\,(X_{d-1}, X_d) \otimes \cdots \otimes \mathcal{C}(X_0, X_1), \mathcal{C}(X_0, X_d)[d]) \quad ,$$

where $\mathrm{Hom}_\Lambda^{\mathbb{Z}/2\mathbb{Z}}$ denotes Λ-linear maps that respect the $\mathbb{Z}/2\mathbb{Z}$-grading. The construction of the differential proceeds as follows. First define the Gerstenhaber product of cochains

$$\phi \circ \psi = \prod_{n \geqslant 1} \sum_{r+s+t=n} (-1)^{rs+t} \phi^{r+1+t}(\mathrm{id}^{\otimes r} \otimes \phi^s \otimes \mathrm{id}^{\otimes t})$$

and the associated $\mathbb{Z}$-graded Lie bracket

$$[\phi, \psi] = \phi \circ \psi - (-1)^{(|\phi|+1)(|\psi|+1)} \psi \circ \phi \quad .$$

These definitions are designed so that the structure maps of $\mathcal{C}$ define a cochain $m^\bullet \in CC^\bullet(\mathcal{C})$, and the A_∞ relations have an elegant reformulation as $m^\bullet \circ m^\bullet = 0$ in this context. Using the Lie bracket, one can define the map $[m^\bullet, \cdot]$ and verify that it is a differential on $CC^\bullet(\mathcal{C})$.

The cohomology of the complex above is the Hochschild cohomology $\mathrm{HH}^\bullet(\mathcal{C})$. There is another useful product on $CC^\bullet(\mathcal{C})$, the Yoneda product, which is defined (up to signs) by

$$\phi \cup \psi = \sum_{r,s,t \geqslant 0} (-1)^? m^\bullet(\mathrm{id}^{\otimes r} \otimes \phi \otimes \mathrm{id}^{\otimes s} \otimes \psi \otimes \mathrm{id}^{\otimes t})$$

At the cohomological level, this makes $\mathrm{HH}^\bullet(\mathcal{C})$ an associative algebra, that can be thought of as a decategorification of $\mathcal{C}$. For any object $X \in \mathcal{C}$, its cohomology $\mathrm{H}(X, X)$ is a module over $\mathrm{HH}^\bullet(\mathcal{C})$, and in this sense one can think of $\mathcal{C}$ as a refinement of the category of modules over the Hochschild cohomology.

B.2. Triangulated closure and generators

Each abelian category has an associated derived category with a canonical triangulated structure. In this section we explain a similar construction in the world of A_∞ categories. The first problem is that there are no direct sums in $\mathcal{C}$. This can be solved by considering the additive enlargement $\Sigma\,\mathcal{C}$. This is an A_∞ category whose objects are formal finite sums $X = \oplus X_i[k_i]$ with $X_i \in \mathrm{Ob}\,\mathcal{C}$ and $k_i \in \mathbb{Z}/2\mathbb{Z}$, and whose morphisms are given by

$$\Sigma\,\mathcal{C}\left(\bigoplus_i X_i[k_i], \bigoplus_j Y_j[l_j]\right) = \bigoplus_{i,j} \mathcal{C}(X_i, Y_j)[l_j - k_i] \quad ,$$

which can be thought of as matrices with morphisms of $\mathcal{C}$ as entries. The A_∞ composition maps are induced by the ones of $\mathcal{C}$ via

$$m^d(a_d, \ldots, a_1)^{ij} = \sum m^d(a_d^{i_{d-1}j}, \ldots, a_1^{ii_1}) \quad .$$

The second problem, which remains in the additive enlargement, is that there are no mapping cones. In the abelian case cones are available by embedding in the category of complexes. In the A_∞ world, cones are available in a further enlargement of $\Sigma\,\mathcal{C}$, the A_∞ category of twisted complexes $\mathrm{Tw}\,\mathcal{C}$ defined below. Objects are given by pairs (X, δ_X) with $X \in \mathrm{Ob}\,\Sigma\,\mathcal{C}$ and $\delta_X \in \Sigma\,\mathcal{C}(X, X)$ called twisting cochain, which is required to be a strictly lower-triangular morphism satisfying the Maurer-Cartan equation:

$$\sum_{d=1}^{\infty} m^d(\delta_X, \ldots, \delta_X) = 0 \quad .$$

This equation makes sense thanks to the following.

Lemma B.2.1. *If $\delta_X = (\delta_X^{ij})$ with $1 \leqslant i, j \leqslant n$ is strictly lower-triangular, then $m^d(\delta_X, \ldots, \delta_X) = 0$ for $d > n - 1$, so that the Maurer-Cartan equation has finitely many terms.*

Proof. Being strictly lower-triangular means that $\delta_X^{ij} = 0$ for $i \leqslant j$. Now observe that

$$\left[\sum_{d=1}^{\infty} m^d(\delta_X, \ldots, \delta_X)\right]^{ij} =$$

$$[m^1(\delta_X)]^{ij} + [m^2(\delta_X, \delta_X)]^{ij} + [m^3(\delta_X, \delta_X, \delta_X)]^{ij} + \ldots =$$

$$m^1(\delta_X^{ij}) + \sum_{i_1} m^2(\delta_X^{i_1 j}, \delta_X^{ii_1}) + \sum_{i_1,i_2} m^3(\delta_X^{i_2 j}, \delta_X^{i_1 i_2}, \delta_X^{ii_1}) + \ldots \quad .$$

Note that the term

$$\sum_{i_1,\ldots,i_{d-1}} m^d(\delta_X^{i_{d-1}j}, \ldots, \delta_X^{ii_i})$$

can possibly be nonzero only when all the inputs are nonzero, so this term is zero unless possibly when $i > i_1 > \cdots > i_{d-1} > j$ due to the fact that δ_X is strictly lower-triangular. But since $1 \leqslant i, j \leqslant n$ this means that the term is zero for $d > n-1$. $\square$

The morphism spaces in $\mathrm{Tw}\,\mathcal{C}$ are the same as in $\Sigma\,\mathcal{C}$. Instead, the composition maps are modified by inserting twisting cochains in all possible ways:

$$m^d = \sum_{i_0,\ldots,i_d} (-1)^? m^{d+i_0+\ldots+i_d}(\delta_{X_d}^{\otimes i_d} \otimes \mathrm{id} \otimes \delta_{X_{d-1}}^{\otimes i_{d-1}} \otimes \cdots \otimes \delta_{X_1}^{\otimes i_1} \otimes \mathrm{id} \otimes \delta_{X_0}^{\otimes i_0}) \quad .$$

This is a finite sum because, as above, the terms in $m^d(a_d, \ldots, a_1)$ must vanish for indices non contained in the cube $i_0 \leqslant N_0, \ldots, i_d \leqslant N_d$ where N_k is the number of summands in the object X_k such that $\delta_{X_k} \in \Sigma\,\mathcal{C}(X_k, X_k)$.

We now describe the construction of cones in $\mathrm{Tw}\,\mathcal{C}$. Given $c \in \mathrm{Tw}\,\mathcal{C}(X_0, X_1)$ such that $m^1(c) = 0$, define $\mathrm{Cone}(c) = (C, \delta_C)$ as the twisted complex given by $C = X_0[1] \oplus X_1$ with twisting cochain given by the matrix

$$\delta_C = \begin{bmatrix} \delta_{X_0} & 0 \\ c & \delta_{X_1} \end{bmatrix} \quad .$$

We are finally ready to defined the derived category of $\mathcal{C}$ as $\mathbf{D}\mathcal{C} = \mathrm{H}(\mathrm{Tw}\,\mathcal{C})$. This category has a natural triangulated structure constructed in the following way: sums and shifts are induced by the ones in $\mathrm{Tw}\,\mathcal{C}$, and the distinguished triangles are those isomorphic to triangles induced by cones in $\mathrm{Tw}\,\mathcal{C}$. Given a set $\mathcal{G}$ of objects in $\mathcal{C}$, one can consider the smallest full triangulated subcategory $\langle\mathcal{G}\rangle \subset \mathbf{D}\mathcal{C}$ whose objects contain $\mathcal{G}$. If $\langle\mathcal{G}\rangle = \mathbf{D}\mathcal{C}$, the objects of $\mathcal{G}$ are called generators of $\mathcal{C}$. In practice, this means that every object of $\mathrm{Tw}\,\mathcal{C}$ is obtained, up to quasi-isomorphism, by taking sums and cones starting from objects of $\mathcal{G}$.

B.3. The monotone Fukaya category

Let (M, ω) be a compact monotone symplectic manifold. For each $\lambda \in \Lambda$, define the monotone Fukaya category $\mathcal{F}_\lambda(M)$ of Lagrangian branes with curvature λ as follows. This is a $\mathbb{Z}/2\mathbb{Z}$-graded A_∞-category, where the objects L_ξ are oriented monotone Lagrangian submanifolds $L \subset X$ equipped with a rank one Λ-linear local system ξ whose holonomy $\mathrm{hol}_\xi : \pi_1(L) \to \Lambda^\times$ satisfies

$$m^0(L_\xi) = \sum_\beta \#\mathcal{M}_J(L;\beta)\,\mathrm{hol}_\xi(\partial\beta) = \lambda \quad .$$

In this equation, the first equality is the definition of curvature given in Appendix A.5.

Given two objects $L^0_{\xi_0}, L^1_{\xi_1}$ of $\mathcal{F}_\lambda(X)$, their set of morphisms $\mathrm{CF}(L^0_{\xi_0}, L^1_{\xi_1})$ is the Floer module of Appendix A.5, whose definition depends on a choice of Floer data (H, J) as in Appendix A.2. Thinking of Hamiltonian chords $x \in \mathrm{CF}(L^0_{\xi_0}, L^1_{\xi_1})$ as intersection points $x(1) \in \Psi^H_1(L_0) \cap L_1$, the $\mathbb{Z}/2\mathbb{Z}$-grading

$$\mathrm{CF}(L^0_{\xi_0}, L^1_{\xi_1}) = \mathrm{CF}^0(L^0_{\xi_0}, L^1_{\xi_1}) \oplus \mathrm{CF}^1(L^0_{\xi_0}, L^1_{\xi_1})$$

is given by the two-fold covering $\mathrm{LGr}^2(T_{x(1)}M) \to \mathrm{LGr}(T_{x(1)}M)$ of the oriented Lagrangian Grassmannian of $T_{x(1)}M$ over the unoriented one: the orientations on the Lagrangians determine two points in the fibers over $T_{x(1)}\Psi^H_1(L^0)$ and $T_{x(1)}L^1$, with $|x| = 0$ if the conventional path (as in Appendix A.4) from $T_{x(1)}\Psi^H_1(L^0)$ to $T_{x(1)}L^1$ in $\mathrm{LGr}(T_{x(1)}M)$ lifts to a path connecting the orientations, and $|x| = 1$ otherwise.

For any $d \geqslant 1$, the A_∞ composition maps

$$m^d : \mathrm{CF}(L^{l-1}_{\xi_{l-1}}, L^d_{\xi_l}) \otimes \cdots \otimes \mathrm{CF}(L^0_{\xi_0}, L^1_{\xi_1}) \to \mathrm{CF}(L^0_{\xi_0}, L^d_{\xi_d})$$

are defined on Hamiltonian chords by

$$m^d(x_d \otimes \cdots \otimes x_1) = \sum_y \left(\sum_\beta \#\overline{\mathcal{M}}_{(H,J)}(x_1, \ldots, x_d, y;\beta)\,\mathrm{hol}_\xi(\partial\beta) T^{\omega(\beta)} \right) y \quad .$$

Here $\mathrm{hol}_\xi(\partial\beta) \in \Lambda^\times$ is obtained as compound holonomy of the local systems $\xi_0, \ldots, \xi_d$

along $\partial\beta$. This construction depends on the choice of Floer data (H, J), but different choices produce equivalent A_∞-categories and $\mathcal{F}_\lambda(X)$ denotes any of them. If $L^0_{\xi_0}$ and $L^1_{\xi_1}$ are two objects in $\mathcal{F}_\lambda(M)$, the condition $m^0(L^0_{\xi_0}) = m^0(L^1_{\xi_1}) = \lambda$ guarantees that $(m^1)^2 = 0$ holds in their Floer module as discussed in Appendix A.5.

Thanks to monotonicity, setting the Novikov variable $T = 1$ makes the Fukaya category linear over $\mathbb{C}$. Denote $\mathrm{QH}(M)$ the quantum cohomology of (M, ω) over $\mathbb{C}$. The operator of quantum multiplication by the first Chern class $c_1\star$ induces a decomposition

$$\mathrm{QH}(X) = \bigoplus_{\lambda\in\mathbb{C}} \mathrm{QH}_\lambda(M)$$

in generalized eigenspaces, labelled by the eigenvalues. Each summand $\mathrm{QH}_\lambda(M)$ can be thought of as a decategorification of $\mathcal{F}_\lambda(M)$ in the following sense.

Theorem B.3.1. *(Sanda [72, Theorem 1.1]) If the A_∞ category $\mathcal{F}_\lambda(X)$ is homologically smooth, then there is an isomorphism of $\mathbb{C}$-algebras*

$$\mathrm{HH}^\bullet(\mathcal{F}_\lambda(M)) \cong \mathrm{QH}_\lambda(M) \quad .$$

It is expected that homological smoothness always holds for the Fukaya category $\mathcal{F}_\lambda(M)$; see Ganatra [32, Section 3.3] for more on this.

We list below some facts that are used throughout the thesis. First, the only $\lambda \in \mathbb{C}$ for which $\mathcal{F}_\lambda(M)$ can be nontrivial are those appearing in the decomposition of quantum cohomology mentioned above.

Theorem B.3.2. *(Auroux [6, Proposition 6.8]) If $\mathrm{HF}(L_\xi, L_\xi) \neq 0$, then $m^0(L_\xi)$ is an eigenvalue of the operator $c_1\star$ acting on $\mathrm{QH}(M)$.*

The case where $L \cong T^N$ is a Lagrangian torus is of particular interest in this thesis. Recall from Appendix A.5 that a monotone Lagrangian torus has an associated disk potential

$$W_L \in \mathbb{C}[z_1^\pm, \dots, z_N^\pm],$$

that can be thought of as a generating function of J-holomorphic disks with Maslov index 2 with boundary on L. One can use the disk potential to completely characterize the nonzero objects of the Fukaya category supported on L.

Theorem B.3.3. *(Auroux [6, Proposition 6.9], Sheridan [77, Proposition 4.2]) If $L \subset M$ is a monotone Lagrangian torus, then hol_ξ is a critical point of W_L if and only if $\mathrm{HF}(L\xi, L_\xi) \neq 0$.*

Finally, the following generation criterion is an adaptation of the one introduced by Abouzaid [1] to the monotone setup.

Theorem B.3.4. *(Sheridan [77, Corollary 2.19]) If $\mathrm{QH}_\lambda(X)$ is one-dimensional, any object L_ξ of $\mathcal{F}_\lambda(X)$ with $\mathrm{HF}(L_\xi, L_\xi) \neq 0$ split-generates $\mathbf{D}\mathcal{F}_\lambda(X)$.*

When one can establish generation by tori, the following gives an efficient description of the Fukaya category as a category of modules over Clifford algebras.

Theorem B.3.5. *(Sheridan [77, Proposition 4.2-4.3 and Corollary 6.5]) If T^N is a monotone Lagrangian torus, then for every nondegenerate critical point hol_ξ of W_{T^N}*

$$\mathrm{HF}(T^N_\xi, T^N_\xi) \cong Cl_N$$

as $\mathbb{C}$-algebras, where Cl_N denotes the Clifford algebra of the quadratic form of rank N on $\mathbb{C}^N$. Moreover if T^N_ξ generates $\mathcal{F}_\lambda(X)$ there is an equivalence of triangulated categories

$$\mathbf{D}\mathcal{F}_\lambda(X) \simeq \mathbf{D}(Cl_N)$$

with the derived category of finitely generated modules over Cl_N.

B.4. The category of singularities

Let U be an affine algebraic variety over $\mathbb{C}$, whose complex dimension is $\dim(U) = N$. Write $U = \mathrm{Spec}(R)$ with R algebra over $\mathbb{C}$ of Krull dimension N, and fix an algebraic function $W \in R$. Smoothness of U guarantees that the sheaf of algebraic one-forms $\Omega^1_{R/\mathbb{C}}$ is locally free of rank N, and the equation $dW = 0$ defines a closed subscheme $Z \subset U$ called critical locus.

The Jacobian ring of W is the ring of algebraic functions on the critical locus $Z = \mathrm{Spec}(\mathrm{Jac}(W))$. The fiber $W^{-1}(\lambda)$ over a closed point $\lambda \in \mathbb{C}$ is also a closed subscheme, with $W^{-1}(\lambda) = \mathrm{Spec}(R/(W - \lambda))$. The critical locus Z decomposes as a union of closed subschemes $Z_\lambda = Z \cap W^{-1}(\lambda)$, and this induces a decomposition

$$\mathrm{Jac(W)} = \bigoplus_{\lambda \in \mathbb{C}} \mathrm{Jac}_\lambda(W) \quad ,$$

where $Z_\lambda = \mathrm{Spec}(\mathrm{Jac}_\lambda(W))$ and $\mathrm{Jac}_\lambda(W) = \mathrm{Jac}(W) \otimes_R R/(W - \lambda)$.

Orlov [62] introduced a triangulated category, the derived category of singularities $\mathbf{D}\mathcal{S}(W^{-1}(\lambda))$, which measures to what extent coherent sheaves on the fiber $W^{-1}(\lambda)$ fail to have finite resolutions by locally free sheaves. When the critical locus is zero-dimensional, Dyckerhoff [23] showed that it is generated by skyscraper sheaves at the singular points. In the context of this thesis, this category typically appears as mirror to the derived Fukaya category $\mathbf{D}\mathcal{F}_\lambda(M)$, in the sense that there is an equivalence of triangulated categories

$$\mathbf{D}\mathcal{F}_\lambda(M) \simeq \mathbf{D}\mathcal{S}(W^{-1}(\lambda)) \quad .$$

When this holds for all $\lambda \in \mathbb{C}$, we say that (U, W) is a Landau-Ginzburg model for the monotone symplectic manifold M in the sense of Homological Mirror Symmetry.

The derived category of singularities of $W^{-1}(\lambda)$ is equivalent to the cohomological category of a differential graded category, called the category of matrix factorizations of $W - \lambda$:

$$\mathbf{D}\mathcal{S}(W^{-1}(\lambda)) \simeq \mathbf{D}\mathcal{M}(R, W - \lambda) \quad .$$

Here, the objects are R-modules $X = X_0 \oplus X_1$ with finitely generated projective summands of degree 0 and 1, and equipped with an R-linear map $d_X : X \to X$ of odd degree satisfying the equation $(d_X)^2 = (W - \lambda)\,\mathrm{id}_X$. Morphisms between two matrix factorizations X and Y in $\mathcal{M}(R, W - \lambda)$ are given by the cycles of a $\mathbb{Z}/2\mathbb{Z}$-graded complex over $\mathbb{C}$ with

$$\mathrm{hom}(X, Y) = \mathrm{hom}^0(X, Y) \oplus \mathrm{hom}^1(X, Y) \quad \text{and} \quad d(f) = d_Y \circ f - (-1)^{|f|} f \circ d_X \quad ,$$

where $f : X \to Y$ denotes an R-linear map of degree $|f|$. The name matrix factorization comes from the fact that, if $X = X_0 \oplus X_1$ with finitely generated free summands, one can pick bases and represent d_X as a matrix

$$d_X = \left(\begin{array}{c|c} 0 & d_X^{01} \\ \hline d_X^{10} & 0 \end{array}\right)$$

and the condition $(d_X)^2 = (W - \lambda)\,\mathrm{id}_X$ implies that X_0 and X_1 have the same rank, with

$$d_X^{10} \circ d_X^{01} = (W - \lambda)\,\mathrm{id}_{X_0} \quad , \quad d_X^{01} \circ d_X^{10} = (W - \lambda)\,\mathrm{id}_{X_1} \quad .$$

Matrix factorizations encode the fact that any coherent sheaf on $W^{-1}(\lambda)$ admits a locally free resolution that eventually becomes two-periodic, as proved by Eisenbud [24].

Bibliography

[1] M. Abouzaid. A geometric criterion for generating the Fukaya category. *Publ. Math. Inst. Hautes Études Sci.*, 112:191–240, 2010.

[2] M. Abouzaid. The family Floer functor is faithful. *J. Eur. Math. Soc. (JEMS)*, 19(7):2139–2217, 2017.

[3] D. Abramovich and Q. Chen. Stable logarithmic maps to Deligne-Faltings pairs II. *Asian J. Math.*, 18(3):465–488, 2014.

[4] D. Abramovich and J. Wise. Birational invariance in logarithmic Gromov-Witten theory. *Compos. Math.*, 154(3):595–620, 2018.

[5] B. H. An, Y. Cho, and J. S. Kim. On the f-vectors of Gelfand-Cetlin polytopes. *European J. Combin.*, 67:61–77, 2018.

[6] D. Auroux. Mirror symmetry and T-duality in the complement of an anticanonical divisor. *J. Gökova Geom. Topol. GGT*, 1:51–91, 2007.

[7] D. Auroux. A beginner's introduction to Fukaya categories. In *Contact and symplectic topology*, volume 26 of *Bolyai Soc. Math. Stud.*, pages 85–136. János Bolyai Math. Soc., Budapest, 2014.

[8] D. Auroux. Infinitely many monotone Lagrangian tori in $\mathbb{R}^6$. *Invent. Math.*, 201(3):909–924, 2015.

[9] A. Bertram. Quantum Schubert calculus. *Adv. Math.*, 128(2):289–305, 1997.

[10] P. Biran and O. Cornea. Lagrangian cobordism and Fukaya categories. *Geom. Funct. Anal.*, 24(6):1731–1830, 2014.

[11] M. Castronovo. ClusterExplorer. https://gitlab.com/castronovo/clusterexplorer, 2019.

[12] M. Castronovo. Fukaya category of Grassmannians: rectangles. *Adv. Math.*, 372:107287, 40, 2020.

[13] F. Charest and C. Woodward. Floer trajectories and stabilizing divisors. *J. Fixed Point Theory Appl.*, 19(2):1165–1236, 2017.

[14] Y. V. Chekanov. Lagrangian tori in a symplectic vector space and global symplectomorphisms. *Math. Z.*, 223(4):547–559, 1996.

[15] Q. Chen. Stable logarithmic maps to Deligne-Faltings pairs I. *Ann. of Math. (2)*, 180(2):455–521, 2014.

[16] D. Cheong and C. Li. On the conjecture $\mathcal{O}$ of GGI for G/P. *Adv. Math.*, 306:704–721, 2017.

[17] C.-H. Cho and Y.-G. Oh. Floer cohomology and disc instantons of Lagrangian torus fibers in Fano toric manifolds. *Asian J. Math.*, 10(4):773–814, 2006.

[18] C.-H. Cho and M. Poddar. Holomorphic orbi-discs and Lagrangian Floer cohomology of symplectic toric orbifolds. *J. Differential Geom.*, 98(1):21–116, 2014.

[19] Y. Cho and Y. Kim. Monotone Lagrangians in flag varieties. *International Mathematics Research Notices*, to appear.

[20] D. A. Cox, J. B. Little, and H. K. Schenck. *Toric varieties*, volume 124 of *Graduate Studies in Mathematics*. American Mathematical Society, Providence, RI, 2011.

[21] N. G. de Bruijn. On the factorization of cyclic groups. *Nederl. Akad. Wetensch. Proc. Ser. A.* **56** = *Indagationes Math.*, 15:370–377, 1953.

[22] J. J. Duistermaat. On global action-angle coordinates. *Comm. Pure Appl. Math.*, 33(6):687–706, 1980.

[23] T. Dyckerhoff. Compact generators in categories of matrix factorizations. *Duke Math. J.*, 159(2):223–274, 2011.

[24] D. Eisenbud. Homological algebra on a complete intersection, with an application to group representations. *Trans. Amer. Math. Soc.*, 260(1):35–64, 1980.

[25] L. Escobar and M. Harada. Wall-crossing for Newton-Okounkov bodies and the tropical Grassmannian. https://doi.org/10.1093/imrn/rnaa230, 2020.

[26] S. Fomin and A. Zelevinsky. Cluster algebras. I. Foundations. *J. Amer. Math. Soc.*, 15(2):497–529, 2002.

[27] S. Fomin and A. Zelevinsky. Cluster algebras. II. Finite type classification. *Invent. Math.*, 154(1):63–121, 2003.

[28] K. Fukaya, Y.-G. Oh, H. Ohta, and K. Ono. *Lagrangian intersection Floer theory: anomaly and obstruction*, volume 46 of *AMS/IP Studies in Advanced Mathematics*. American Mathematical Society, Providence, RI; International Press, Somerville, MA, 2009.

[29] K. Fukaya, Y.-G. Oh, H. Ohta, and K. Ono. Lagrangian Floer theory on compact toric manifolds. I. *Duke Math. J.*, 151(1):23–174, 2010.

[30] W. Fulton. *Introduction to toric varieties*, volume 131 of *Annals of Mathematics Studies*. Princeton University Press, Princeton, NJ, 1993. The William H. Roever Lectures in Geometry.

[31] S. Galkin, V. Golyshev, and H. Iritani. Gamma classes and quantum cohomology of Fano manifolds: gamma conjectures. *Duke Math. J.*, 165(11):2005–2077, 2016.

[32] S. Ganatra. Automatically generating Fukaya categories and computing quantum cohomology. https://arxiv.org/abs/1605.07702, 2019.

[33] N. Gonciulea and V. Lakshmibai. Degenerations of flag and Schubert varieties to toric varieties. *Transform. Groups*, 1(3):215–248, 1996.

[34] M. Gromov. Pseudo holomorphic curves in symplectic manifolds. *Invent. Math.*, 82(2):307–347, 1985.

[35] M. Gross, P. Hacking, S. Keel, and M. Kontsevich. Canonical bases for cluster algebras. *J. Amer. Math. Soc.*, 31(2):497–608, 2018.

[36] M. Gross and B. Siebert. Mirror symmetry via logarithmic degeneration data. I. *J. Differential Geom.*, 72(2):169–338, 2006.

[37] M. Gross and B. Siebert. Mirror symmetry via logarithmic degeneration data, II. *J. Algebraic Geom.*, 19(4):679–780, 2010.

[38] M. Gross and B. Siebert. From real affine geometry to complex geometry. *Ann. of Math. (2)*, 174(3):1301–1428, 2011.

[39] M. Gross and B. Siebert. Logarithmic Gromov-Witten invariants. *J. Amer. Math. Soc.*, 26(2):451–510, 2013.

[40] V. Guillemin and S. Sternberg. The Gelfand-Cetlin system and quantization of the complex flag manifolds. *J. Funct. Anal.*, 52(1):106–128, 1983.

[41] M. Harada and K. Kaveh. Integrable systems, toric degenerations and Okounkov bodies. *Invent. Math.*, 202(3):927–985, 2015.

[42] S. N. Karp. Moment curves and cyclic symmetry for positive Grassmannians. *Bull. Lond. Math. Soc.*, 51(5):900–916, 2019.

[43] K. Kato. Logarithmic structures of Fontaine-Illusie. In *Algebraic analysis, geometry, and number theory (Baltimore, MD, 1988)*, pages 191–224. Johns Hopkins Univ. Press, Baltimore, MD, 1989.

[44] K. Kato. Toric singularities. *Amer. J. Math.*, 116(5):1073–1099, 1994.

[45] K. Kaveh and A. G. Khovanskii. Newton-Okounkov bodies, semigroups of integral points, graded algebras and intersection theory. *Ann. of Math. (2)*, 176(2):925–978, 2012.

[46] K. Kaveh and C. Manon. Khovanskii bases, higher rank valuations, and tropical geometry. *SIAM J. Appl. Algebra Geom.*, 3(2):292–336, 2019.

[47] A. Knutson, T. Lam, and D. E. Speyer. Positroid varieties: juggling and geometry. *Compos. Math.*, 149(10):1710–1752, 2013.

[48] A. Knutson, T. Lam, and D. E. Speyer. Projections of Richardson varieties. *J. Reine Angew. Math.*, 687:133–157, 2014.

[49] M. Kontsevich. Homological algebra of mirror symmetry. In *Proceedings of the International Congress of Mathematicians, Vol. 1, 2 (Zürich, 1994)*, pages 120–139. Birkhäuser, Basel, 1995.

[50] T. Y. Lam and K. H. Leung. On vanishing sums of roots of unity. *J. Algebra*, 224(1):91–109, 2000.

[51] B. Leclerc. Cluster structures on strata of flag varieties. *Adv. Math.*, 300:190–228, 2016.

[52] G. Lusztig. Total positivity in partial flag manifolds. *Represent. Theory*, 2:70–78, 1998.

[53] R. J. Marsh and K. Rietsch. The B-model connection and mirror symmetry for Grassmannians. *Adv. Math.*, 366:107027, 131, 2020.

[54] R. J. Marsh and J. S. Scott. Twists of Plücker coordinates as dimer partition functions. *Comm. Math. Phys.*, 341(3):821–884, 2016.

[55] D. McDuff and D. Salamon. *J-holomorphic curves and symplectic topology*, volume 52 of *American Mathematical Society Colloquium Publications*. American Mathematical Society, Providence, RI, second edition, 2012.

[56] M. McLean. Reeb orbits and the minimal discrepancy of an isolated singularity. *Invent. Math.*, 204(2):505–594, 2016.

[57] M. McLean, M. Tehrani, and A. Zinger. Normal crossings singularities for symplectic topology. *Adv. Math.*, 339:672–748, 2018.

[58] T. Nishinou, Y. Nohara, and K. Ueda. Toric degenerations of Gelfand-Cetlin systems and potential functions. *Adv. Math.*, 224(2):648–706, 2010.

[59] Y. Nohara and K. Ueda. Toric degenerations of integrable systems on Grassmannians and polygon spaces. *Nagoya Math. J.*, 214:125–168, 2014.

[60] Y. Nohara and K. Ueda. Potential functions on Grassmannians of planes and cluster transformations. *J. Symplectic Geom.*, 18(2):559–612, 2020.

[61] Y.-G. Oh. Addendum to: "Floer cohomology of Lagrangian intersections and pseudo-holomorphic disks. I." [Comm. Pure Appl. Math. **46** (1993), no. 7, 949–993; MR1223659 (95d:58029a)]. *Comm. Pure Appl. Math.*, 48(11):1299–1302, 1995.

[62] D. O. Orlov. Triangulated categories of singularities and D-branes in Landau-Ginzburg models. *Tr. Mat. Inst. Steklova*, 246(Algebr. Geom. Metody, Svyazi i Prilozh.):240–262, 2004.

[63] Y. Ostrover and I. Tyomkin. On the quantum homology algebra of toric Fano manifolds. *Selecta Math. (N.S.)*, 15(1):121–149, 2009.

[64] J. Pardon. An algebraic approach to virtual fundamental cycles on moduli spaces of pseudo-holomorphic curves. *Geom. Topol.*, 20(2):779–1034, 2016.

[65] S. Piunikhin, D. Salamon, and M. Schwarz. Symplectic Floer-Donaldson theory and quantum cohomology. In *Contact and symplectic geometry (Cambridge, 1994)*, volume 8 of *Publ. Newton Inst.*, pages 171–200. Cambridge Univ. Press, Cambridge, 1996.

[66] A. Postnikov. Total positivity, Grassmannians, and networks. https://arxiv.org/abs/math/0609764, 2006.

[67] K. Rietsch. Quantum cohomology rings of Grassmannians and total positivity. *Duke Math. J.*, 110(3):523–553, 2001.

[68] K. Rietsch. A mirror construction for the totally nonnegative part of the Peterson variety. *Nagoya Math. J.*, 183:105–142, 2006.

[69] K. Rietsch. A mirror symmetric construction of $qH_T^*(G/P)_{(q)}$. *Adv. Math.*, 217(6):2401–2442, 2008.

[70] K. Rietsch and L. Williams. Newton-Okounkov bodies, cluster duality, and mirror symmetry for Grassmannians. *Duke Math. J.*, 168(18):3437–3527, 2019.

[71] J. Sacks and K. Uhlenbeck. The existence of minimal immersions of 2-spheres. *Ann. of Math. (2)*, 113(1):1–24, 1981.

[72] D. Salamon. Lectures on Floer homology. In *Symplectic geometry and topology (Park City, UT, 1997)*, volume 7 of *IAS/Park City Math. Ser.*, pages 143–229. Amer. Math. Soc., Providence, RI, 1999.

[73] F. Sanda. Computation of Quantum Cohomology From Fukaya Categories. *Int. Math. Res. Not. IMRN*, (1):766–800, 2021.

[74] J. S. Scott. Grassmannians and cluster algebras. *Proc. London Math. Soc. (3)*, 92(2):345–380, 2006.

[75] P. Seidel. *Fukaya categories and Picard-Lefschetz theory*. Zurich Lectures in Advanced Mathematics. European Mathematical Society (EMS), Zürich, 2008.

[76] V. Shende, D. Treumann, H. Williams, and E. Zaslow. Cluster varieties from Legendrian knots. *Duke Math. J.*, 168(15):2801–2871, 2019.

[77] N. Sheridan. On the Fukaya category of a Fano hypersurface in projective space. *Publ. Math. Inst. Hautes Études Sci.*, 124:165–317, 2016.

[78] B. Siebert and G. Tian. On quantum cohomology rings of Fano manifolds and a formula of Vafa and Intriligator. *Asian J. Math.*, 1(4):679–695, 1997.

[79] R. P. Stanley. Theory and application of plane partitions. I, II. *Studies in Appl. Math.*, 50:167–188; ibid. 50 (1971), 259–279, 1971.

[80] A. Strominger, S.-T. Yau, and E. Zaslow. Mirror symmetry is T-duality. *Nuclear Phys. B*, 479(1-2):243–259, 1996.

[81] D. Tonkonog. From symplectic cohomology to Lagrangian enumerative geometry. *Adv. Math.*, 352:717–776, 2019.

[82] U. Varolgunes. *Mayer-Vietoris property for relative symplectic cohomology*. 2018. Thesis (Ph.D.)–MIT.

[83] E. Witten. Two-dimensional gravity and intersection theory on moduli space. In *Surveys in differential geometry (Cambridge, MA, 1990)*, pages 243–310. Lehigh Univ., Bethlehem, PA, 1991.

[84] H. Yuan. Family Floer program and non-archimedean SYZ mirror construction. https://arxiv.org/abs/2003.06106, 2020.